APPLICABILITY OF COAGULATION TECHNOLOGIES FOR HIGH-TURBIDITY COAL SEAM GAS WATER TREATMENT

Syeda Nishat Ashraf

Master of Science

Submitted in fulfilment of the requirements for the degree of

Doctor of Philosophy (Research)

School of Civil Engineering and Built Environment

Science and Engineering Faculty

Queensland University of Technology

2019

Keywords

Aluminium electrodes (Al), Aluminium-iron combined electrodes (Al-Fe), Brine, Chemical Coagulation (CC), Coal Seam Gas (CSG) Water, Dissolved ions, Electrocoagulation (EC), Flocs, High Efficiency Reverse Osmosis (HERO), High Turbidity, Hydraulic Retention Time (HRT), Iron electrodes (Fe), Polarity Reversal Time (PRT), Reverse Osmosis (RO), Silicates.

Abstract

Coal Seam Gas (CSG), an increasingly important source of energy, has become one of the major sources of revenue in Queensland, Australia. Depressurising of coal seams is required to extract methane gas which causes the release of 'produced water' from coal seams. CSG (produced) water profile varies within a small territory; but in general, contains high sodium chloride, sodium bicarbonate, and alkaline earth ions. Other important ions, such as boron (B^+) and silicon (Si^{4+}) can be found in lower concentrations. Typically, CSG water turbidity can be below 50 NTU, however, values of 500 NTU and above are not uncommon and have been reported by the industry. Since a large quantity of water is being produced in the CSG sector, it is a great challenge to the CSG operators to manage the safe disposal, abiding discharge guidelines imposed by the Queensland Government. Therefore, the purpose of this study is to improve the currently available treatment technologies, specially, pre-treatment technologies for safe disposal of CSG produced water into the environment or make it suitable for other applications such as irrigation.

Several treatment technologies are currently used in practice to treat CSG water, where desalination is the core treatment process. In Australia and places in the USA, reverse osmosis (RO) is the central desalination unit. RO is a membrane technology, which is very susceptible to biofouling, blockage with suspended solids and scaling by dissolved ions. During the desalination of CSG water, the concentration of dissolved ions determines the efficiency of RO treated water recovery. High-efficiency reverse osmosis (HERO) is an improved version of RO containing specially designed pre-treatment stages before the raw water enters the RO system. HERO can recover more

water than conventional RO and depending on feed water quality HERO can recover up to 99% water. Consequently, brine rejected by HERO is more concentrated than RO brine.

The reduction of dissolved ions prior to either RO or HERO treatment can protect the membranes, thereby, considerably reducing the operation and maintenance cost of the system. In earlier studies, chemical coagulation (CC) and electrocoagulation (EC) have been considered as effective pre-treatment methods for industrial wastewater from textiles, tannery, hospitals, pharmaceutical and cosmetics manufacturers, dairy and so on. Though limited study is found on pre-treatment of CSG water using CC and EC, the effect of raw water turbidity on the efficiency of both processes in removing dissolved ions has not been studied extensively. Therefore, the development of appropriate pre-treatment technologies for CSG produced water containing high turbidity is of significant benefit to the CSG industry. This study is focused on (i) the effectiveness of CC for pre-treatment of CSG water in the presence of turbidity, (ii) influence of high-turbidity on the performance of EC for pre-treatment of CSG water, and (iii) applicability of EC to treat HERO brine from CSG water.

In this study, both laboratory simulated samples and real CSG water were tested using a jar test apparatus with either aluminium chlorohydrate (ACH), aluminium sulphate (alum) or ferric chloride as coagulants. All coagulants reduced the turbidity significantly (> 96%) and dissolved silicates moderately (< 37.82 %). The use of AqMB software demonstrated that the formation of a muscovite-like material was responsible for the silicate removal. However, aluminium based coagulants were preferred in terms of their ability to promote the formation of aluminosilicates which

were responsible for the reduction in dissolved silicate content of the CSG associated water. Alkaline earth ions removal was found to be insignificant by chemical coagulation. Surprisingly, alkaline earth ions and dissolved silica removal were greater in real CSG water compared to simulated water. Furthermore, in the tested range of turbidity (up to 500 NTU), the coagulants' performance in removing alkaline earth ions, boron, or dissolved silica was not influenced by the turbidity present in the feed water.

This study also focused upon the controlling parameters of EC to treat turbid CSG water and HERO brine. For this, the EC cell, equipped with multi-electrodes was used in the continuous mode of operation. For both types of water samples, either aluminium (Al), iron (Fe) or combined (Al-Fe) electrodes were employed at three different hydraulic retention times (HRT: 20, 30 and 60 s) and three different polarity reversal times (PRT: 1, 3 and 5 min).

For all electrodes and PRT, more than 99% turbidity was removed at 20 s HRT. At 60 s HRT, Al electrodes exhibited the best performance in removing dissolved ions (calcium, magnesium, boron, barium, strontium, and silica) and had the least electrode dissolution (1.46 g/L) compared to other electrode combinations. Though Fe electrodes were not efficient enough to reduce dissolved ions from CSG water, rapid floc sedimentation was observed (up to 75% volumetric reduction within an hour). However, PRT has not affected the removal efficiency significantly, but it had a notable bearing on the power consumption.

The study on the applicability of EC to treat HERO brine showed that at 60 s HRT, Fe electrodes achieved highest dissolved ions removal (except silicates) compared to other electrode combinations. On the other hand, more than 98% of silicates were removed by both Al and Al-Fe combined electrodes. Removal of dissolved species by Al-Fe combined electrodes were in between the removal by Al and Fe electrodes individually. Surprisingly, residual aluminium content was 29.5 mg/L for Al-Fe electrodes while the amount was 20.9 mg/L for Al electrodes. Irrespective of HRT and PRT, Al electrodes produce the least amount of flocs (0.40 g/L) while both Fe and Al-Fe electrodes produced more than 0.75 g/L flocs. In contrast, the amount of Fe electrode dissolution was the highest among all electrode combinations (0.703 kg/KL) followed by Al-Fe electrodes (0.418 kg/KL) and Al electrodes (0.205 kg/KL). Therefore, the selection of electrode material depends on variety of ions to remove. The impact of PRT was independent of EC performance in treating HERO brine, due to the presence of high concentrations of chlorides (21560 mg/L).

In summary, EC demonstrates better performance than CC in pre-treating CSG water with or without turbidity. This study reveals new information about optimising the EC process regarding electrodes combinations, hydraulic retention times, and polarity reversal times. This new knowledge will assist CSG industries to choose EC with appropriate parameters as a pre-treatment method for CSG produced water according to the requirements. Besides, EC exhibits conservable promise as a treatment method for HERO brine from CSG water. Most importantly, silicates, the most critical salts in CSG water and HERO brine, was reduced to a great extent by EC equipped with any combination of electrodes at any HRT and PRT. Therefore, EC

would be a promising application in removing silicates from HERO brine, which will

benefit downstream treatment processes.

Table of Contents

List of Figures

List of Tables

List of Abbreviations

BOD   Biochemical Oxygen Demand

CBM   Coal Bed Methane

COD   Chemical Oxygen Demand

CS   Coal Seam

CSG   Coal Seam Gas

EC   Electrocoagulation

EDL   Electric Double Layer

HERO   High Efficiency Reverse Osmosis

HRT   Hydraulic Retention Times

ICP-OES   Inductively Coupled Plasma Optical Emission Spectroscopy

NOM   Natural Organic Matter

PRT   Polarity Reversal Times

RO   Reverse Osmosis

SAR   Sodium Adsorption Ratio

SEM   Scanning Electron Microscopy

TDS   Total Dissolved Solids

TOC   Total Organic Carbon

TSS   Total Suspended Solids

Please note, abbreviations for all equations are provided in the first instance of their use for the readers' ease of understanding.

List of Publications

1. S.N. Ashraf, J. Rajapakse, L.A. Dawes, G.J. Millar, Electrocoagulation for the purification of highly concentrated brine produced from reverse osmosis desalination of coal seam gas associated water, Journal of Water Process Engineering, 28 (2019) 300-310.

2. S.N. Ashraf, J. Rajapakse, L.A. Dawes, G.J. Millar, Coagulants for removal of turbidity and dissolved species from coal seam gas associated water, Journal of Water Process Engineering, 26 (2018) 187-199.

3. S.N. Ashraf, J. Rajapakse, G. Millar, L. Dawes, Performance Analysis of Chemical and Natural Coagulants for Turbidity Removal of River Water in Coastal Areas of Bangladesh, in: International Multidisciplinary Conference on Sustainable Development (IMCSD) 2016, 2016, pp. 172.

Statement of Original Authorship

The work contained in this thesis has not been previously submitted to meet requirements for an award at this or any other higher education institution. To the best of my knowledge and belief, the thesis contains no material previously published or written by another person except where due reference is made.

Signature: _QUT Verified Signature_

Date: _07/03/2019_

Acknowledgements

My foremost gratitude goes towards my principal supervisor Dr Jay Rajapakse for his constant support and technical contribution to overcoming the hurdles and challenges throughout my PhD journey. My special thanks to my associate supervisor Professor Les Dawes for supporting me whenever I was in need.

I gratefully acknowledge my associate supervisor Prof Graeme Millar for his financial, technical, and analytical support for the laboratory experiments, patient guidance, and useful critiques of this research work. This PhD journey was impossible to come to the completion without your immense support. Thank you, Sir.

I would like to acknowledge all the technical staff who provided me instrumental training and inductions. I am thankful for the assistance given by Dr Natalia Danilova and Dr Chris East for SEM, Dr Sanjleena Singh for Optical Microscopy, Mr John Outram for ICP-OES and Mr Daniel Wellner for Electrocoagulation. I am grateful to Mr Kenneth Nuttall, Mr Mitchell de Bruyn and Mr Dominic Alexander for their continuous support throughout my lab experiments. I thank the Central Analytical Research Facility (CARF) in the Institute for Future Environments at QUT for access to their facilities.

The dream of a PhD wouldn't have been accomplished without the financial support provided by QUT (QUTPRA and QUT tuition fees waiver). My heartfelt thanks to my family and friends in Australia and Bangladesh, whose indispensable moral supports certainly led me towards the completion of my PhD study.

Chapter 1: Introduction

1.1   BACKGROUND

Clean water is one of the vital needs of living species [2]. According to the World Economic Forum, the water crisis imposes one of the greatest risks to the global society [3]. In 2015, 663 million people globally, relied on unimproved water sources, with an additional 159 million individuals depending on surface water [4]. The World Health Organisation [4] estimated that half of the world's population will be living in water-stressed areas by 2025. Along with numerous man-made hazards, the development of the coal seam gas (CSG) industry affects local ecosystems. This occurs through the generation of large volumes of produced water that worsens the already stressed aquifers by lowering the water levels in surface bores used for water supply, irrigation and stock watering [5]. Nevertheless, appropriate treatment of CSG water can be made suitable for aquifer injection for future potable purposes, water suitable for irrigation or for release into local watercourses, particularly where water is in short supply [1].

Although seawater is 97% of the water on the planet, this water is not favoured for drinking or for irrigation due to its high salt content [6]. Therefore, to meet the growing demand for fresh water, desalination has drawn the attention of researchers. Desalination is a process or a combination of processes that reduce salt, mineral contents and other impurities from saline water so that it can be used for drinking or alternative uses [7]. Globally, 60% of desalination capacity treats seawater, while the remainder treats brackish and saline feed water from groundwater or industrial

wastewater. It is predicted that 14% of the world's demand for water will depend on desalination by 2025 [8]. Mining industries withdraw a significant amount of brackish water, which can be a potential source of water for beneficial alternative uses [9]. Amongst the many technologies available, reverse osmosis (RO) is the preferred method for desalination [10]. In fact, it is also one of the core units of the CSG water treatment process in Australia and places in the USA [11].

CSG is a natural gas trapped in coal seams by water and ground pressure [12]. To release gas from coal seams, withdrawal of water is required for depressurisation [13-16]. The production volume of CSG water varies significantly with geological and hydrogeological profiles of the seams [13, 17]. In spite of that, it has been estimated that in the future on average 110 giga-litres (GL) of CSG water will be produced annually in Queensland, Australia [18]. Unfortunately, this large volume of water is not suitable for release into the environment because of its high salt content [15, 16, 19]. As a result, the treatment of CSG water using RO technology is being considered with high importance, as RO treated water is suitable for alternative uses such as irrigation or safe disposal into the environment [14, 15].

The selection of the most appropriate method for feedwater pre-treatment is critical as it can represent up to 20% of the overall cost for desalination [20]. Pre-treatment od feed water prior to RO process to remove common dissolved ions found in CSG water are sodium (Na), potassium (K), calcium (Ca), magnesium (Mg), Strontium (Sr), Barium (Ba), silicon (Si), and Boron (B) can potentially reduce the fouling of RO membranes [21]. In water and wastewater treatment coagulation has been used for removal of particulate contaminants from water, including inorganic and

natural organic materials through charge neutralisation and bridging or sweeping coagulation. In principle, coagulation cannot removal simple dissolve salts or ions, such as NaCl, and KCl [22, 23]. Alkaline earth ions, such as Ca, Mg, Sr, and Ba barely removed by the addition of coagulants rather removed by chemical precipitation [24]. Precipitation of metal hydroxide can effectively remove dissolved alkaline earth metals by sweep flocculation [25]. Metal salts can remove silicates from the solution as metal silicate precipitates. Metal salts potentially reduce the solubility of silica and influence the polymerisation rate which forms precipitates [26]. Boron is found in water as boric acid, borates or anionic polyborates [27], which can be reduced by chemical coagulation as precipitates [28]. Electrocoagulation has been proven in removing boron efficiently compared to chemical coagulation. During electrocoagulation boric acid convert to negatively charged borates and adsorbed on positively charged metal hydroxides, thus is removed from the solution. This study focused on improvements in current CSG water treatment practices by treating CSG water before and after the RO process.

1.2   CONTEXT

In Australia, RO is the most popular and effective treatment method used for CSG water [11]. This process forces the water to pass through increasingly finer mesh membranes [13, 29]. RO membranes are highly susceptible to fouling and scaling. This is a process of accumulation of solutions or particles on membrane surface or in membrane pores [11, 30] and this system requires extensive pre-treatment facilities [1]. As pre-treatment methods, chemical coagulation-flocculation and dissolved air floatation (DAF) can remove particulate contaminants, however, the simultaneous removal of suspended solids (turbidity) and dissolved ions from CSG water is still not available [19].

Recovery of water in a RO unit usually depends on feed water quality, temperature, feed pressure and membrane type [31]. However, the application of high-efficiency reverse osmosis (HERO) has become very popular to increase the recovery rate. HERO includes three steps before RO i.e., removing hardness, decarbonation and pH elevation, which enables this technology to recover a substantially higher amount of water [32]. Consequently, the rejected concentrates (HERO brines) contain more salts and chemicals compared to RO brines. HERO brine can be managed using several methods, such as surface disposal, reinjection, storage dam, membrane treatment technologies, thermal technologies and crystallisation [5]. In general, the selection of methods depends on local regulations, distances of plants from disposal points and, most importantly, on disposal costs. Notably, HERO brine from CSG water contains a high concentration of silica (up to 1500 mg/L). Brine with high silica content is problematic to transport because it precipitates in piping systems, which affects the brine flow and induces corrosion. Silica also affects the downstream brine treatment unit [33]. In this regard, treatment of HERO brine to reduce silica content is one of the major concerns for CSG operators.

Therefore, this study focuses on the pre-treatment of CSG water and treatment of HERO brine as important additions to knowledge for current practices.

1.3 AIM AND OBJECTIVES

The aim of this study is to develop a process for pre-treating CSG water to facilitate the efficient operation of RO desalination units and to promote the ability to remove salts from brine solutions. To achieve the aim, the following objectives were developed:

1. To evaluate the performance of various chemical coagulants to pre-treat CSG water in the presence of turbidity.

2. To investigate the influence of turbidity on the performance of electrocoagulation systems equipped with either (a) aluminium, (b) iron or (c) combined aluminium/iron electrodes.

3. To assess the applicability of electrocoagulation to treat HERO brine from CSG water.

1.4   RESEARCH SIGNIFICANCE

In Queensland, Australia, current practices for the pre-treatment of CSG water are a combination of processes, such as holding pond, microfiltration, ultrafiltration, disc filtration, ion-exchange and ballast flocculation [5]. New approaches include chemical coagulation (CC) [22, 23] and electrocoagulation (EC) [34, 35]. However, the effect of turbidity on the performance of CC and EC has been overlooked by researchers. On the other hand, treatment of HERO brine from CSG industries has been studied for EC equipped with iron electrodes only. This research aims to fill these knowledge gaps.

This study also contributes to the knowledge of the influence of hydraulic retention time (HRT) and polarity reversal time (PRT) on EC performance while treating either CSG water or HERO brine. In this study, HERO brine is treated by EC equipped with either aluminium, iron or aluminium-iron combined electrodes to evaluate the applicability of EC in this sector.

1.5 SCOPE OF THIS RESEARCH

This research focuses on the efficiency of chemical coagulation (CC) and electrocoagulation (EC) in removing dissolved species (alkaline earth ions, boron, and silica) from CSG water in the presence of high turbidity. Feed water of reverse osmosis (RO) unit must be free from turbidity to protect the membranes from fouling. Among several dissolved ions, the emphasis of the study is on the removal of common scalant species in CSG water treatment, such as calcium, magnesium, strontium, barium, boron, and silica. CC experiments are carried out using three commercially available coagulants used for water treatment, such as alum, aluminium chlorohydrate (ACH) and ferric chloride. EC experiments for the treatment of CSG water and HERO brine included a combination of two most commonly used electrodes (aluminium and iron). This study focuses on the effect of operating parameters of EC with particular emphasis on hydraulic retention time (HRT) and polarity reversal time (PRT).

1.6 CHAPTER OVERVIEWS

In order to address the challenges allied with the treatment processes of CSG water and HERO brine, the research has been divided into three phases.

The first phase starts with a literature review. Among the available resources, relevant and useful literature are enlisted in EndNote software and categorised according to their research outcomes. From the literature review, the research field was narrowed down to address the gaps in knowledge identified. Details of the literature review are presented in Chapter 2. The next phase involved research planning and laboratory experiments. Research gaps identified in literature formed the basis of the research questions (included in chapter 4-8). The final phase involves a comparison of collected data with published literature relevant to each parameter. These observations

and literature review analysis present findings that add value to existing knowledge. Figure 1-1 shows the research process employed in this thesis to address the overcoming research aim of developing a process for pre-treating CSG water to facilitate the more efficient operation of RO desalination units and to promote the ability to remove salts from brine solutions.

Chapter 2

A review of the literature on CSG, the produced water, RO, HERO brine, water quality parameters, and CC and EC have been provided in this chapter.

Chapter 3

This chapter explains the laboratory experimental methods. The theory behind two treatment methods used in this study, electrocoagulation and chemical coagulation is described in detail. This chapter also includes the details of chemicals used to simulate the water samples and the analytical methods used to analyse the samples.

Chapter 4

Chemical coagulation of CSG water is discussed in this chapter. It contains a brief literature review on water quality, available coagulants, and applicability of coagulants on reducing turbidity and dissolved ions. The performance of aluminium and iron coagulants is presented here. The performance analysis is based on required coagulants' doses, suspended solids removal and dissolved species reduction efficiency and flocs characteristics.

Chapter 5

This chapter focuses on the effect of turbidity, HRT, and PRT on the performance of electrocoagulation (EC) while treating turbid CSG water. The up-flow

EC cell is equipped with 13 aluminium electrodes. The performance analysis has been done depending on dissolved species removal efficiency, floc characteristics, power requirement, electrode dissolution and residual ion concentrations from electrodes.

Chapter 6

This chapter presents findings on the influence of turbidity on the performance of the same EC set up as presented in chapter 5 where iron electrodes are used instead of aluminium electrodes. Three HRT (20, 30 and 60 s) and three PRT (1, 3 and 5 min) have been studied.

Chapter 7

Based on the findings from Chapter 5 and Chapter 6, aluminium electrodes reduce ion concentration effectively than iron electrodes. On the other hand, aluminium electrodes pollute the treated water with residual aluminium, while iron electrodes do not keep any trace of residual iron ion. To combine the benefit of both electrodes, similar EC experiments as in Chapter 5 and Chapter 6, were carried out using aluminium and iron combined electrodes. The effect of PRT and HRT on the performance of EC to treat CSG water using aluminium-iron combined electrodes has been described in Chapter 7.

Chapter 8

A comparative study is carried out and discussed regarding the results obtained from laboratory experiments for different electrodes, HRT and PRT combinations. In this chapter, EC equipped with either aluminium, iron or combined electrodes are experimented to evaluate for applicability to treat HERO brine. Chapter 8 presents a

literature review on HERO, HERO brine profile, and available brine treatment technologies.

Chapter 9

A thorough conclusion covering the completed research work is presented in Chapter 9. It combines all the results and outcomes obtained from the research work in Chapters 4, 5, 6, 7 and 8. The comparative study of the performance of EC based on electrodes, HRT, and PRT is also presented here. Finally, recommendations for future research directions are listed in this chapter.
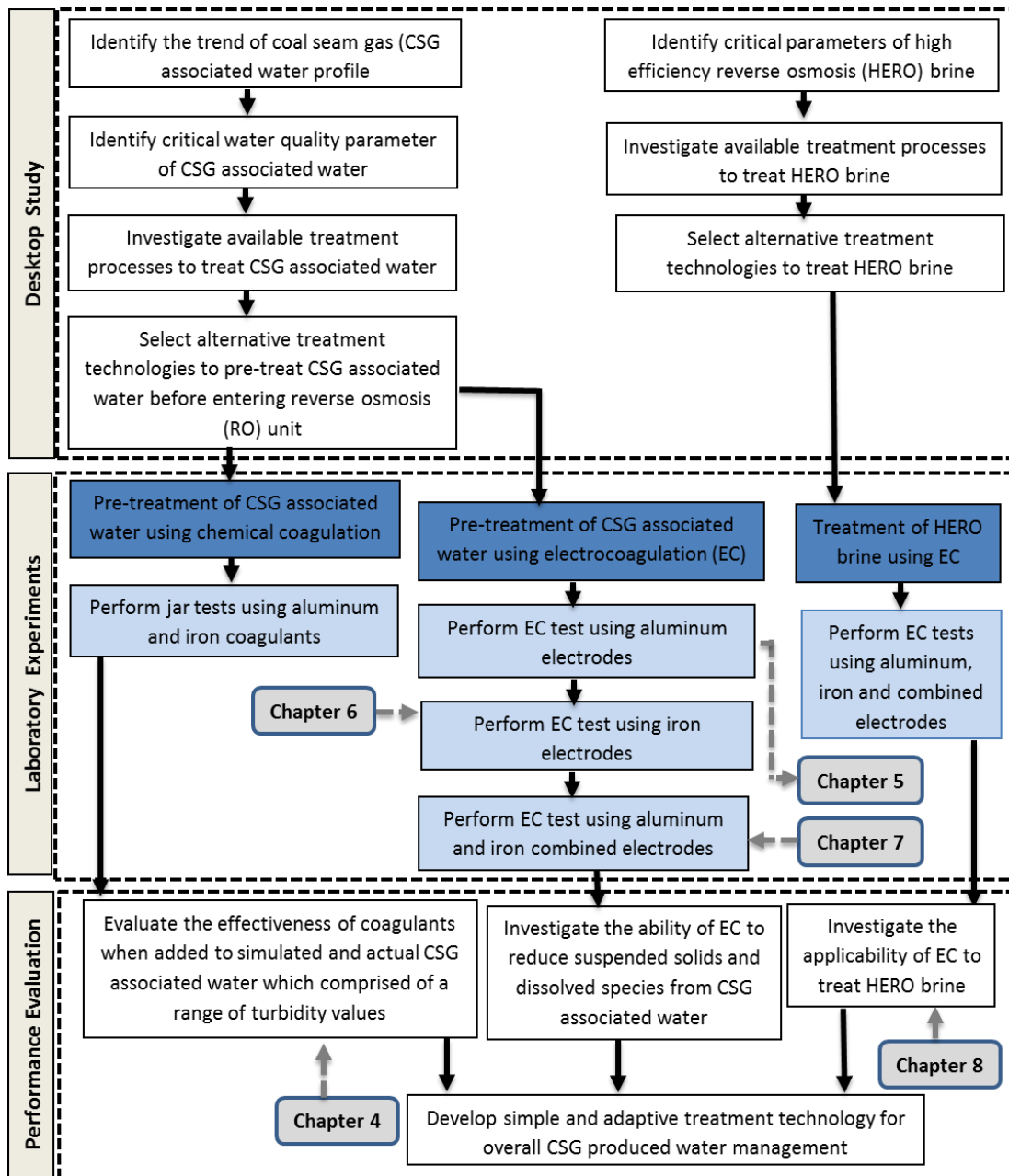
Figure 1-1: Schematic diagram showing a detailed representation of research undertaken highlighting research design and chapters.

Chapter 2: Literature Review

2.1 HIGH-TURBIDITY COAL SEAM GAS (CSG) WATER

For the past few decades, coal seam gas (CSG) or coal bed methane (CBM) has been a rapidly growing industry in many regions [21, 36]. United States (US), Canada, Australia, India, and China are the leading countries involved in CSG exploration and production [37]. The US is dominating the market by contributing around 80% of the world's CSG production. The largest CSG project in the US is situated in the Powder River Basin. Nearly one million oil or gas wells are actively operated in the US [38-40]. China has developed rapidly in the CSG sector. China's active CSG well number reached to 2500 in the year 2008 while it was only 250 in 2003 [41]. It is estimated that in China the storage of CSG is nearly 36.81 trillion cubic meters less than 2000m in depth [42]. Australia has a massive deposit of CSG. In the Australian context, 90% of coal seam gas production occur in Queensland with particular commercial focus is on the Surat and Bowen Basins [21, 43]. In Queensland, Santos GLNG, Queensland Gas Corporation (QGC), Arrow Energy and Australia Pacific LNG are four major CSG production companies [44]. Worldwide reserves of CSG are estimated to be *ca.* 1.4×10^{14} m^3 [37]. CSG is a combination of methane and carbon dioxide gases [37]. The emission of carbon dioxide from the CSG industry contributes to greenhouse gas, is a considerable problem for the world environment [45].

As shown in Figure 2-1, the CSG is trapped in coal cleats due to water pressure, extraction of the gas is invariably accompanied with the production of water especially in the initial years of the well-life [46]. Along with gas, CSG water is also extracted

as wells are depressurized in order to allow the gas to flow [1, 19]. It may require to pump the CSG water for more than 6 months before starting to withdraw of gas [47].
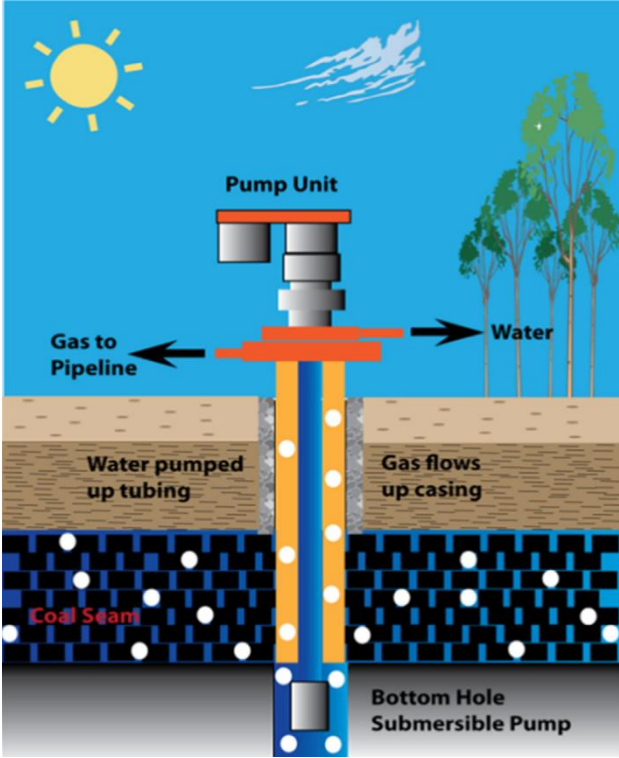
Figure 2-1: Illustration of the coal seam gas (CSG) and associated water extraction process (Adapted from [1]).

There are some factors (geological and hydrological) that control the production volume of CSG water [13, 17]. Volumes of produced water in Queensland are currently 44 GL per year and may increase to 110 GL per year in the future [48, 49]. Most of this associated water requires pre-treatment before beneficial reuse as dissolved salt concentrations in the water are typically too high to comply with environmental regulations [1, 5]. The quality of CSG water depends upon the depth of the coal bed and the formation profiles of coal and basin as well [50]. CSG water composition varies greatly depending upon several factors [21]. Dahm et al. [51]

created a geochemical database for CSG water produced in the Rocky Mountain region, USA which revealed that the chemical composition varied with coal type, freshwater recharge availability, and basin geology. Typically, CSG water is potentially contaminated salty water [14]. Dahm et al. [52] reported the major cations present as sodium, potassium, calcium, magnesium, strontium, barium, iron and aluminium. Whereas, anions of interest were chloride, bicarbonate, carbonate, fluoride, and bromide. Irrespective of location, the main constituents of CSG water are chloride, sodium, and bicarbonate [21, 49, 52-54]. In Australia, the salt concentrations of CSG water ranging from *ca.* 200 to 10,000 mg/L [55]. Outside of Australia, the salinity of the associated water from CSG operations can be significantly greater [51, 56, 57]. On average sodium, bicarbonate and chloride species are dominant in CSG water [58]. Minor ions also present in the water include calcium, magnesium, sulphate, aluminium, iron, manganese, fluoride, barium and strontium [19, 55, 59]. Rebello et al. [21] tested the CSG water samples collected from three different fields (named as A, B, and C) of Surat Basin and found a variety of water composition (Table 2-1).

Another important CSG water quality parameter to consider is the turbidity level. Turbidity is the cloudiness of water. Technically, it is the optical determination of water transparency measured as the amount of light scattered by particles in solution [60]. Turbidity is caused mainly due to suspended solids (silt, clay, and inorganic particles) but can include organic matter (algae, plankton, decaying materials etc.), dyes, such as coloured dissolved organic matter and fluorescent dissolved organic matter [61, 62].

Table 2-1: Range and mean values (in brackets) for water quality parameters – surat basin CSG water (in terms of mg/L otherwise labeled) [21].

Parameter	A field (54 wells)	B field (73 wells)	C field (23 wells)
EC (mS/cm)	3850 – 13300 (7084)	3630 – 9410 (6743)	5150 – 17200 (9765)
SAR (ratio)	69.6 – 177 (120.0)	86.4 – 163 (121.2)	62 – 156 (112.5)
pH	7.92 – 8.89 (8.47)	7.94 – 8.76 (8.43)	7.83 – 8.63 (8.30)
TSS	5–7560 (435)	6–1520 (272)	7–265 (72)
TDS	2940 – 7600 (4444)	2190 – 5790 (4046)	3050 – 10200 (5655)
Hardness (mg/l as CaCO3)	276 – 1620 (38)	12 – 80 (30)	12 – 482 (102)
Bicarbonate alkalinity mg/l as CaCO3	5 – 2030 (1039)	470 – 1540 (960)	108 – 1350 (714)
Bromide	1.93 – 12.7 (6.0)	2.82 – 11.7 (5.6)	2.75 – 16.6 (8.9)
Chloride	471 – 4390 (1595)	875 – 2930 (1579)	823 – 5910 (2938)
Sulfate	1 – 18 (4.4)	1 – 48 (8.0)	1 – 5 (3.3)
Calcium	2 – 55 (9.0)	3 – 19 (7.0)	3 – 137 (26.2)
Magnesium	1 – 16 (3.8)	1 – 8 (3.1)	1 – 34 (8.8)
Sodium	909 – 2700 (1487)	786 – 2010 (1452)	1130 – 3700 (2098)
Potassium	4 – 14 (6.9)	3 – 10 (6.1)	5 – 20 (10.6)
Aluminium	0.02 – 40.9 (2.9)	0.01 – 17.8 (2.1)	0.01 – 2.08 (0.65)
Manganese	0.002 – 0.54 (0.06)	0 – 3.59 (0.11)	0 – 0.13 (0.04)
Strontium	0.65 – 9.03 (2.30)	0.7 – 4.5 (2.12)	0.99 – 20.2 (5.52)
Boron	0.22 – 0.54 (0.34)	0.24 – 0.68 (0.41)	0.17 – 0.61 (0.31)
Iron	0.16 – 45.1 (5.12)	0.09 – 35.1 (8.73)	0.3 – 6.16 (2.44)
Silica	13.1 – 19.6 (16.9)	13.9 – 23.1 (17.7)	13.8 – 19.2 (16.5)
Fluoride	0.8 – 3.2 (2.2)	1 – 3.3 (2.0)	0.4 – 2.7 (1.6)
Barium	0.53 – 4.39 (1.37)	0.38 – 2.32 (1.18)	0.62 – 9.38 (2.73)
Total Organic Carbon	1 – 71 (19)	1 – 138 (25)	4 – 138 (27)

Because of this close relationship between turbidity and suspended solids, turbidity can be used as a surrogate for rapid suspended solids evaluation [63-65].

Turbidity is measured by a turbidity meter and generally, turbidity is reported in Nephelometric Turbidity Unit (NTU). Turbidity is an important parameter to determine water quality. Clearwater is considered healthy water because turbidity can provide food and shelter for bacteria, viruses, and parasites [62]. Moreover, turbidity can interfere disinfection process by protecting microorganisms from the disinfectants [61].

Rebello et al. [21] analysed the water composition from 150 CSG wells located in the Surat Basin in Queensland. These authors found an average total suspended solids (TSS) value of 300 mg/L with the highest value of 7560 mg/L. Similarly, Benko and Drewes [66] examined a variety of produced water samples in the USA and reported that TSS levels could be as high as 1000 mg/L. Ali et al. [67] studied CSG water from seven different coal mine sites in south Sydney and turbidity level was found up to 300 NTU. Qian et al. [68] evaluated a pilot plant system for treating CSG water using a central reverse osmosis unit. Notably, the feed water was characterized as having a high turbidity value of 409 NTU. The main portion of suspended solids is comprised of sand, silt, clay and other solids produced during bore operation [69]. The situation in Queensland is exacerbated by the fact that regular flooding events occur which encourage surface run-off to receive waterways such as CSG water storage dams [70].

There are strict regulations regarding the beneficial reuse of CSG water as not only may the salinity be too high but also the sodium absorption ratio (SAR) may exceed the recommended limits for direct soil irrigation [16]. Vance et al. [71] investigated the impact of irrigation of soils with CSG water and noted that not only

did soil electrical conductivity increase but also plant diversity decreased. Additionally, Burkhardt et al. [72] discovered that irrigation with CSG water could lead to a reduction in the oil content of crops and high sodium content in the leaves of mints. Therefore, the general necessity of treating CSG water prior to crop irrigation is important.

Desalination is the core treatment technology in relation to treating CSG water for beneficial reuse. Both ion exchange (IX) [73] and RO [74, 75] are presently employed commercially to reclaim purified water from CSG water. With either technology, there is a requirement to protect the membrane or resins from fouling [76]. The selection of the most appropriate method for feedwater pre-treatment is critical as it can represent up to 20% of the overall cost for desalination [77]. Consequently, one must consider the impact of turbid water upon the latter desalination methods. A range of pre-treatment processes are available for reducing the turbidity of water samples, *e.g.* chemical coagulation, electrocoagulation, ballasted flocculation, dissolved air flotation, microfiltration, and ultrafiltration [1, 34, 78-81]. Major CSG companies in Queensland utilise a combination of pre-treatment methods commonly, holding ponds, coarse filtration, fine filtration and ion exchange units [Figure 2-2]. Le [82] removed suspended solids from CSG water sourced in New South Wales, Australia using a combination of a treatment pond, disc filtration, and microfiltration. Alternatively, Carter [83] reported that the QGC CSG water treatment facility located near Chinchilla in Queensland, Australia included an ultrafiltration stage.

Despite the demonstrated success of filtration technologies to control turbidity in CSG water, there is also a need to remove dissolved species such as alkaline earth

ions and silicates. These species cause problems such as scale formation and membrane fouling which ultimately result in a decrease in water treatment plant performance [84, 85]. Ion exchange softening can be employed to reduce the alkaline earth ion content of the CSG water [86]; albeit, this method requires the onsite storage and handling of substantial amounts of potentially hazardous acid and alkali. Coagulation is well proven for a reduction in the suspended solid content of wastewater [87], but the removal of dissolved ions from CSG water is more challenging [22, 23].
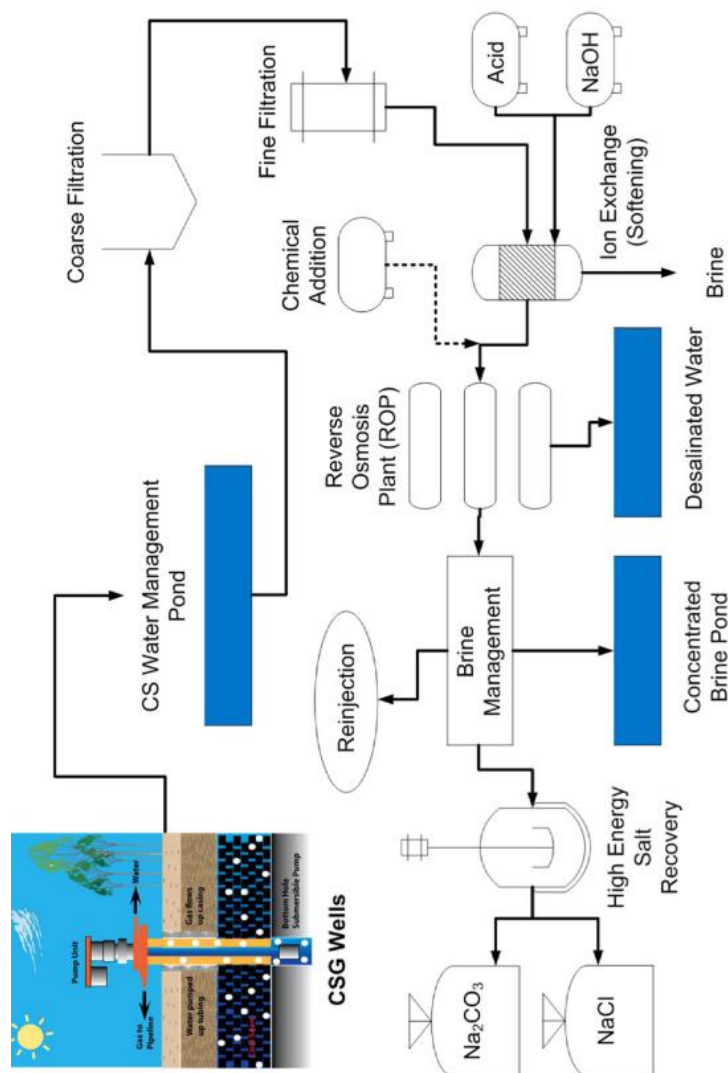
Figure 2-2: Process flow for coal seam water treatment using reverse osmosis (Adapted from [1])

2.2 REVERSE OSMOSIS (RO) FOR CSG WATER TREATMENT

Osmosis is a naturally occurring process in which a liquid pass through a membrane spontaneously. In this process, a semipermeable membrane allows the water molecules to pass through but restricts the salt molecules. The liquid flows naturally to the high salt concentration side to even out the concentration levels [88]. On the other hand, when the direction of liquid flow is opposite to this is called reverse osmosis (RO). By pressurising the high salt concentration side RO process is achieved. As the semipermeable membrane does not allow salt molecules to pass through, clean water accumulates on the other side [89]. In reverse osmosis, high-pressure pumps are used to provide the driving force needed to overcome the osmotic pressure of the feed water. With the increase in recovered water, the salt concentration increases in the feed water side i.e., the osmotic pressure also increases. Therefore, it requires more driving force to continue to recover clean water.

2.2.1 The necessity of pre-treatment for RO

In the RO process, after a certain amount of water recovery, the feed water reaches the solubility limit of the salt content [90]. At this point, RO stops recovering further recovery. This is how the recovery of clean water from feed water using RO technology is limited due to thermodynamic restrictions [91]. Besides, energy required to gain driving force, conventional RO unit faces the challenge of membrane fouling often. Membrane fouling is a process where a solution or particles deposited on a membrane surface or clog the membrane pores. This process degrades the membrane performance and affects the recovered water quality. Severe fouling may require intense chemical cleaning and in the worse case, it requires to change the membrane.

This increases the cost of water treatment [92]. Therefore, pre-treatment can protect the membranes by reducing the dissolved species content, thereby, can substantially save the operation and maintenance costs.

2.2.2 High-efficiency reverse osmosis (HERO) brine

To increase the water recovery without fouling the membrane, RO system was incorporated with a few pre-treatment steps and was named as high-efficiency reverse osmosis (HERO). HERO is operated in three steps mainly [93]. Initially, the ration of hardness and alkalinity is adjusted by adding alkali. Then, the concentration of calcium hardness and alkalinity is reduced to a minimum level to minimize the hardness leakage from the pre-treatment ahead of the RO. Weak acid cation exchange resins or lime softening are preferred as the reduction medium here, depending on feed water quality [94]. Then feed water is decarbonated at acidic pH to remove carbon dioxide in a degasification process. Because this carbon dioxide is converted to alkalinity at a high pH level [95, 96]. Finally, the pH level of the feed water is elevated by sodium hydroxide before passing through the RO unit. Figure 2-3 represents the steps of the HERO process.

Elevation in pH level highly ionized silica, thus, increases the solubility. It has been reported that at a pH level above 10 the solubility of silica increases exponentially. Therefore, in the HERO process, the preferable pH is 10.5 or above. The solubility of silica may increase up to 1500 mg/L in the rejected water [97]. This is how the recovery rate from feed water can be achieved by more than 90% [98]. Along with high water recovery, the HERO process has other benefits like high salt

rejection, high flux, and reduced fouling. Therefore, HERO reduces operating costs [99].
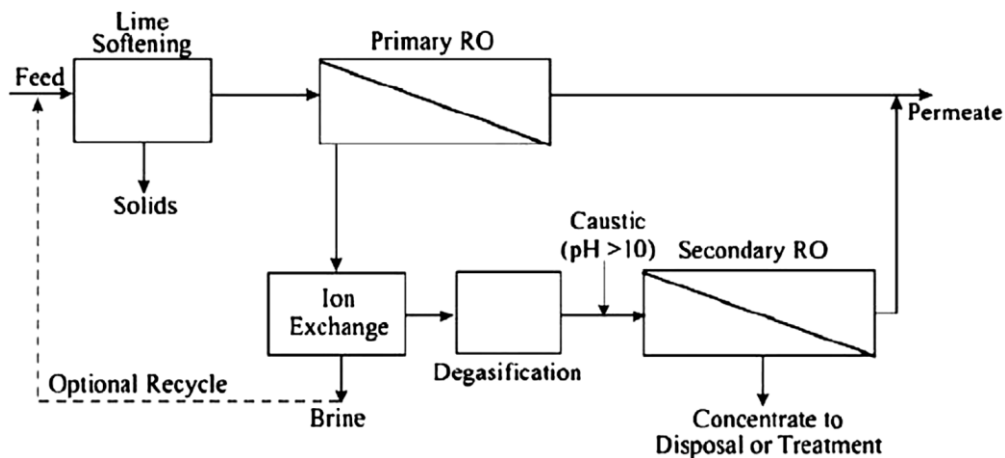
Figure 2-3: Diagram of high-efficiency reverse osmosis (HERO) [100].

The rejected water from HERO is highly concentrated. It contains alkaline metal cations, mono, and divalent anions and a high concentration of dissolved silica [33]. The composition of HERO brine from CSG water was not available to the present study, therefore, a water treatment software namely, AqMB was used to simulate the treatment of CSG water by HERO. The composition of brine produced from the simulated treatment process was used to prepare synthetic HERO brine for the study.

2.3 COAGULATION TECHNOLOGIES

2.3.1 Chemical coagulation (CC)

Coagulation-flocculation is a widely used scientific method for removing turbidity. Particles in natural water are either hydrophobic (water repelling) or hydrophilic (water attracting) [101]. The principal electrical property of suspended particles is the surface charge. This charge influences the particle to achieve stability in the suspension. Therefore, particles do not settle rather float in the suspension.

Generally, particles in suspension aggregate and settle if adequate time is allowed. However, this process is time-consuming which is not economically feasible.
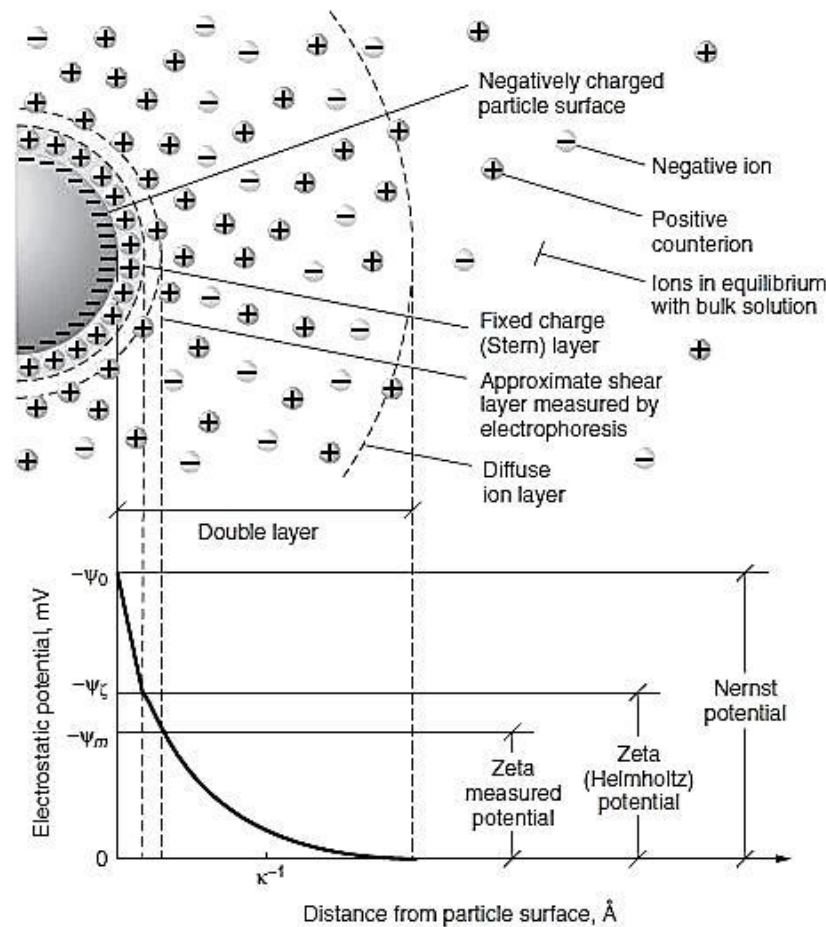
Figure 2-4: Structure of the electrical double layer in solution [90].

In natural waters, pollutant particulates are negatively charged and adsorb positive counter-ions on and around the particle's surface to create electro-neutrality, thus forms Helmholtz layer [Figure 2-4]. This layer appears as a negative electric field which attracts an excess of positive ions and consequently, attracts other negative ions. The excess cations outspread into the solution until electro-neutrality is achieved. After the Helmholtz layer, negative and positive ions continue to accumulate until the charge

becomes zero. The layer of these ions is called the diffuse layer [102]. The Helmholtz layer and diffuse layer together are named as the electric double layer (EDL).

There is no available method to directly measure the electric potential surrounding a particle or to estimate the amount of coagulant addition to destabilize the particles. However, zeta potential is an indirect method to measure the surface potential of the particles in solution. This is the electrostatic potential of EDL surrounding a particle [103].

The stability of particles in solution depends on a balance between the physical forces on the particle surface, the repulsive force, and the attractive (Van Der Waals) force. The addition of coagulants (simple salts) increases the ionic strength of the solution and contributes opposite ions to the particles to reduce the repulsive force which accelerates flocculation [90]. Higher ionic strength causes the compression in EDL, thus, reduces the zeta potential of the particles. Therefore, particles aggregate due to Brownian motion.

At neutral pH range, between pH 6 and 8, the pollutant particles in natural waters are negatively charged. Those particles can be destabilized by positively charged ions. Therefore, coagulants commonly contain positive ions. Hydrolyzed and pre-hydrolyzed metal salts work efficiently as coagulants. Cationic organic polymers are used as preliminary coagulants to clump the particles together and generally, they are used in combination with inorganic coagulants [90]. Generally, the optimum dose of selected coagulant or combination of coagulants is achieved when the particle

surrounding is covered less than 50%. When the appropriate number of ions is adsorbed, the charge of the particle becomes zero. Consequently, the charged neutralized particles flocculate. If an excessive amount of polymer is added, the particles become positively charged and become stable again [104].

2.3.2 Electrocoagulation (EC)

Electrocoagulation (EC) is a technique involving the electrolytic addition of coagulating metal ions directly from sacrificial electrodes. These ions work in a similar manner to the chemical coagulant. They coagulate with turbidity agents in the water and allow the easier removal of the pollutants [105].
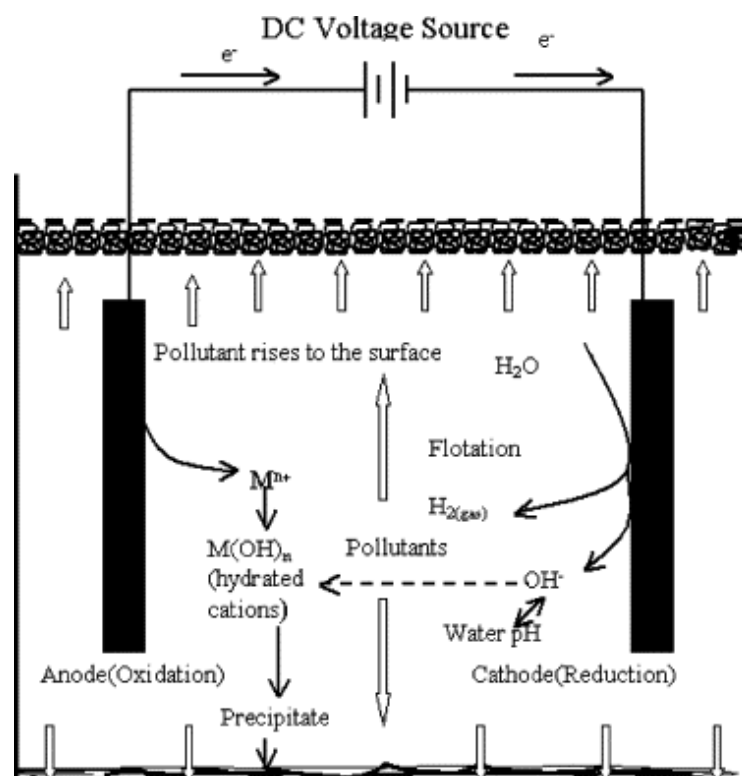
Figure 2-5: Illustration of the mechanisms in electrocoagulation (EC) cell [106].

EC is accepted as an alternative, and economically feasible process to treat water effectively removes suspended solids (turbidity), alkaline earth ions, heavy metals, emulsifiers and other dissolved species in solutions, such as boron, silicates etc. [33, 34]. This technique possesses many advantages over the available conventional processes in terms of its simple equipment, such as easy operation, instantaneous reaction, reduction or absence in chemicals requirement, rapid sedimentation of electro-generated flocs, and less sludge production [25, 26].

EC is a progressing technology that has been effectively worked in the industrial wastewater treatment containing different types of pollutants [107-109]. It is a simple and efficient method. In this method, the coagulating agent is produced in-situ by dissolving ions from metal electrodes [Figure 2-5]. Commonly, aluminium and/or iron electrode is used in the EC process [110, 111]. Coagulants come into the solution from the anodes during the electrocoagulation process. Iron anodes produce ferrous or ferric ions according to Equation 2-2. Hydroxides of ferrous and ferric ions are produced as Equation 2-3 and 2-4, where n is a pH-dependent variable [112]. Equation 2-1 shows the hydrogen production reaction. This is the main reduction reaction during the EC process [113].

Reaction on Cathode
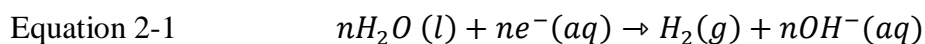
Equation 2-1 $$nH_2O \ (l) + ne^-(aq) \rightarrow H_2(g) + nOH^-(aq)$$

Reaction on Anode

Equation 2-2 $$M \ (s) \ \rightarrow M^{n+}(aq) + ne^-(aq)$$

At alkaline conditions

Equation 2-3 $$M^{n+}(aq) + nOH^-(aq) \rightarrow M(OH)_n \downarrow (s)$$

At acidic conditions

Equation 2-4 $$M^{n+}(aq) + nH_2O \ (l) \rightarrow M(OH)_n \downarrow (s) + nH^+(aq)$$

Polymer formation

Equation 2-5 $$mM(OH)_n \rightarrow M_m(OH)_{nm}$$
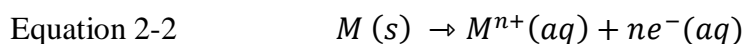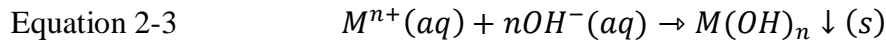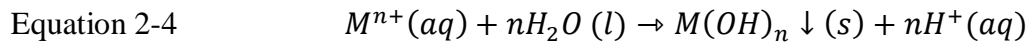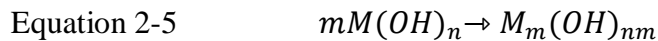
Hydrogen production can cause particles flotation [113]. This electro-flotation technique can be applied for effective precipitated, coagulated, or flocculated material separation [108]. This technique shows many advantages over conventional practices with respect to its simplicity. The operation process is easy and quick. It reduces the amount of chemical dosing, and sometimes it doesn't require chemicals. Most importantly, electro-coagulation produces the one-fifth amount of sludge compared to the chemical coagulation [114, 115]. Butler et al. [116] found EC as an economically beneficial method for wastewater treatment over the chemical coagulation processes.

A number of studies have been found on EC to treat drinking water and industrial wastewater [117]. EC has been tested on several water types, such as synthetic natural water [118], laundry wastewaters [119] pasta and cookie processing wastewaters [120], dairy wastewaters [121], alcohol distillery wastewaters [122] and distillery effluents [123]. EC is very popular in treating wastewater from dairy industry [121, 124, 125]. Increase in removal efficiency of chemical oxygen demand (COD),

biological oxygen demand (BOD), and total suspended solids (TSS) from dairy wastewater is observed using the EC process [126].

Aluminium (Al) and iron (Fe) are the two most popular metals used in EC [127]. Turbidity removal rate by Aluminum (Al) electrodes appears to be higher than that by Iron (Fe) and Steel (St) electrodes [105]. Al electrodes required lower current for minimum time to obtain the highest amount of turbidity removal than Fe and St electrodes. Adapureddy and Goel [128] found that the efficiency of EC to reduce turbidity depends on several factors, such as applied voltages, solution pH, and electrode spacing. This study observed that the effect of turbidity level has a very significant effect on EC performance. According to Perez-Sicairos et al. [129], reported some other factors, such as the arrangement of electroplates, current density, feed water flow rate and the active surface of electrodes, that influence the turbidity removal efficiency by continuous EC reactor.

2.3.2.1 Polarity Reversal Time (PRT)

In terms of EC operation, there are some key factors which need to be addressed because those have received insufficient attention in the literature (albeit, for practical use, these parameters are highly pertinent). It is widely reported that during EC operation the electrodes can become passivated with an oxide film [130]. Hence, strategies to clean the electrode surface have been introduced such as polarity reversal; which involves switching the polarity of the electrode plates from "positive" to "negative" at prescribed time intervals. Gobbi et al. [131] employed a polarity reversal time (PRT) of 10 s when treating oily water using an EC unit equipped with Al electrodes. However, these authors did not investigate the impact of decreasing or increasing the PRT upon EC performance. As indicated by Wellner et al. [132] the

polarity reversal time is important with respect to minimization of electrode passivation. In their study, they discovered that a 3 min PRT was optimal when EC was conducted with sodium chloride solutions and used aluminium electrodes. This finding was in harmony with the idea of Fekete et al. [133] that a certain time was required in order for the passivated layer to be removed from the electrode surface. Timmes et al. [134] also intimated that the PRT required to be adjusted in order to maintain the performance of a pilot plant electrocoagulation system employed to pre-treat seawater prior to a reverse osmosis desalination stage. In terms of EC treatment of CSG water, published studies both reported use of a fixed PRT of 30 s [135, 136], and hence there is a need to examine the influence of PRT upon water treatment performance.

2.3.2.2 Hydraulic Retention Time (HRT)

Another key parameter with regards to EC performance is the hydraulic retention time (HRT) in the EC unit. Often the influence of HRT upon EC performance has been evaluated for batch systems [137]; however, continuous EC units are more relevant to practical application as they offer greater throughput of water. Amani et al. [138] studied a continuous EC process for compost leachate remediation. HRT was discovered to be an important parameter in terms of chemical oxygen demand (COD) and total suspended solids (TSS) removal. In the latter study, HRT was tested in the range 30 to 90 min and the optimal value was determined to be 75 min. In contrast, Mores et al. [139] investigated the use of both aluminium and iron electrodes for the EC treatment of swine wastewater. These authors reported that HRT did not have a significant impact upon turbidity removal which was attributed to the dominating influence of current density. Alternatively, Kobya et al. [140] observed substantial diminishment in the ability of an EC unit to remove COD, turbidity and total organic

carbon (TOC) from dye-house wastewater as the hydraulic retention time was reduced. Notably, previous literature relating to EC purification of CSG water has not investigated the impact of HRT upon the effluent water quality, with only 30 s HRT data reported [135, 136]. Therefore, elucidation of the effect of increasing or decreasing HRT for CSG water treatment would be beneficial with regards to EC process optimization.

2.4 RESEARCH GAP IDENTIFIED

From the above literature, it is clear that there is a lack of information on pre-treatment of high-turbidity CSG water. While the application of EC instead of traditional CC demonstrated better-suspended solids, and dissolved species removal from a variety of waters, the effect of turbidity on dissolved species removal by EC has not been studied for CSG water. The implementation of EC for the treatment of HERO brine is absent in the published literature. Consequently, the aim of this study was to evaluate the applicability of chemical coagulation and electrocoagulation to pre-treat CSG water and performance analysis of electrocoagulation to remove some salts from HERO brine.

Chapter 3: Materials and Methods

3.1 MATERIALS

3.1.1 Chemicals used for feed water simulation

Simulated CSG water and HERO brine samples were prepared by adding the required amount of technical grade chemicals to deionised water. The chemicals used in this study, have been listed in Table 3-1. Kaolin clay named Snobrite55® was supplied by Unimin Australia and was added to the simulated CSG water to provide required levels of turbidity.

Table 3-1: Chemicals used to simulate CSG water and HERO brine from CSG water.

Chemical used	Molecular formula
Aluminium chloride	$AlCl_3.6H2O$
Boric acid	H_3BO_3
Barium chloride	$BaCl_2.2H_2O$
Calcium carbonate	$CaCl_2.2H_2O$
Iron (III) chloride	$FeCl_3.6H_2O$
Potassium chloride	KCl
Magnesium chloride	$MgCl_2.6H_2O$
Sodium meta-silicate	$Na_2SiO_3.5H_2O$
Strontium chloride	$SrCl_2.6H_2O$
Sodium chloride	$NaCl$
Sodium bicarbonate	$NaHCO_3$
Sodium sulphate	$Na_2SO_4.10H_2O$

3.1.2 Chemical coagulants

Among the most common commercial chemical coagulants, two aluminium and one iron based coagulants were used in this study. The coagulants' properties are presented in Table 3-2.

Table 3-2: Characteristics of chemical coagulants.

	Aluminium Sulphate (Alum)	Aluminium Chlorohydrate (ACH)	Ferric Chloride
Supplier	Omega Chemicals	Hardman Chemicals	Omega Chemicals
Formula	$Al_2(SO4)_3.14H_2O$	$Al_2(OH)_5Cl$	$FeCl_3.6H_2O$
Specific Gravity (g/ml)	1.35	1.36	1.45
Mass Al/Fe per L of Solution (g/L)	57.59	201.54	209.67
Mass Coagulant per L of Solution (g/L)	634.29	651.54	609.00

3.1.3 Electrocoagulation reactor

An electrocoagulation unit with the specifications shown in Table 3-3 was set up to treat CSG water and HERO brine.

Table 3-3: Electrocoagulation reactor specification.

Electrode	Specification
Electrode material	Aluminium (Al) and/or Iron (Fe)
Electrode Shape/ Size	Rectangular (10 cm x 15 cm x 0.3 cm)
Number of Electrode	13 (Active electrodes 12)
Effective electrode surface area	1800 cm^2
Plate / electrode arrangement	Parallel
Inter-electrode gap	0.3 cm
Power supply	DC
Connection mode	Bipolar
Polarity reversal	Yes
Reactor material	Acrylic
Reactor mode	Continuous

3.1.4 Coal Seam Gas Associated Water Samples

Appropriate amounts of salts were weighed and mixed with deionized (Milli-Q) water to form simulated CSG associated water. For each experiment, 10 L of feedwater was prepared. The chemicals were dissolved in water separately and mixed one by one in a 10 L container. The container was manually agitated until the salts were fully dissolved. An actual CSG associated water sample from an operating site in Queensland was also acquired for this study (due to confidentiality reasons the identity of the company cannot be revealed). The compositions and physical properties of the CSG associated water samples used are displayed in Table 3-4.

Table 3-4 Initial properties of simulated and actual CSG associated water

Species	Units	Sample 1: Low TDS CSG Associated Water	Sample 2: High TDS CSG Associated Water	Real CSG Associated Water
Sodium	mg/L	665.3	1786	1667
Potassium	mg/L	36.58	7.028	7.687
Calcium	mg/L	3.571	5.566	3.966
Magnesium	mg/L	3.082	3.519	3.203
Barium	mg/L	0.256	0.871	0.935
Strontium	mg/L	0.44	1.578	1.64
Silicon	mg/L	12.02	6.388	5.877
Boron	mg/L	0.878	0.458	0.484
Sulphur	mg/L	0.66	0.66	1.14
Solution pH		8.99	8.48	9.06
Solution Conductivity	µS/cm	2880	6930	7290
Turbidity	NTU	210	210	210
True Colour	Pt-Co	14	19	65
Apparent Colour	Pt-Co	1090	1370	2180
Suspended Solids	mg/L	305	305	305
UV254nm	Abs	0.45	0.94	8.6
Bicarbonate	mg/L	840	n.d.	n.d.
Chloride	mg/L	602.8	n.d.	n.d.

n.d. = not determined

3.2 **EXPERIMENTAL METHODS**

Two experimental methods namely the jar test (chemical coagulation) and electrocoagulation test have been used in this study.

3.2.1 Jar tests

A digitally controlled Platypus Jar Tester supplied by Aquagenics, Australia was used. This apparatus consisted of four 2 L square jars with supernatant sample taps. An 80 mm x 35 mm butterfly paddle was placed in each jar and this paddle could operate with programmable speed and time settings. Both jars and paddles were made of clear polycarbonate material. Jar tests were done according to ASTM D2035 − 13. The first stage involved the rapid mixing of the coagulant at the rate of 100 rpm for 1 min. The second maturation stage was operated at 30 rpm for 10 min. From the jar tester manufacturers chart the velocity gradients were estimated at 195 and 32 s^{-1} for rapid and slow mixing steps, respectively. Following the maturation step, the sample was allowed to settle under static conditions in a 1 L measuring cylinder for 30 min. The volume of solid-liquid interface was recorded regularly in order to determine floc settling rates. At the endpoint, 200 ml of supernatant was collected for further analysis of dissolved ions.

3.2.2 Electrocoagulation testing

Operation of the EC process started with the preparation of electrodes. Metal electrodes were cleaned with 3% Hydrochloric acid and were scrubbed lightly to remove all the greasy and loose particles from the surface. Then kept in the oven overnight at 60°C. The electrodes were removed and rested for 4 hours to bring it to room temperature. Then every electrode plate was weighed and recorded separately. An electrocoagulation unit [Figure 3-1] was employed which comprised 13 vertical

electrode plates. Each plate had an active dimension of 15 x 10 x 0.3 cm. The plates were spaced equally by 0.3 cm. Therefore, the surface area of one side of each plate was 150 cm^2 and a total number of active surfaces was 24.
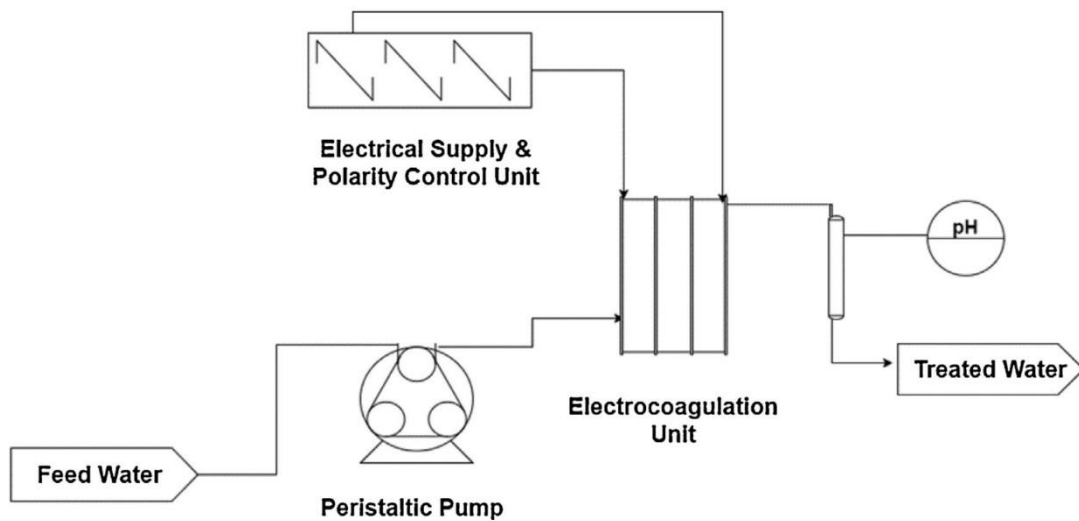
Figure 3-1: Configuration of electrocoagulation testing system [132].

The EC unit was connected to a DC power supply and an option existed to apply polarity reversal. The power supply was connected to the two outermost electrodes, which keeps the EC cell simple and effective [141]. WinTPS software was used to continuously record the voltage (V) and current (A). A pH meter and conductivity meter were connected to a data logger to record pH and conductivity (mS/cm) throughout the entire EC test. A peristaltic pump (Masterflex II) was used to deliver feed water into the EC reactor (inlet diameter 0.625 cm). The EC cell was consist of a vertical up-flow configuration wherein feedwater entered from the bottom of the unit and exited at the top. According to the experimental parameters, the flow rate was varied in order to create an average residence time of 20, 30, or 60 s in the EC unit.

For 30 s HRT, three different PRT (1, 3 and 5 min) were employed to evaluate the effect of PRT. More details can be found in Wellner et al. [31, 36]. Treated water samples were transferred to a 2 L measuring cylinder in order to record the floc settling rates. After 30 minutes of sedimentation samples for analysis were collected from approximately 1.5 cm below the water surface to minimize contamination by floating flocs. Electrode mass loss during EC operation was calculated based upon weighing the electrodes before and after use. To ensure accuracy the electrodes were oven dried overnight at $95^{\circ}C$ to remove water contamination.

3.3   ANALYTICAL METHODS

3.3.1 Inductively coupled plasma - optical emission spectroscopy (ICP-OES)

Solutions were analysed using a Perkin Elmer Optima 8300 DV ICP-OES instrument to identify elemental traces of alkaline earth ions, boron and silica. For online internal standardisation and auto dilution, this instrument was connected to an ESI SC-4DX autosampler and PrepFAST 2 sample handling unit. ICP-MS grade single element solution supplied by High-Purity Standards, Charleston, USA was used to calibrate the instrument. The wavelengths used were as follows (nm); Al (396.153), B (249.677), Ba (455.403), Ca (317.933), Fe (259.939), K (766.490 – Rad), Mg (285.213 – Rad), Na (589.592 – Rad), S (181.975), Si (251.611), and Sr (407.771). The samples were filtered through 0.45µm filters and diluted in a 1:10 ratio by purified nitric acid to reduce the pH to 2.

3.3.2 Solution pH and conductivity

pH and conductivity were measured by using a Labchem-CP benchtop Conductivity/TDS - pH/mV - temperature meter supplied by TPS, Australia. The pH meter was calibrated using pH buffer 4.00, 7.00 and 10.06 standard solutions. The

solution conductivity was expected to be high. Therefore, conductivity (Sensor K=10) meter was calibrated using 58.00 mS/cm conductivity standard manufactured by the manufacturing company.

3.3.3 Apparent colour/true colour and UV-254 nm absorbance

A Hach DR5000 UV-VIS spectrophotometer was used to measure apparent colour/true colour and UV254 nm absorbance. Platinum-Cobalt Standard Method (Hach method 8025) and Direct Reading Method (Hach method 10054) were used for measuring colour and UV-254, respectively. Solutions were filtered through 0.45 µm filters before measuring true colour.

3.3.4 Turbidity

A Hach 2100Q portable turbidity meter (EPA method 180.1) was used to measure turbidity. The meter was calibrated with 10, 20, 100 and 800 NTU turbidity standards. Both standard and sample vials were coated with silicone oil to avoid the effect of glass scratches.

3.3.5 Scanning electron microscopy (SEM)

Floc analysis was conducted by a JEOL 6360A SEM instrument operating at an accelerating voltage of 15 KV. An Energy Dispersive Spectroscopy (EDS) detector was used to measure the percentage of ions present on the sample surface. The wet floc samples were dried by compressed Nitrogen gas. Before placing in the SEM, dried samples were carbon coated using a Cressington 208 Carbon Coater to avoid charging effects.

3.3.6 Optical microscopy

Flocs images were taken by a Nikon SMZ 1500 stereoscopic zoom microscope. Wet samples were placed on a frosted microscope slide in a very thin layer to capture the shape and colour of floc.

3.3.7 Floc settling rates

Just after the slow mixing treated solutions were transferred to 2 L graduated cylinders the settling height was recorded at time intervals 5, 10, 15, 20, 25, 30, 40 and 60 minutes.

3.3.8 Mass balance

Each plate was weighted separately before and after the experiment. Plates were washed, oven dried for overnight and cooled to the room temperature prior to weighing. The difference between before and after weights denoted the electrodes dissolution. Theoretical dissolution was calculated by using the Faradic yields as shown in Equation 3-1.

Equation 3-1 $\qquad m = {ItM}/{zF}$

Here, m is the mass of iron released to the solution (g), I is the average current applied through the experiment (A), t is the runtime (s), M is the atomic mass of iron (55.845 g/mol) or Aliminium (27 g/mol), z is the number of electrons transferred during anodic dissolution (3) and F stands for Faraday's Constant (96,486 C/mol).

3.3.9 Power consumption

Power consumed during the experiment was calculated using the following equation, where P is the power consumed in Watt-hr/L, I is the average current (A), V is the average voltage (V) and Q is the flow rate of influent (L/hr).

Equation 3-2 $\qquad P = {IV}/{Q}$

3.4   COMPUTATION MODELLING

3.4.1 Chemical Coagulation Process Simulation
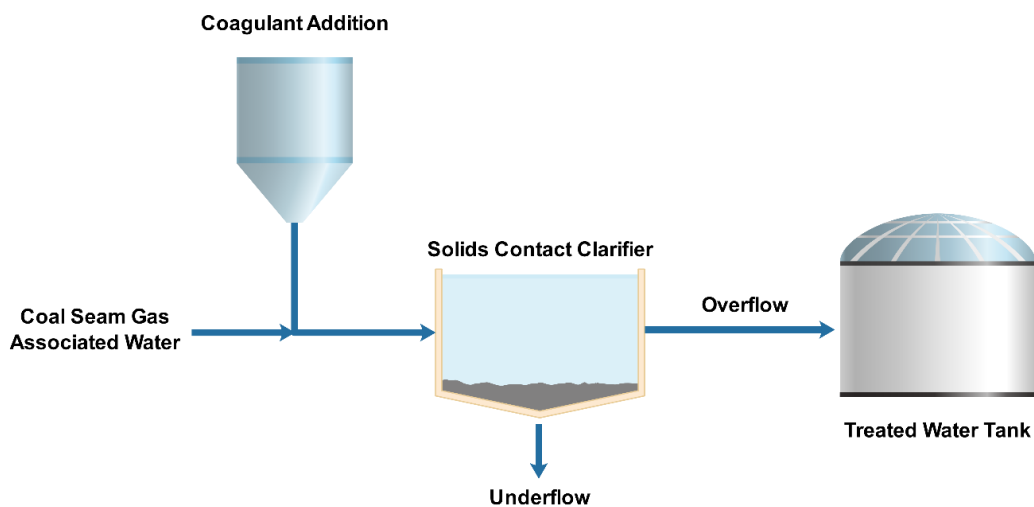
Figure 3-2: Process Flow Diagram for AqMB simulation of coagulant addition to CSG associated water

AqMB software is a process engineering simulation package designed specifically for the water treatment industry [29]. AqMB can simulate a wide range of unit operations including coagulant addition to suitable equipment such as solid contact clarifier, thickener and lamella clarifier.

The clarifier had the following design criteria: surface loading rate of 3 m/h; floc/contact zone detention 5 min; K-factor to determine rake drive torque 70 N/m and mixer power number 0.35.

Chapter 4: Chemical Coagulants for Removal of Turbidity and Dissolved Species from Coal Seam Gas Associated water

4.1 INTRODUCTION

Production of coal seam gas (CSG) also known as coal bed methane (CBM) has expanded in recent years around the world [19]. In the Australian context, the largest deposits of coal seam gas occur in Queensland with the particular commercial focus centered on the Surat and Bowen basins [21]. As the coal seam gas is trapped in coal cleats due to water pressure, extraction of the gas is invariably accompanied by the production of water especially in the initial years of the well-life [46]. Towler *et al.* [49] reported that volumes of associated water collected from operating CSG wells in Queensland were presently averaging 120 ML/day (44 GL/year). The CSG associated water is saline in character with salt concentrations ranging from *ca.* 200 to 10,000 mg/L [1]. Outside of Australia, the salinity of the associated water from CSG operations can be significantly greater [37, 51, 57]. Dahm *et al.* [51] created a geochemical database for CSG associated water produced in the Rocky Mountain region of the USA which revealed that the chemical composition varied with coal type, freshwater recharge availability, and basin geology. Typically, sodium bicarbonate and chloride species are dominant in CSG associated water [58]. Minor species also present in the associated water include calcium, magnesium, dissolved silicates, dissolved organic matter, suspended solids, sulphate, aluminium, iron, manganese, fluoride, barium and strontium [1, 19, 59].

There are strict regulations regarding the beneficial reuse of CSG associated water as for example; not only may the salinity be too high but also the sodium adsorption ratio (SAR) can be in excess of recommended limits for direct soil irrigation [16]. Vance *et al.* [71] investigated the impact of irrigation of soils with CSG associated water and noted that not only did soil electrical conductivity increase but also plant diversity decreased. Burkhardt *et al.* [72] additionally discovered that irrigation with CSG associated water could lead to a reduction in the oil content of crops and high sodium content in the leaves of mints. Therefore, the general necessity of treating CSG associated water prior to crop irrigation is illustrated.

Reverse osmosis (RO) is the principal desalination process for treating CSG associated water [75, 142, 143]. Ion exchange has also been reported to be especially viable for CSG associated water with high alkalinity [73, 144, 145]. With either technology, there is a requirement to protect the membrane or resins from fouling [76]. The selection of the most appropriate method for feedwater pre-treatment is critical as it can represent up to 20 % of the overall cost for desalination [77]. In terms of the presence of suspended solids, it has been reported that CSG associated water can be highly turbid in some instances. For example, Rebello *et al.* [21] analyzed associated water from 150 different wells in the Surat Basin, Queensland; and discovered that total suspended solids (TSS) concentrations ranged from 5 to 7560 mg/L. Qian *et al.* [68] evaluated a pilot plant system for treating CSG associated water using a central reverse osmosis unit. Notably, the feed water was characterized as having a high turbidity value of 409 NTU. Hence, a range of unit operations such as greensand filters, sand filters, coagulants, and ultrafiltration was required to pre-treat the water prior to the RO membranes. The situation in Queensland is exacerbated by the fact

that regular flooding events occur which encourage surface run-off to receiving waterways such as CSG associated water storage dams [70].

Chemical coagulation methods are widely used for reducing the turbidity of water and wastewater samples [146, 147]. However, the application of coagulants for the treatment of CSG associated water has been limited. Lin *et al.* [22] recently described the addition of aluminium based coagulants to both simulated and actual CSG associated water samples. Dissolved silicates were removed effectively by the use of aluminium sulphate (alum) or aluminium chlorohydrate (ACH) (> 85 %). A lesser but nonetheless significant decrease in the concentration of alkaline earth ions was also evident. Barium ions were most readily removed from the CSG associated water sample whereas magnesium ions were relatively difficult to remediate. Iron based coagulants for CSG associated water treatment have also been described [23]. Similar behaviour of ferric sulphate and ferric chloride to the aluminium based coagulants was observed [22]. An interesting finding in the latter two studies was the reduced efficiency of inorganic coagulants when applied to real CSG associated water compared to simulated solutions. For example, when ACH was used as a coagulant the silicate removal was reduced from 12 mg/L to *ca.* 50 %. The factors not addressed in simulated solutions included lack of species which caused turbidity, organic carbon and potentially the presence of microorganisms such as algae.

Inspection of the existing literature has revealed that there are no published studies regarding the reduction in turbidity in CSG associated water by the use of coagulants; despite the importance to CSG companies who need to ensure that the associated water does not foul and degrade downstream desalination equipment.

Therefore, the objective of this study was to examine the effectiveness of both aluminium and iron based coagulants when added to simulated and actual CSG associated water which comprised of a range of turbidity values. The hypothesis was that coagulation methods may have to be tailored to adequately treat CSG associated water which comprised of not only varying water composition but also differing levels of turbidity and dissolved organic carbon. Consequently, the following research questions were addressed to support this latter idea: (1) How does the identity of the inorganic coagulant impact CSG associated water quality? (2) Which dissolved and suspended solids are removed as a function of the coagulant dose? (3) What are the properties of the flocs produced? (4) Is the salinity of the CSG associated water important in terms of coagulant performance? (5) What is the difference in behaviour between simulated and actual CSG associated water? Jar tests were conducted in order to address these challenges and computational modelling using AqMB water process software also applied in order to predict coagulant performance. Both simulated and real CSG associated water were tested and turbidity produced by added kaolin was examined in accord with the methodology of Mahdavi *et al.* [148].

4.2   RESULTS AND DISCUSSION

4.2.1 Comparison of Various Coagulants for Treatment of Simulated CSG Associated Water

4.2.1.1   Solution Physical Parameters

Simulated CSG associated water sample 1 was chosen to investigate the baseline performance of coagulant addition. Figure 4-1 displays the impact of coagulant identity and dose rate upon the solution conductivity and pH of the simulated CSG associated water.
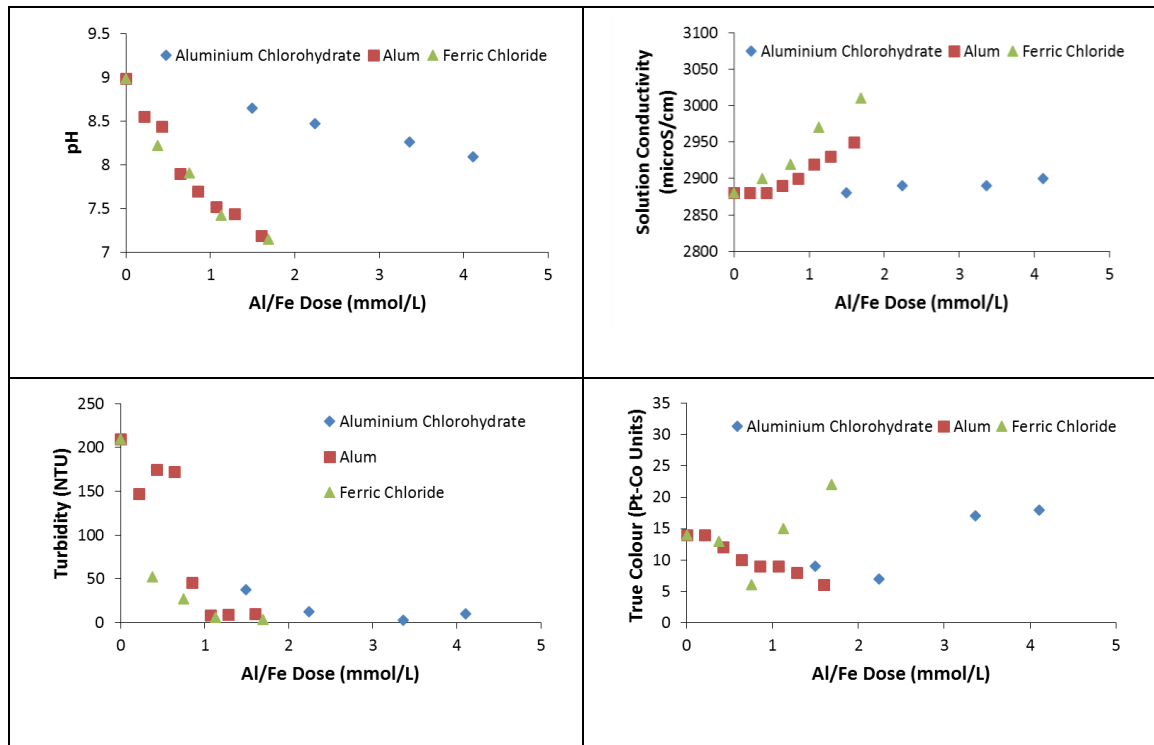
Figure 4-1 Solution changes as a function of coagulant type and dose when added to simulated CSG associated water sample 1

In general, the solution pH gradually diminished with increasing coagulant dose, with the precise rate of pH decrease dependent upon the coagulant type. Alum and ferric chloride induced the greatest reduction in solution pH which was *ca.* 7.1 at the end of the coagulant addition stage. Notably, the rate of pH decreased when aluminium chlorohydrate was employed, was significantly slower than when either alum or ferric chloride was applied to the simulated CSG associated water. To understand the pH behaviour, we need to consider Equations 4-1 to 4-3.

Equation 4-1: $Al_2(SO_4)_3 . 14H_2O \rightarrow 2\,Al(OH)_3 + 6\,H^+ + 3\,SO_4^{2-} + 8\,H_2O$

Equation 4-2: $2\,FeCl_3 . 6H_2O \rightarrow 2\,Fe(OH)_3 + 6\,H^+ + 6\,Cl^- + 6\,H_2O$

Equation 4-3: $Al_2(OH)_5Cl \rightarrow 2\,Al(OH)_3 + H^+ + Cl^-$
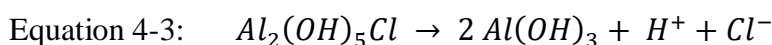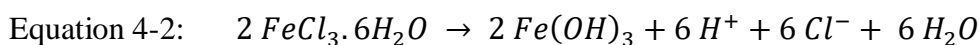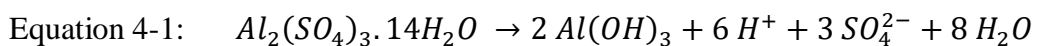
It can be seen that for the same dose rate of iron or aluminium the amount of protons generated in the treated solution was the same for both alum and ferric chloride (6 H^+) ions; thus, it was not unexpected that the pH profile would be similar in both instances. In contrast, only one H^+ species was released when using ACH [Equation 4-3]; hence, the decrease in solution pH was diminished compared to the other coagulants employed. Figure 4-1 also revealed that the solution conductivity remained relatively constant when dosing with ACH (2880 to 2900 µS/cm), whereas the conductivity steadily increased for both alum (2880 to 2980 µS/cm) and ferric chloride (2880 to 3010 µS/cm) coagulants (which probably correlated with the greater evolution of protons and anions with these two coagulants compared to ACH).

From Figure 4-1 it was noted that a similar dose rate of 1 mmol/L Al or Fe was required for alum and $FeCl_3$ to achieve high turbidity removal efficiency. The initial turbidity was reduced from 210 to 6.44 NTU using $FeCl_3$ and to 8.33 NTU using alum coagulant. Baghvand *et al.* [149] reported comparable behaviour when either alum or $FeCl_3$ was used to remove turbidity from a turbid water sample. In contrast, ACH required a higher dose rate (3.4 mmol/L as Al) to remove turbidity; albeit, it was noted that ACH performed best as turbidity was diminished to 2.56 NTU. In this study, the apparent colour was also measured and the trend in value mirrored the turbidity behaviour with coagulant addition (results not shown for sake of brevity). Alternatively, the true colour values did not follow the turbidity trend when the coagulants were added to the turbid CSG associated water sample. The initial true colour of the raw water was 14 Pt-Co unit, which reduced to 6 Pt-Co units for 0.76 mmol/L Fe dose (as $FeCl_3$). When the Fe dose was increased to 1.15 and 1.72 mmol/L

true colour values also increased to 15 and 22 Pt-Co units, respectively. This behaviour was consistent with the presence of residual iron in the treated water which was measured as 0.046, 0.169, and 0.210 mg/L for iron doses of 0.76, 1.15, and 1.72 mmol/L, respectively. Visually the colour of the effluent was yellow-orange which was typical of dissolved iron species. Along with residual iron, very fine flocs (less than 0.45 µm) remained in the filtered effluent and thus also may have contributed to the true colour values. Interestingly, the true colour of ACH treated CSG associated water was recorded as 7, 17, and 18 Pt-Co units for Al doses of 2.2, 3.4 and 4.1 mmol/L, respectively [Figure 4-1]. It was tentatively concluded that the true colour in this instance was due mainly to the presence of fine flocs in the solution. Alum addition similarly gave rise to true colour values which were best attributed to fine flocs in the sample.

4.2.1.2 Species Removed from CSG Associated Water due to Coagulant Addition

No discernible impact upon the concentrations of sodium or potassium ions was found when analysing the treated CSG associated water samples for all three coagulants employed, which was in agreement with previously published studies [22, 23]. Figure 4-2 shows the degree of alkaline earth ion and dissolved silica removal from CSG associated water for the three coagulants used in addition to changes in chloride and sulphate concentration. In all cases, barium ions were removed to the highest extent (*ca.* 42 to 64 %), followed by silicates (*ca.* 25 to 40 %), calcium (*ca.* 17 to 31 %), and strontium (*ca.* 20.5 to 24 %). Magnesium ions were not removed to any discernible level (removal rates within errors in experimental measurement). Du et al. [150] found in a study of cooling water softening with alkali and coagulant that barium was the easiest species to remove followed by silica and strontium. The formation of highly insoluble barium carbonate was suggested to be the reason why barium

concentration was reduced by the greatest extent. Coagulation didn't cause the formation of barium carbonate rather the co-presence of barium and high concentration of carbonate and bicarbonate ions was the reason.
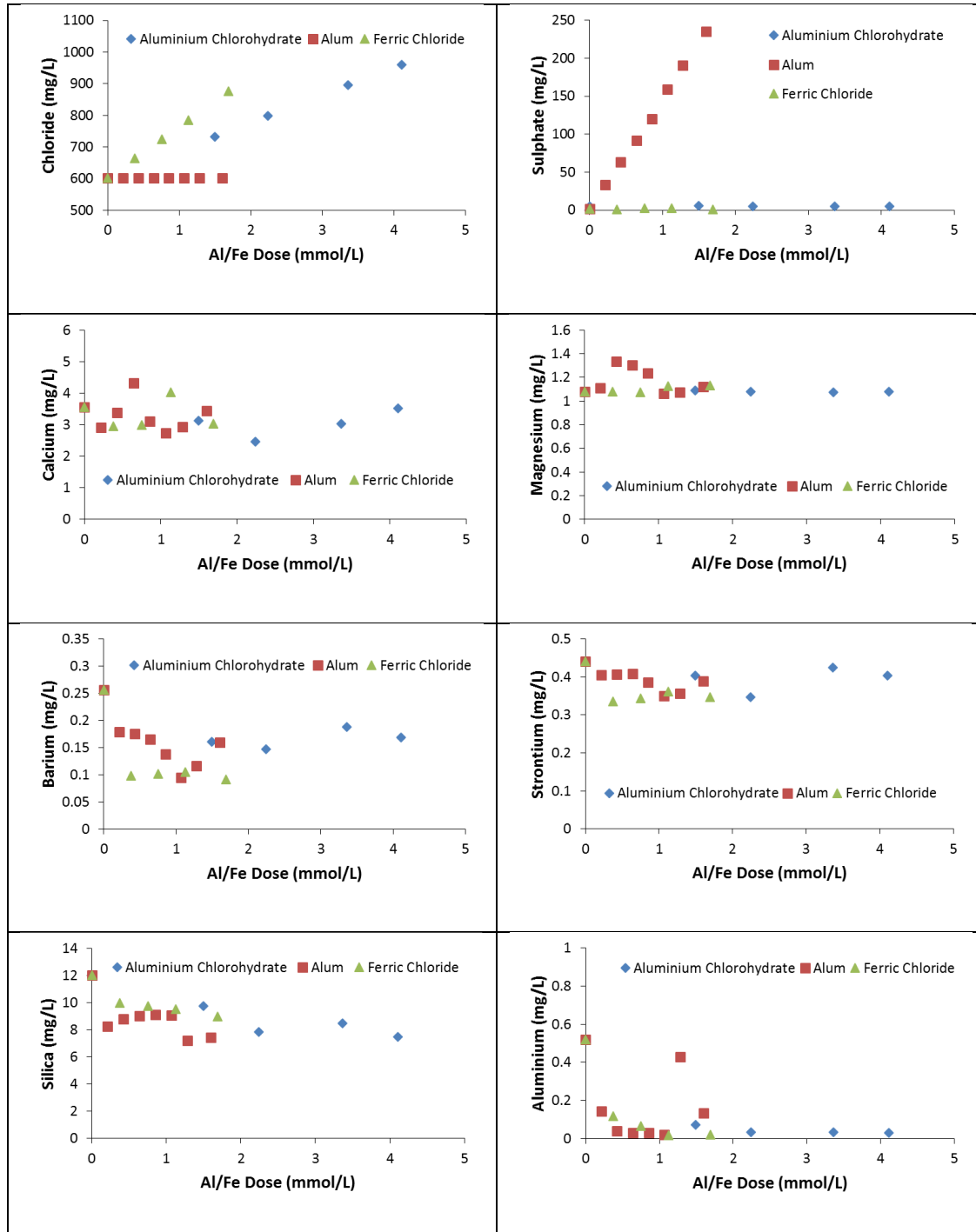
Figure 4-2: Impact of coagulant dose rates upon dissolved species in CSG associated

water sample 1

O'Donnell *et al.* [151] studied the removal of strontium ions from drinking water using both aluminium and iron based coagulants. Removal rates were typically less than 6.5 % regardless of strontium concentration, solution pH or turbidity level; which was significantly less than the maximum value of 24 % recorded in this study when ferric chloride was added. However, upon addition of calcium (in the form of lime) and soda ash, once a pH of 8.8 was attained the removal of strontium ions was accelerated. This behaviour was attributed to the formation of a solid solution of strontium ions in the lattice of precipitated calcium carbonate. Notably, the presence of sufficient alkalinity was required to allow the precipitation of carbonate species to occur. CSG associated water inherently contains substantial amounts of bicarbonate and carbonate species and thus the observed higher level of strontium ion removal in this solution compared to the surface water studied by O'Donnell *et al.* [151] was not unexpected.

O'Donnell *et al.* [151] also noted that magnesium ions did not exhibit similar chemistry to calcium ions in the water samples studied. Magnesium was not significantly removed until a pH > 9.8 upon which time $Mg(OH)_2$ precipitated. This discovery was in accord with the data recorded in this investigation wherein the pH was a maximum of 9 in the coagulation tests and no magnesium precipitation was thus possible. Cheng *et al.* [152] added alum to brackish water and found that up to 65 % of dissolved silica could be removed. These authors indicated that the silica removal was by means of precipitation with aluminium hydroxide flocs.

The chloride content of the CSG associated water was controlled by the nature of the coagulant used. In harmony with the fact that aluminium sulphate did not

contain any chloride ions in its structure, the chloride ion concentration in the treated CSG associated water was not observed to change in value relative to the feed (602.8 mg/L Cl). In contrast, both ferric chloride (737.7 mg/L Cl) and aluminium chlorohydrate (895.8 mg/L Cl) released chloride ions into the treated CSG associated water sample. Likewise, the only coagulant to influence sulphate ion concentration in the CSG associated water was alum.

Lin *et al.* [22] evaluated the behaviour of ACH and alum coagulants to treat CSG associated water without the presence of turbidity. In this study, dissolved silica was mainly removed using ACH addition, whereas barium, strontium, and magnesium ion concentrations were minimally influenced by the presence of the coagulant. Calcium was removed but only by *ca.* 20 % at a comparable CSG associated water quality. As kaolin was used as the source of turbidity it is possible that this material may have ion exchanged some of the alkaline earth ions from solution. For example, Kleven and Alsted [153] investigated the exchange behaviour of alkaline earth ions with kaolin and discovered that barium ions were preferred to calcium ions which was consistent with our data.

The dose rate of ACH required to remove dissolved silica was not only significantly increased relative to the study of Lin *et al.* [22] when turbidity was present (*c.f.* 2.24 compared to 0.56 mmol/L Al) but also the removal of dissolved silica was inhibited (*c.f.* 34.9 to 86.5 %). However, it was noted when Lin *et al.* [22] investigated actual CSG associated water from an operating gas field that the amount of aluminium dosed was higher (up to 2.80 mmol/L Al) and the degree of silica removal less (50 %). The real CSG associated water sample did exhibit turbidity, but

only 8.4 NTU which was a value substantially less than used in CSG associated water sample 1 (210 NTU). Consequently, it can be deduced that turbidity causing species can potentially inhibit coagulant performance in relation to the removal of dissolved species from CSG associated water but that other factors must also be considered. In this study, turbidity was simulated using an inorganic material namely kaolin. In an actual CSG associated water sample, it is entirely possible that the species responsible for turbidity could be partially organic in character [154].

The presence of residual iron or aluminium was also considered following the coagulation process. For ACH and alum, the aluminium concentrations were 0.03 and 0.02 mg/L, respectively; whereas for ferric chloride the residual iron content was 0.17 mg/L (result not shown for sake of brevity). These latter values were all within typical guidelines for water discharge [155]. This data was also consistent with the report by Knowles *et al.* [155] that application of iron based coagulants normally results in a higher concentration of residual iron in solution compared to residual aluminium produced by aluminium based coagulants.

4.2.1.3 Simulation of Coagulant Performance

Using AqMB software a scenario was developed wherein CSG associated water sample 1 was dosed with either ACH, alum or ferric chloride and passed into a solid contact clarifier vessel. Based on typical mobile reverse osmosis (RO) plant, an arbitrary flow rate of 100 m^3/h was chosen for simulation purposes.

Addition of ACH was predicted to result in a slight increase in solution pH as the dose of ACH was increased (8.99 to 9.40), whereas in the actual jar test the pH decreased to *ca.* 8.1. A decrease in pH was expected on the basis of the process

described in Equation 4-3. In harmony with the increase in pH was a lowering of the bicarbonate concentration and an increase in carbonate species. The discrepancy in pH values between simulation and experimental needs to be considered in the context that the software is estimating the performance of a commercial clarifier unit complete with overflow and underflow streams, whereas in a lab only a stirred solution is evaluated. The influence of the underflow stream can be seen when inspecting the overflow flowrates when different coagulant doses are used: a reduction from an initial flow rate of 99.99 m^3/h to 79.35 m^3/h was observed when 4.1 mmol/L Al was added. However, it is possible that dissolved carbon dioxide in the simulated CSG associated water was displaced by oxygen in the air which would promote a rise in solution pH.

In all instances, the removal of total suspended solids was estimated to be > 96.5 % which was in agreement with experimental studies [Figure 4-1], and concomitantly the turbidity was suitably diminished in value. It was predicted that some residual aluminium would be present in the treated water; albeit, at about an order of magnitude greater than the experimental values. Likewise, chloride ions increased in concentration as more ACH was added which was in harmony with Equation 4-3.

Notably, AqMB suggested that the reduction in dissolved silicates induced by ACH addition was related to the formation of muscovite [Table 4-2]. Muscovite materials have the general formula $KAl_2(Si_3AlO_{10})(OH)_2$ (potassium ions can be exchanged with other single charged ions such as sodium, a situation most likely for the current evaluation of CSG associated water). The only other precipitate which was proposed to be present was the gibbsite-like floc formed by ACH dosing.

Table 4-1 AqMB simulation of ACH coagulant addition to CSG associated water

sample 1

	Units	Feed	ACH Concentration		
			195 mg/L (2.2 mmol/L Al)	293 mg/L (3.4 mmol/L Al)	358 mg/L (4.1 mmol/L Al)
pH (25 ºC)		8.99	9.26	9.39	9.40 (6.74 feed)
Alkalinity (total)	mg CaCO$_3$/L	707.7	652.3	626.3	608.8
Conductivity (25 ºC)	µS/cm	3052	3080	3096	3107
Flowrate	m^3/hr	99.99	85.73	81.9	79.35
TDS	mg/L	2085.9	1997	1967	1960
TSS	mg/L	305.0	10	10	10
Turbidity	NTU	291.0	9.54	9.54	9.54
Aluminium (total)	mg/L	0	0.84	0.99	1.06
Barium (total)	mg/L	0.256	0.256	0.256	0.256
Bicarbonate (total)	mg/L as HCO$_3$	713.8	572.1	499	476.9
Carbonate (total)	mg/L as CO$_3$	68.24	101.6	119.2	118.4
Chloride (total)	mg/L	602.8	606.4	626.3	639.4
Silica	mg/L	25.7	11.31	16.23	18.99
Sulphate (total)	mg/L as SO$_4$	1.32	1.32	1.32	1.32

Table 4-2: Prediction of precipitate formation as a function of ACH dose to CSG associated water sample 1

Precipitate (mol/h)	ACH Concentration		
	195 mg/L	293 mg/L	358 mg/L
Muscovite	7.998	5.262	3.726
Gibbsite	196.9	317.1	396.1

A similar evaluation of alum addition to CSG associated water was conducted using AqMB software [Table 4-3]. In this instance, the solution pH was predicted to significantly decrease as alum was added (8.99 to 6.93) which was in agreement with the data shown in Figure 4-1 and described in Equation 4-1.

Accordingly, the total alkalinity of the solution decreased with the presence of carbonate almost reduced and a gradual decline in the concentration of bicarbonate species (as summarized in Equations 4-4 & 4-5].

Equation 4-4: $CO_3^{2-} + H^+ \leftrightarrow HCO_3^-$

Equation 4-5: $HCO_3^- + H^+ \leftrightarrow CO_2 + H_2O$
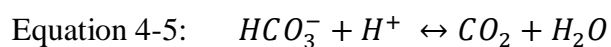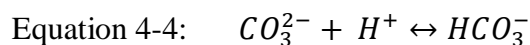
Again, the removal of suspended solids and reduction in turbidity was successfully predicted in agreement with the experimental data. Similarly, a substantial increase in sulphate species was estimated due to the process shown in Equation 4-1. Silicate species were again predicted to be removed from the solution, although only at the lowest coagulant dose rates. In contrast to the results for ACH

addition, alum dosing of the CSG associated water was suggested to be able to remove some barium ions from solution [Table 4-3]. Table 4-4 provides some insight as the chemistry occurring as barite (barium sulphate) was indicated to precipitate at increasing amounts with increasing alum addition. Muscovite was also predicted to form, but the quantity precipitated decreased with increasing alum dose. Hence, silicate removal was estimated to decrease with increasing coagulant addition. As described by Hermosilla *et al.* [156] alkaline pH favours the solubility of dissolved silicates; hence, the lower pH values induced by the addition of alum would inhibit the formation of aluminosilicate phases. Also, Iler [157] reported that any surface containing both Al_2O_3 and SiO_2 has lower solubility than individuals.

Ferric chloride addition to CSG associated water was evaluated using AqMB software [Table 4-5]. Consistent with the release of protons upon addition of ferric chloride [Equation 4-2] the solution pH was significantly reduced from 8.99 to 6.99. In harmony with the fact that both alum and ferric chloride release 3 protons per Al or Fe ion, the magnitude of the pH reduction was comparable for both coagulants. Therefore, the decrease in alkalinity, reduction in carbonate concentration and a decrease in bicarbonate concentration was not unexpected. The degree of suspended solids removal was the same for all three coagulants studied. Due to the lack of sulphate addition to the CSG associated water sample, no barium removal was predicted. Moreover, no silicate removal was estimated to form due to the lack of aluminium added to the solution. In practice, some silicate was recorded to be removed from the CSG associated water, albeit iron chloride was found to be the least effective of the three coagulants tested (which was in agreement with the

computational data). The only precipitate formed according to AqMB was amorphous

ferrihydrite (FeOOH).

Table 4-3: AqMB simulation of alum coagulant addition to CSG associated water

sample 1: Values represent the composition of the overflow from solid contact

clarifier

	Units	Feed	Alum Concentration		
			127 mg/L (0.43 mmol/L Al)	254 mg/L (0.85 mmol/L Al)	476 mg/L (1.6 mmol/L Al)
pH (25 ºC)		8.99	8.40	7.67	6.93
Alkalinity (total)	mg CaCO$_3$/L	707.7	647.9	594.1	496.7
Conductivity (25 ºC)	µS/cm	3052	3072	3099	3138
Flowrate	m^3/hr	99.99	92.31	91.25	89.08
TDS	mg/L	2085.9	2110	2141	2202
TSS	mg/L	305.0	10	10	10
Turbidity	NTU	291.0	9.54	9.54	9.54
Aluminium (total)	mg/L	0	0.265	0.46	0.69
Barium (total)	mg/L	0.256	0.256	0.185	0.112
Bicarbonate (total)	mg/L as HCO$_3$	713.8	748.2	712.9	598.5
Carbonate (total)	mg/L as CO$_3$	68.24	18.34	3.823	0.5
Chloride (total)	mg/L	602.8	566.8	566.7	566.5
Silica	mg/L	25.7	11.68	20.59	25.68
Sulphate (total)	mg/L as SO$_4$	1.32	56.23	111.1	206.7

Table 4-4: Prediction of precipitate formation as a function of alum dose to CSG
associated water sample 1

Precipitate (mol/h)	Alum Concentration		
	127 mg/L	254 mg/L	476 mg/L
Muscovite	7.795	2.839	0
Gibbsite	13.82	66.16	140.6
Barite	0	0.052	0.105

Table 4-5: AqMB simulation of ferric chloride coagulant addition to CSG associated
water sample 1: Values represent the composition of the overflow from solid contact
clarifier

	Units	Feed	Ferric Chloride Concentration		
			61 mg/L (0.18 mmol/L Fe)	122 mg/L (0.37 mmol/L Fe)	183 mg/L (0.55 mmol/L Fe)
pH (25 ºC)		8.99	8.77	7.41	6.99
Alkalinity (total)	mg CaCO$_3$/L	707.7	653.0	599.5	546.4
Conductivity (25 ºC)	µS/cm	3052	3088	3128	3162
Flowrate	m^3/hr	99.99	92.54	91.06	89.6
TDS	mg/L	2085.9	2090.0	2145	2173
TSS	mg/L	305.0	10	10	10
Turbidity	NTU	291.0	9.54	9.54	9.54
Aluminium (total)	mg/L	0	0	0	0
Barium (total)	mg/L	0.256	0.256	0.256	0.256

Bicarbonate (total)	mg/L as HCO$_3$	713.8	703.7	720.8	654.5
Carbonate (total)	mg/L as CO$_3$	68.24	41.61	3.79	3.95
Chloride (total)	mg/L	602.8	606.9	646.8	686.7
Iron (total)	mg/L	0	0.66	1.82	3.083
Silica	mg/L	25.7	25.7	25.7	25.69
Sulphate (total)	mg/L as SO$_4$	1.32	1.32	1.32	1.32

4.2.1.4 Floc Characteristics

When evaluating the effectiveness of coagulants, one must consider the settling behaviour of the resulting flocs. Figure 4-3 shows the settling behaviour of flocs resulting from the addition of ACH to CSG associated water. It is noted that no clear solid-liquid interface was observed for either alum or ferric chloride (albeit some dense flocs at the bottom of the vessel were visually observed) and thus no discussion of settling behaviour could be provided. Figure 4-3 reveals that the rate of settling and volume of floc after 60 minutes depended upon the amount of coagulant added. At the lowest dose studied there was no observable "mud line" which suggested the flocs were colloidal in nature.
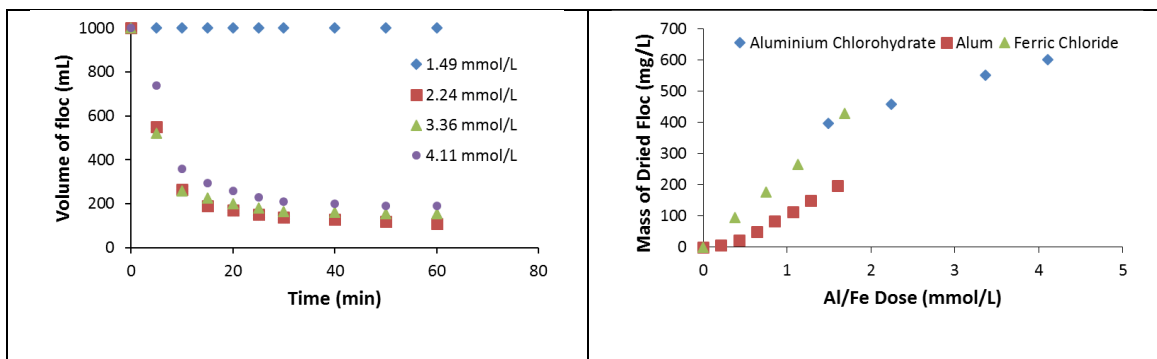
Figure 4-3: Floc settling behaviour after ACH addition and dry mass of flocs after coagulant addition for CSG associated water sample 1

However, upon increasing the aluminium dose to 60.5 mg/L (2.24 mmol/L) the flocs settled reasonably quickly with the majority of the settling completed within the initial 10 minute period. The final settled volume of floc was smallest for the least amount of coagulant used (2.24 mmol/L Al) and increased as the amount of coagulant dosed was increased. This behaviour may simply reflect the enhanced quantity of flocs formed in the process which occupied more volume of the treated solution. Correspondingly, Figure 4-3 confirmed that the amount of floc increased almost linearly with the coagulant dose. Overall, ferric chloride and aluminium chlorohydrate addition resulted in the highest mass of floc formed. The higher floc mass of ferric chloride relative to alum could be explained simply as the difference in atomic mass of iron (55.845 amu) compared to aluminium (26.982 amu). For ACH the same explanation did not appear to apply. Undoubtedly higher dose rates were used for ACH and the predicted formation of gibbsite was substantially greater for ACH compared to alum. However, the data in Figure 4-3 was based upon moles of aluminium added and thus allowed direct comparison between alum and ACH behaviour. One possible explanation was that the floc composition for ACH addition was different from that of alum. For example, chloride ions may have incorporated in the floc when using ACH. Guseva *et al.* [158] examined the electrochemical dissolution of aluminium in the presence of dissolved salt and suggested that chloride ions could incorporate within the floc material ($Al(OH)Cl^+$, and $Al(OH)_2Cl$). The higher mass of chloride (35.45 amu) relative to OH (17 amu) would then explain the higher mass of floc recorded for ACH compared with alum.

Further information about the floc characteristics was gained from the optical microscopy images in Figure 4-4. It was evident that ACH and $FeCl_3$ produced very

fine flocs with respect to alum flocs. This observation was consistent with the facts that the true colour for ACH and $FeCl_3$ treated CSG associated water was at least partially explained by the presence of fine flocs in these materials (hence the higher true colour values compared to alum [Figure 4-1]). Lin *et al.* [23] described the flocs produced when ferric chloride was added to CSG associated water as "thin-networked", which was comparable to the floc found in our study. Closer inspection of the optical images in Figure 4-4 suggested that the ferric chloride flocs were fractal in nature. Li *et al.* [159] examined flocs produced by the addition of alum coagulant to a solution dosed with kaolin. The flocs were also shown to be fractal in character which was again consistent with the image shown in Figure 4-4. Jiao *et al.* [160] noted that the alum flocs were particularly suited to removing suspended solids *via* sweep flocculation. Chakraborti *et al.* [161] also recorded the growth of flocs resulting from alum addition to lake water containing suspended clay particles. The mechanism for clay removal varied from charge neutralization to sweep flocculation as time progressed.

| ACH | Alum | Ferric Chloride |
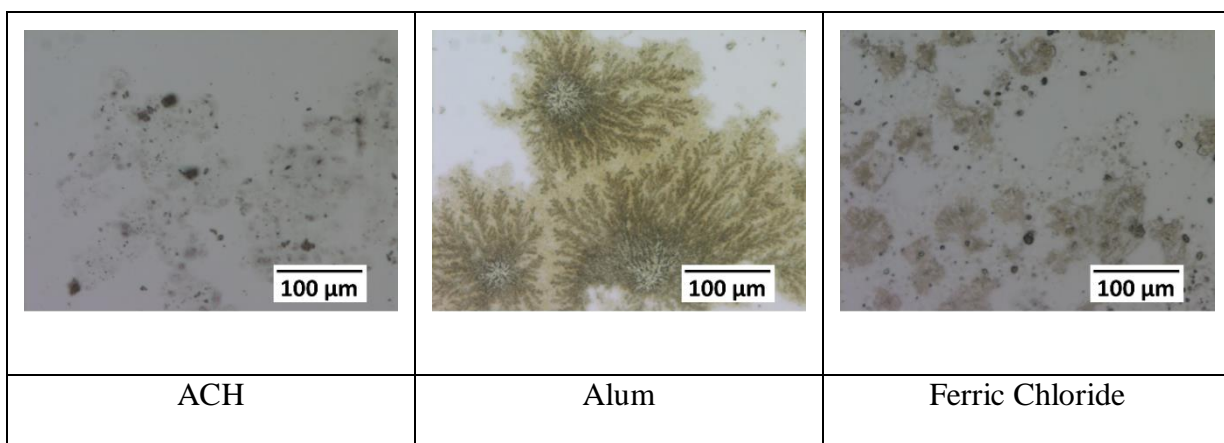
Figure 4-4: Optical Microscopic images of flocs formed after coagulant addition to simulated CSG associated water

4.2.2 Effect of CSG Associated Water Composition upon Coagulant Performance

The composition of CSG associated water varies greatly in practical situations [1, 19, 59]. Therefore, it was necessary to examine the effect of coagulant performance with CSG associated water of varying dissolved ion compositions. Furthermore, an understanding of the differences between simulated and real CSG associated water samples was also required. Consequently, tests were conducted using ACH coagulant to treat CSG associated water sample 2 and a real CSG associated water sample from an operating field in Queensland [Figures 4-5 & 4-6]. An important aspect was that the composition of CSG associated water sample 2 was chosen to mimic that of the real CSG associated water. This situation facilitated not only insight into the factors which may not be taken into account in the simulated sample but also what the performance variations were.

The pH gradually reduced for both the CSG associated water types which was consistent with the fact that ACH does not release a significant amount of protons into solution [Figure 4-5]. Similarly, minimal changes in solution conductivity were observed which was in agreement with the data shown in Figure 4-1. It was noted that the pH diminished to a lesser extent with the high TDS CSG associated water sample compared to the low TDS sample. This behaviour can be attributed to the greater buffering capacity of the high TDS sample. Although turbidity was majorly diminished for both water samples it was noted that the clarity of the real CSG associated water was generally not as good as the simulated sample. Substantial differences in the true colour of the water samples after coagulation were apparent. It was clear that the simulated sample did not replicate the real sample in terms of species

which gave rise to a coloured solution (the true colour was initially 62 Pt-Co units for the real sample compared to 20 Pt-Co units for the simulated sample). When ACH was added the true colour did not exhibit a definitive change from the initial value (within error), whereas the true colour of the CSG associated water sample 2 steadily decreased with increasing coagulant dose. The salinity of the CSG associated water did not appear to significantly influence the ability of the coagulant to reduce turbidity as the removal performance was similar for both high and low TDS samples. This result was in contrast to the study of Pontius [162] who found that reduction of turbidity using ACH coagulant was challenging when attempting to clarify highly saline water with a TDS of 70,000 mg/L. However, it was noted that the TDS of the CSG associated water was significantly lower than 70,000 mg/L. As outlined by Umar *et al.* [163] higher salinity samples tend to solubilize aluminium coagulants and inhibit the formation of flocs. Therefore, the recorded effectiveness of ACH to remove turbidity over the salinity range evaluated for CSG associated water was in accord with the relative stability of flocs under the experimental conditions. In terms of what caused the colour in the real sample, organic species would be expected to be present and support for this assertion was provided by the relatively high UV254 value shown in Table 3-4 for the real sample. In agreement, Le [82] analysed the composition of CSG associated water from the Narrabri Gas Project in New South Wales and found not only dissolved organic carbon (14.3 mg/L) but also algae (>600,000 cells/mL).

The presence of organic material is problematic in terms of downstream stability of the reverse osmosis desalination unit, and thus Le [82] employed biocides to control the algae growth and a microfiltration stage. De Julio *et al.* [164] reported that humic substances caused the true colour of aqueous samples to increase, and the

presence of such species in CSG associated water is considered plausible. Coagulation is usually a reliable method to reduce natural organic matter from water samples. Staaks *et al.* [165] evaluated the performance of both alum and ACH to reduce the organic content of three types of water samples from South Australia. These authors found that generally, alum was more effective than ACH for the water samples tested and that the reduction in organic content was between 31 and 52 %. Greater ability to reduce organic matter levels by alum was correlated to the degree of hydrophobic character of the organic material. Comparison of the true colour values for the high and low TDS CSG associated water samples revealed that the colour was lower as the salinity increased. This behaviour may be due to the greater dissolution of small floc material (<0.45 microns) in the high salt solution [163].
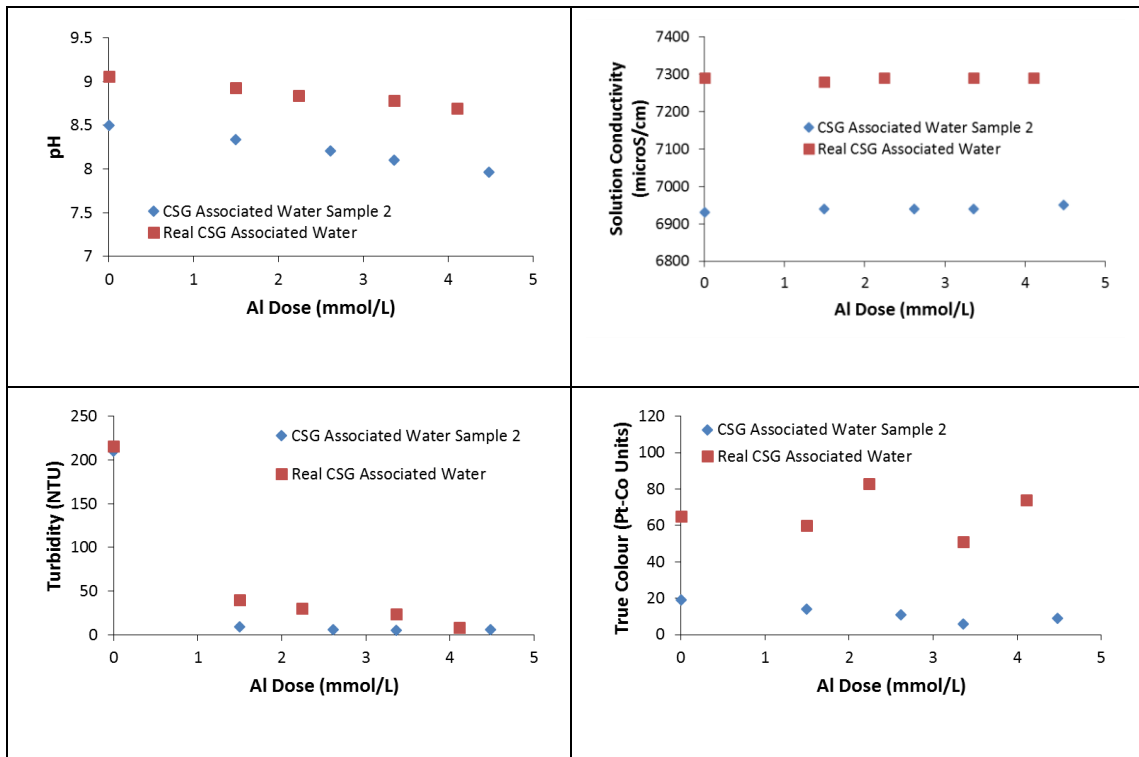
Figure 4-5: Solution changes as a function of ACH coagulant dose to simulated CSG associated water sample 2 and real CSG associated water
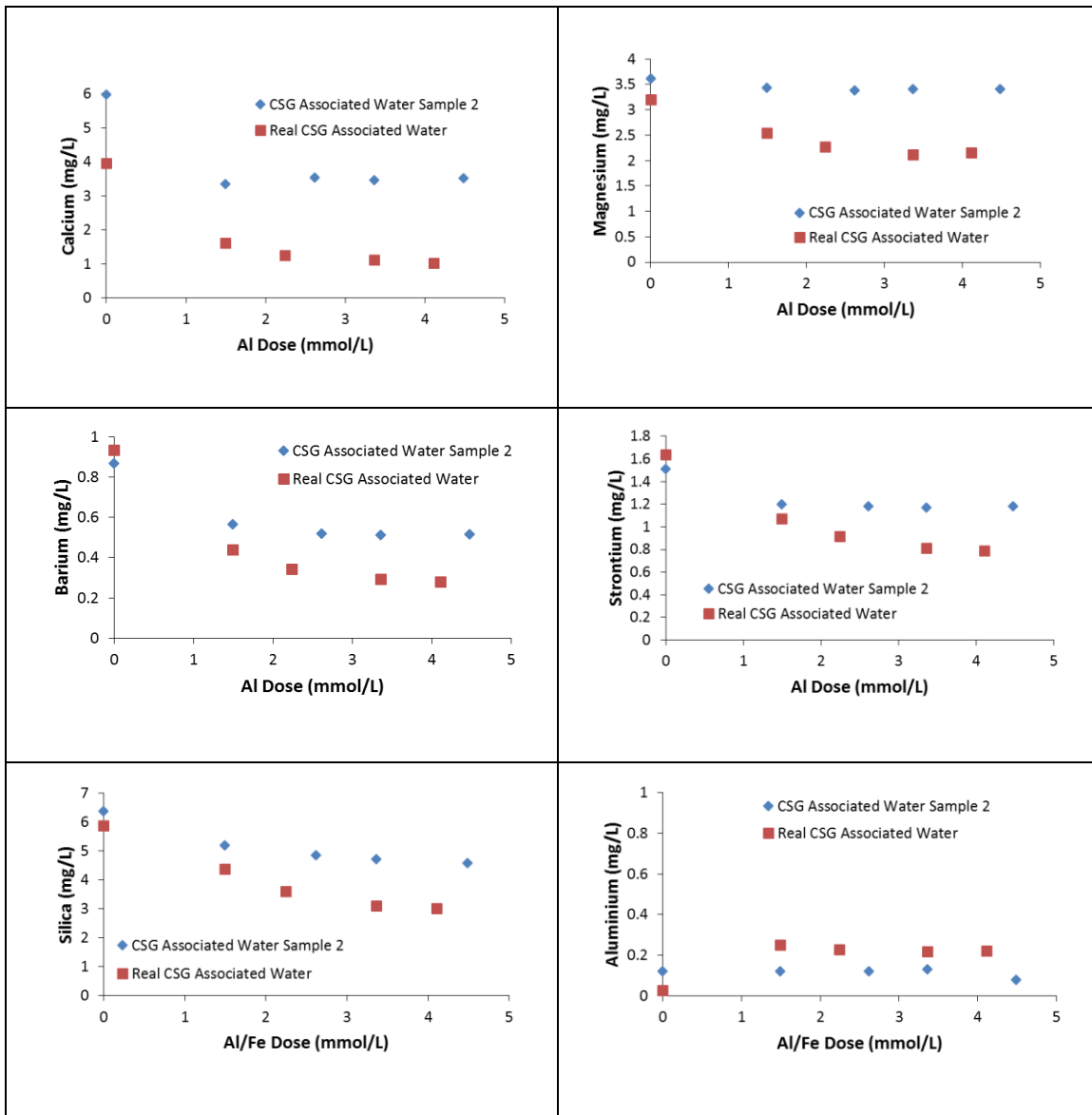
Figure 4-6: Impact of ACH coagulant dose rates upon dissolved species in CSG associated water sample 2 and real CSG associated water

Figure 4-6 shows the variation of dissolved ions in ACH treated water as a function of the coagulant dose. Overall, the removal of alkaline earth ions and dissolved silicates was promoted by the use of real CSG associated water compared to the simulated solution. As stated above, the major difference in the real water was the presence of dissolved organic carbon, with the inorganic ions being very similar in

concentration for both samples. Lin *et al.* [22] found that the coagulation performance of a real CSG associated water sample was inferior to simulated solutions. It was thus inferred that the presence of dissolved organic carbon inhibited the coagulation/flocculation process. The contrary results in this study suggested that the combination of turbidity and dissolved organic carbon was actually promoting the removal of dissolved species (Ca, Mg, Ba, B Sr and Si) from the CSG associated water. Hermosilla *et al.* [156] noted that organic species in solution can react with the inorganic ions from the coagulant. Xue *et al.* [166] discovered that the co-existence of silica and natural organic matter in river water influenced the characteristics of the floc. In particular, the formation of Al_b (polymeric) and Al_c (colloidal) species was promoted and the coagulation performance enhanced. Notably, the only instance where coagulation of real CSG associated water showed inferior performance was in relation to the presence of residual aluminium in solution. Kimura *et al.* [167] studied the removal of NOM in river water using aluminium based coagulants. A key finding was that the formation of residual aluminium in solution was correlated with the increasing presence of Al_a species (monomeric). Hence, it was concluded that with real CSG associated water samples the formation of Al_b and Al_c species was promoted and concomitantly the presence of Al_a was reduced.

Comparison of the dissolved species removal efficiency between the high and low TDS CSG associated water samples did not reveal any significant difference in the performance of the ACH coagulant. This observation was in harmony with the conclusion that the floc species were mainly stable in waters of the salinity range studied.
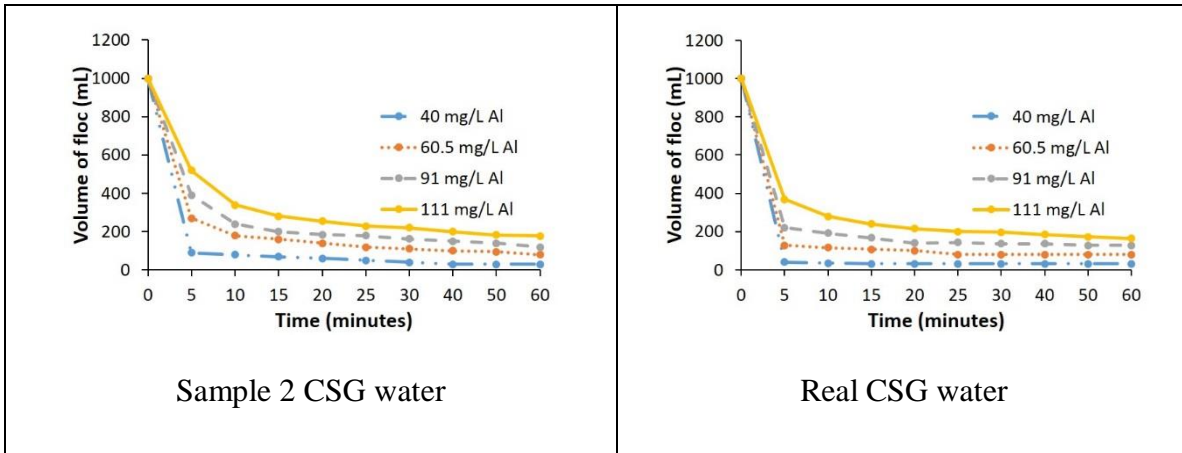
Figure 4-7: Floc settling rate of ACH treated CSG water
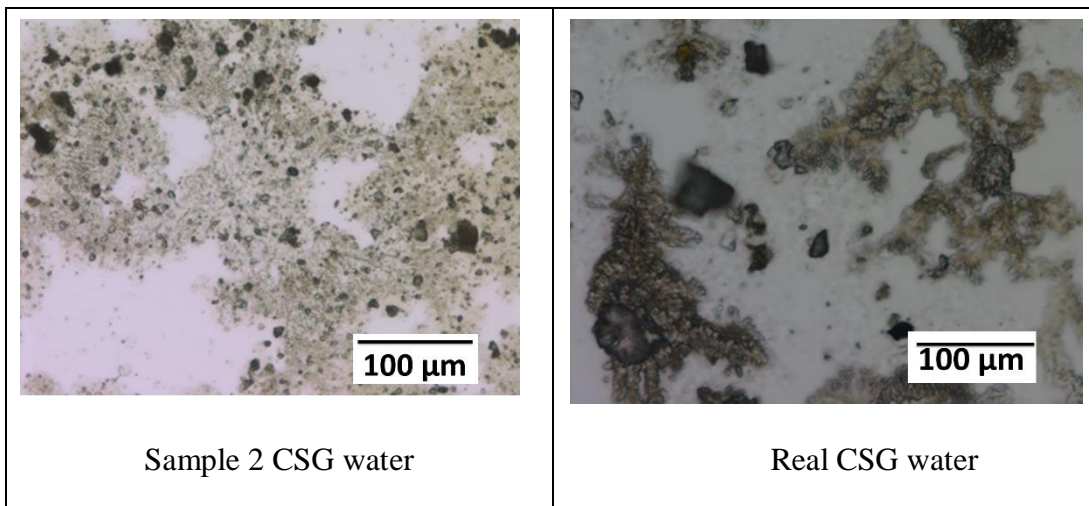
Figure 4-8: Optical microscopic images of ACH treated CSG water

The settling behaviour of the flocs formed by ACH addition to CSG associated water sample 2 and real CSG associated water was also examined [Figure 4-7]. In general, the final settled volume of flocs formed with either water sample was similar, and the time required for the flocs to settle satisfied typical commercial timeframes of 60 min or less. The most notable aspect was the more rapid settling of the flocs generated by ACH addition to real CSG associated water during the initial 10 min period. Figure 4-8 provided greater insight into the settling process as the optical

microscopy images revealed that the flocs from the real CSG associated water were denser than those for the simulated sample. The observation of ACH flocs which were different in shape from those shown in Figure 4-4 was consistent with the established view that variables such as pH and water composition influence floc structure and performance [168].

4.2.3 Effect of Turbidity Level in CSG Associated Water upon Coagulant Performance

The impact of turbidity level was also investigated in relation to coagulant performance when treating CSG associated water as this parameter is known to vary over a significant range in real CSG associated water samples [21]. Hence, three additional samples were prepared using real CSG associated water wherein: no additional kaolin was added ("no turbidity"); kaolin was added until turbidity was approximately 100 NTU (low turbidity); and finally, kaolin was dosed to give a turbidity of 800 NTU (high turbidity). ACH coagulant was dosed to the three samples of varying turbidity and the results shown in Figure 4-9. The changes in pH and solution conductivity were similar for all three water types regardless of the turbidity level.

Interestingly, the effectiveness of the coagulant was essentially unaffected by the extent of turbidity present, which was important in respect to the practical application where turbidity of CSG associated water was dependent upon the location of well, the residence time in storage ponds and climatic conditions [21]. It was observed that the true colour of the real CSG associated water was related to the amount of kaolin added to create turbidity. The trend was increasing turbidity as more kaolin was added, although not in a linear relationship. This observation indicated that

organic species were not the only source of colour in the water sample. The identity of the species causing the residual colour was not unequivocal. The true colour measurement involved the application of a 0.45 micron filter to the water sample; hence, if the kaolin was causing the detection of colour in solution then these materials would be of very fine size.

The data displayed in Figure 4-9 was also enlightening in relation to providing an insight as to how species such as alkaline earth ions and silicates were removed from the solution. One possibility for the reduction in alkaline earth ion concentration was the ion exchange of these ions with surface sites on the kaolin. For example, Ockert *et al.* [169] investigated the ion exchange properties of kaolin and calcium ions in a marine setting. Not only was the exchange relatively rapid (*ca.* 2 min) but also up to 20 % of the exchange sites were occupied by calcium ions even with the strong competition from the abundant sodium ions in the seawater medium. Gasco and Mendez [170] studied the exchange behaviour of calcium, magnesium, sodium and potassium ions with kaolin in aqueous solution. Magnesium and calcium ions were preferentially sorbed on the kaolin surface and the uptake of these ions was favoured by increasing pH (6.5 to 9) and greater initial concentrations in solution. Nevertheless, as shown in Figure 4-9 the data recorded was essentially the same whether kaolin was present or not in the CSG associated water sample. Hence, the reduction in the concentration of both alkaline earth ions and silicate species was due to not only the coagulant addition but also from Figure 4-6, the presence of organic matter. This latter conclusion supported the deduction that Al_b and Al_c species were promoted when both kaolin and dissolved organic carbon were present in the CSG associated water sample.
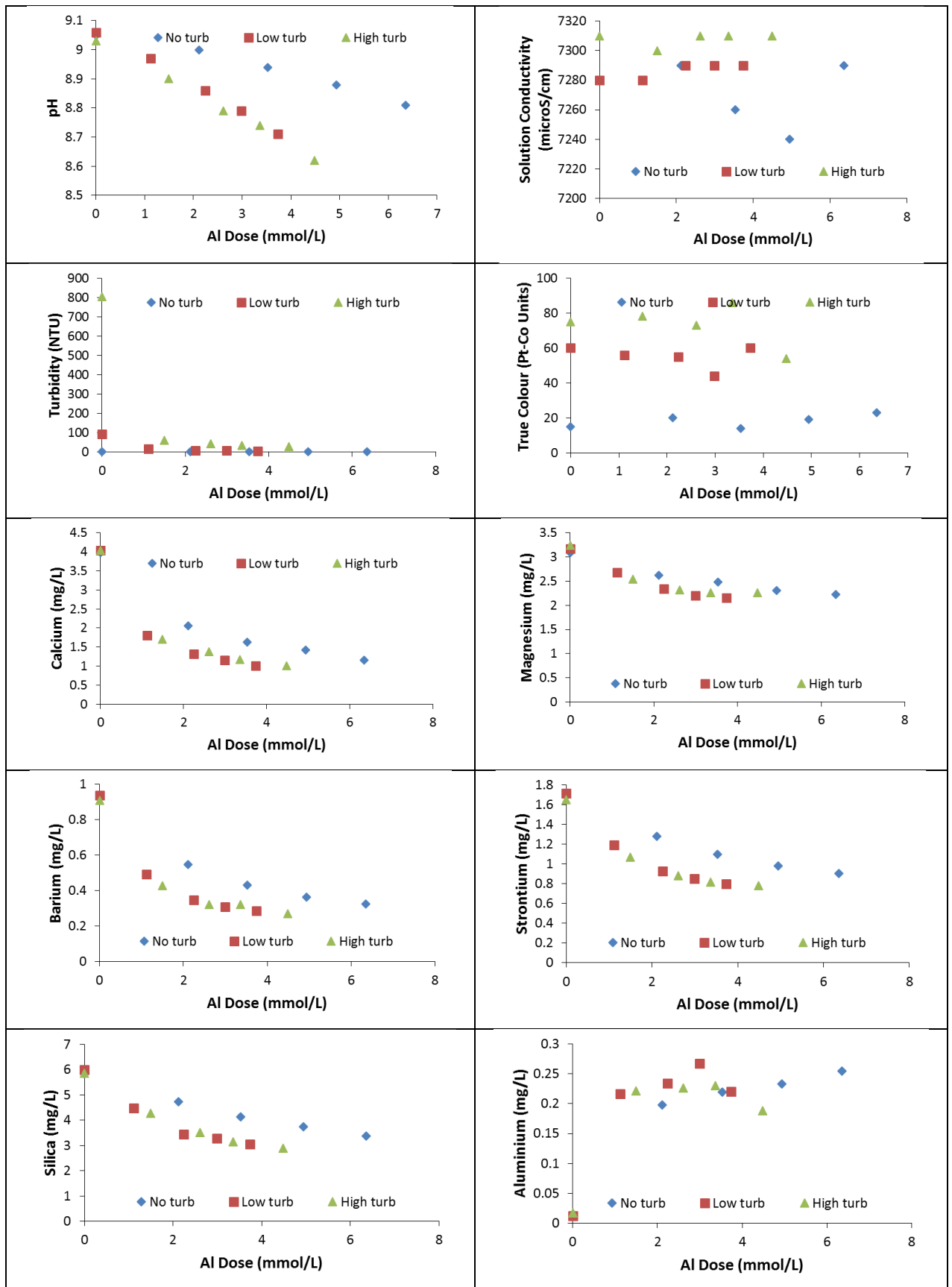
Figure 4-9: Impact of ACH coagulant dose rates upon characteristics of real CSG

associated water sample with different turbidity levels

4.3   **CONCLUSIONS**

Addition of inorganic coagulants can effectively reduce not only the turbidity of CSG associated water but also the presence of alkaline earth ions and dissolved silicates. All three coagulants studied were capable of reducing the content of alkaline earth ions. However, aluminium based coagulants were preferred in terms of their ability to promote the formation of aluminosilicates which were responsible for the reduction in dissolved silicate content of the CSG associated water. Modeling predicted that muscovite type minerals were formed due to the interaction of dissolved aluminium and silicate species. ACH did not introduce sulphate species to the CSG associated water unlike alum; therefore, this may be a preferable trait depending upon which downstream technologies are employed to desalinate the water sample.

The flocs produced by coagulant addition generally settled within 60 minutes. The alum based flocs were larger and fractal in character. However, problems were found in relation to the settling ability of flocs produced from both alum and ferric chloride addition to CSG associated water. Therefore, consideration must be given to not only the extent of turbidity and dissolved species removal from solution but also the practicality of floc separation from the treated water sample.

Coagulants performed equally as well under a wide range of turbidity values. A key finding was that the co-presence of kaolin and dissolved organic carbon in real CSG associated water promoted the formation of Al_b and Al_c species. The polymeric and colloidal forms of aluminium complexes in solution performed better than solutions where monomeric Al_a species were relatively more abundant. Simulated

solutions could not adequately mimic the range of organic species which may be in CSG associated water; hence, testing of real solutions was recommended.

The salinity of the CSG associated water did not appear to be a critical parameter with respect to coagulant performance. This observation suggested that coagulation processes may cope with the variation in CSG associated water quality expected in an actual CSG operation.

Coagulation is currently not a core technology for treating CSG associated water, yet this study has shown that it can be highly effective at reducing the impact of problematic alkaline earth ions and dissolved silicates which both can foul downstream membranes used for desalination.

Chapter 5: Electrocoagulation with Aluminium Electrodes for High-turbidity CSG Water Treatment

5.1 INTRODUCTION

For the past few decades, coal seam gas (CSG) (coal bed methane (CBM)) has been a rapidly growing industry in many regions [21, 36]. Worldwide reserves of CSG are estimated to be *ca.* 1.4 x 10^{14} m^3 and the United States of America, Canada, Australia, India, and China are the leading countries involved in CSG exploration and production [37]. Along with gas, associated water (CSG associated water) is also extracted as wells are depressurized in order to allow the gas to flow [1, 19]. Volumes of associated water in Queensland are currently 44 GL per year and may increase to 110 GL per year in the future [48, 49]. Most of this associated water requires pre-treatment before beneficial reuse as dissolved salt concentrations in the water are typically too high to comply with environmental regulations [1, 5]. Depending upon several factors CSG associated water composition varies greatly [21]. Dahm *et al.* [52] reported the major cations present as sodium, potassium, calcium, magnesium, strontium, barium, iron and aluminium. Whereas, anions of interest were chloride, bicarbonate, carbonate, fluoride, and bromide. Irrespective of the location the main constituents of coal seam gas produced water are chloride, sodium, and bicarbonate [21, 49, 52-54]. Another important CSG associated water quality parameter to consider is the turbidity level. Rebello *et al.* [21] analysed the water composition from 150 CSG wells located in the Surat Basin in Queensland. These authors found an average total suspended solids (TSS) value of 300 mg/L with the highest value of 7560

mg/L. Similarly, Benko and Drewes [66] examined a variety of produced water samples in the USA and reported that TSS levels could be as high as 1000 mg/L.

Desalination is the core treatment technology in relation to treating CSG associated water for beneficial reuse. Both ion exchange (IX) [73] and reverse osmosis (RO) [74, 75] are presently employed commercially to reclaim purified water from CSG associated water. Consequently, one must consider the impact of turbid water on the latter desalination methods. A range of pre-treatment processes are available for reducing the turbidity of water samples, *e.g.* chemical coagulation, electrocoagulation, ballasted flocculation, dissolved air flotation, microfiltration, and ultrafiltration [1, 34, 78-81]. Le [82] removed suspended solids from CSG associated water sourced in New South Wales, Australia using a combination of a treatment pond, disc filtration, and microfiltration. Alternatively, Carter [83] revealed that the QGC CSG associated water treatment facility located near Chinchilla in Queensland, Australia included an ultrafiltration stage.

Despite the demonstrated success of filtration technologies to control turbidity in CSG associated water, there is a need to also remove dissolved species such as alkaline earth ions and silicates. These species can cause problems such as scale formation and membrane fouling which ultimately result in a decrease in water treatment plant performance [84, 85]. Ion exchange softening can be employed to reduce the alkaline earth ion content of the CSG associated water [86]; albeit, this method requires the onsite storage and handling of substantial amounts of potentially hazardous acid and alkali. Coagulation is well proven for a reduction in the suspended

solid content of wastewater [87], but the removal of dissolved ions from CSG associated water is more challenging [22, 23].

Therefore, alternate technologies which can remove both turbidity causing species and dissolved ions responsible for scale formation are desirable. Electrocoagulation (EC) has been employed to treat coal seam gas associated water prior to the central desalination technology [34]. EC involves the dissolution of primarily aluminium or iron based anodes and subsequent formation of metal hydroxide flocs [171]. EC appears to be prospective for this application as it has been shown to be capable of significantly reducing the concentration of scale forming species such as calcium, magnesium, strontium, and silicates present in the CSG associated water to low levels [135, 172]. However, the influence of turbidity upon the ability of EC to remove both suspended solids and dissolved species is as yet unknown. Nevertheless, there is significant literature which describes the applicability of EC to other wastewater types for suspended solids reduction. For example, Bellebia *et al.* [173] used EC to remove 99.93 % of turbidity when treating cardboard paper mill effluent. Similarly, Chou *et al.* [174] reduced the turbidity of chemical mechanical polishing wastewater by 98 %.

In terms of EC operation, there are some key factors which need to be addressed which have received insufficient attention in the literature (albeit, for practical use, these parameters are highly pertinent). It is widely reported that during EC operation the electrodes can become passivated with an oxide film [130]. Hence, strategies to clean the electrode surface have been introduced such as polarity reversal; which involves switching the polarity of the electrode plates from "positive" to "negative" at

prescribed time intervals. Gobbi *et al.* [131] employed a polarity reversal time (PRT) of 10 s when treating oily water using an EC unit equipped with aluminium electrodes. However, these authors did not investigate the impact of decreasing or increasing the polarity reversal period upon EC performance. As indicated by Wellner *et al.* [132] the polarity reversal time is important with respect to minimization of electrode passivation. In their study, they discovered that a 3 minute PRT was optimal when electrocoagulation was conducted with sodium chloride solutions and used aluminium electrodes. This finding was in harmony with the idea of Fekete *et al.* [133] that a certain time was required in order for the passivated layer to be removed from the electrode surface. Timmes *et al.* [134] also intimated that the PRT required to be adjusted in order to maintain the performance of a pilot plant electrocoagulation system employed to pre-treat seawater prior to a reverse osmosis desalination stage. In terms of EC treatment of CSG associated water, published studies both reported use of a fixed PRT of 30 s [135, 136]; and hence there is a need to examine the influence of PRT upon water treatment performance.

Another key parameter with regards to EC performance is the hydraulic retention time (HRT) in the EC unit. Often the influence of HRT upon EC performance has been evaluated for batch systems [137]; however, continuous EC units are more relevant to practical application as they offer greater throughput of water. Amani *et al.* [138] studied a continuous EC process for compost leachate remediation. HRT was discovered to be an important parameter in terms of chemical oxygen demand (COD) and total suspended solids (TSS) removal. HRT was tested in the range 30 to 90 minutes and the optimal value was determined to be 75 minutes. In contrast, Mores *et al.* [139] investigated the use of both aluminium and iron electrodes for the EC

treatment of swine wastewater. These authors reported that HRT did not have a significant impact upon turbidity removal which was attributed to the dominating influence of current density. Alternatively, Kobya *et al.* [140] described substantial diminishment in the ability of an EC unit to remove COD, turbidity and total organic carbon (TOC) from dyehouse wastewater as the hydraulic retention time was reduced. Notably, previous literature relating to EC purification of CSG associated water has not investigated the impact of HRT upon the effluent water quality, with only 30 s HRT data reported [135, 136]. Therefore, elucidation of the effect of increasing or decreasing HRT for CSG associated water treatment would be beneficial with regards to EC process optimization.

At present, no published studies currently exist in relation to the effectiveness of EC to treat CSG associated water which comprises of high levels of turbidity. Therefore, the objective of this study was to investigate the ability of EC to remove turbidity causing species from CSG associated water and examine the influence of turbidity causing species upon the usefulness of EC to remove dissolved ions. The underlying hypothesis was that EC could prove to be a versatile method for reducing not only suspended solids but also dissolved species from CSG associated water; thus, potentially simplifying the overall water treatment process design. Consequently, the following questions were addressed to support the latter hypothesis: (1) can EC effectively remove turbidity causing moieties from CSG associated water? (2) how does polarity reversal time influence EC treatment performance?; (3) what is the effect of hydraulic retention time upon the removal of suspended solids and dissolved species in CSG associated water? and (4) what are the recommended experimental conditions for application of electrocoagulation to pre-treat CSG associated water prior to a

reverse osmosis desalination stage. To answer the aforementioned questions a bench-top electrocoagulation unit equipped with aluminium electrodes was employed which comprised of multiple electrodes and was operated in continuous mode.

5.2 RESULT AND DISCUSSION

5.2.1 Impact of Hydraulic Retention Time (HRT) upon Electrocoagulation Performance

A series of tests were conducted wherein CSG associated water with turbidity of 434 NTU (created by kaolin addition), was treated by the EC unit equipped with aluminium electrodes at various flow rates; which resulted in retention times in the EC unit of 20, 30, and 60 s. The aim of these experiments was to understand whether the removal of turbidity causing species and dissolved ions such as alkaline earth ions and silicates were impacted by the time of residence in the EC unit.

5.2.1.1 Variation in Effluent pH and Turbidity of Treated CSG Associated Water

Figure 5-1 shows the variation in treated CSG associated water pH and turbidity after EC treatment as a function of hydraulic retention time. Solution conductivity did not exhibit substantial changes as a function of HRT when treating the CSG associated water (results not shown for sake of brevity) which was consistent with earlier research which reported that conductivity was not significantly influenced by EC treatment [34]. The pH of the EC treated CSG associated water sample exhibited a notable increase as the HRT period was increased, from a starting value of 8.58 to 10.81 for the 60 s retention time solution. Mores *et al.* [139] explained this process as a function of aluminium hydroxide production; essentially the longer the water stayed in the reactor the concentration of alkaline species increased and thus elevated solution pH.
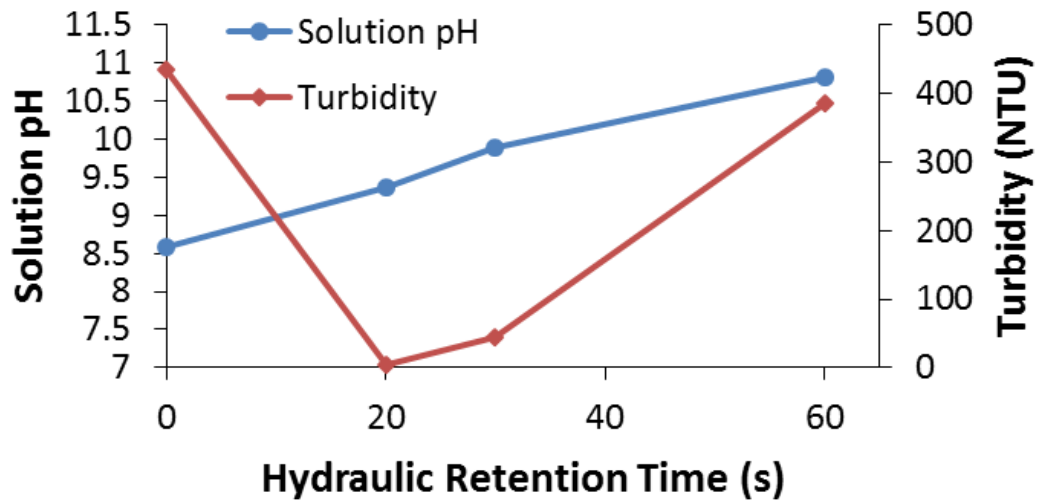
Figure 5-1 Impact of hydraulic retention time upon effluent pH and turbidity of EC treated CSG water sample; polarity reversal period 3 min; test time 40 min

The highest turbidity removal (99.0 %) was recorded when the HRT was 20 s. Notably, as the HRT was increased the turbidity reduction was diminished to 90.0 and 11.3 % for 30 and 60 s retention periods, respectively. Correspondingly, the Apparent Colour of the EC treated sample was initially 1550 Pt-Co units and this decreased to 66 Pt-Co units when a 20 s retention time was employed but then increased to 550 and 1640 Pt-Co units for retention times of 30 and 60 s, respectively (which paralleled the turbidity trend as a function of HRT). Notably, the True Colour was 0 to 1 Pt-Co units for these treated samples which meant that the particles were > 0.45 microns in size.

Mores *et al.* [139] examined the ability of a continuous electrocoagulation process to treat swine wastewater produced after up-flow anaerobic sludge blanket digestion of swine manure. In this study, the authors changed hydraulic retention time from 31.8 to 88.2 min and concluded that this parameter did not significantly impact

the removal of turbidity causing species. Instead, they demonstrated that current density was the major factor which influenced EC performance. However, it was noted that the low turbidity in the starting solution may have been a reason why the HRT value was not important in this situation. Benazzi *et al.* [175] studied the ability of an EC unit equipped with aluminium electrodes to treat simulated dairy wastewater. Again, HRT values were in the order of hours (0.5 to 1.5 h) and not a minute or less as employed in this investigation. Longer retention times were found to promote turbidity removal. It was suggested that the increased dissolution of aluminium ions into the wastewater resulted in greater floc formation and thus improved turbidity removal. Also, the lower flow rates used when increasing the HRT would have reduced turbulence in the EC unit and thus potentially promoted the flotation process. Mahesh *et al.* [176] also used a continuous EC unit but in this instance, they treated wastewater from a pulp and paper mill. With a residence time in the region 2 to 4 h, the turbidity was reduced from an initial value of 182 NTU to less than 10 NTU. However, when the residence time was limited to 0.5 h the turbidity actually increased to 418 NTU. Observation of optimum residence time for the feedstream in an EC unit in relation to maximising turbidity reduction has also been reported by Moosavirad [177]. After 5 min contact time, the turbidity of a greywater sample from a village in Iran actually increased in turbidity before decreasing as the operational time was elongated.

Based upon the above literature evaluation, the fact that turbidity removal was related to the hydraulic residence time of the CSG associated water in the EC unit was not unexpected. However, the decrease in turbidity removal with longer hydraulic retention time was initially surprising. Nevertheless, it was also evident that the

performance of the EC was not impacted significantly at high pH values. Therefore, it can be concluded that the majority of the flocs were still present (confirmed in Section 5.2.1.2). An explanation for the upward trend in the turbidity level when using a retention time greater than 20 s was the presence of suspended flocs in the treated water sample. Section 5.2.1.4 illustrates the fact that flocs produced at longer HRT values tended to float and thus when the water was sampled for turbidity analysis it was entirely plausible that the turbidity measured was majorly due to the presence of the floc material which did not settle.

5.2.1.2 Variation in Residual Aluminium, Floc Mass, and Electrode Consumption

In relation to the aforementioned discussion in Section 5.2.1.1, it was pertinent to investigate whether residual aluminium in the treated CSG associated water was related to HRT, and also how electrode consumption and floc formation was impacted [Figure 5-2]. The residual aluminium content in the treated CSG associated water did indeed show an increasing trend as the HRT value was increased. The aluminium concentrations were 28.5, 31.4, & 86.4 mg/L for retention times of 20, 30 and 60 s, respectively. Therefore, this data was consistent with the hypothesis that at longer HRT values the elevated solution pH promoted dissolution of a fraction of the aluminium flocs. However, it was also observed that both the electrode consumption and floc mass produced were enhanced by the longer residence times of the feed solution in the EC unit. For example, the electrode consumption increased from 0.46 to 1.46 g/L of CSG water treated when HRT changed from 20 to 60 s. Likewise, the floc mass grew from 1.85 to 4.78 g/L when HRT changed from 20 to 60 s.
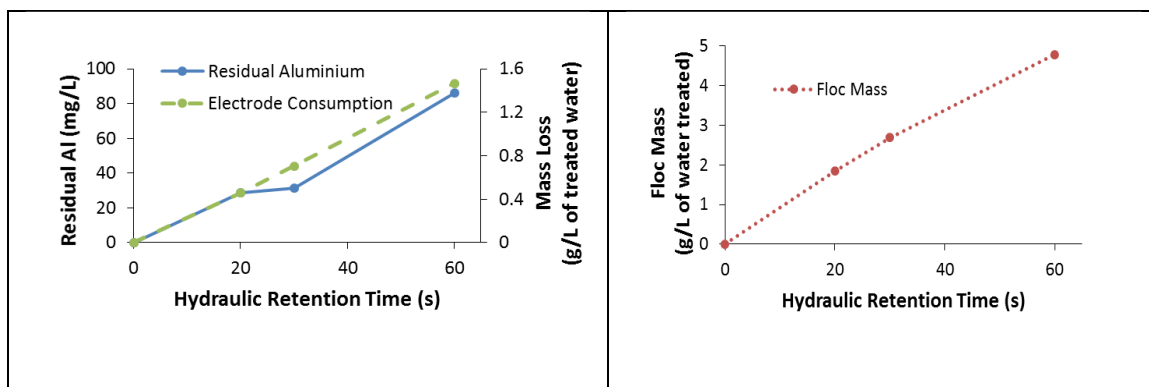
Figure 5-2: Impact of HRT upon residual aluminium, floc mass formed and electrode consumption for CSG water sample; PRT 3 min; test time 40 min

The question arises as to why the consumption of electrode material was promoted by increasing the HRT value. Closer inspection of the electrode consumption data shows that as the HRT was tripled in value the electrode consumption also increased by a factor of *ca.* 3.2. Likewise, the floc mass increased by *ca.* 2.6 and residual aluminium by *ca.* 3.0 when HRT was increased from 20 to 60 s. Consequently, we can assume that in terms of these outlined parameters a simple relationship existed wherein the longer the water resided in the EC unit the electrode mass loss, floc production and residual aluminium formation correspondingly directly increased.

In theory, if all aluminium dissolved from the electrodes was hydrolysed to aluminium hydroxide ($Al(OH)_3$) then the ratio of floc mass to electrode consumed would be 2.89. Measured values in this study corresponded to ratios of 4.02, 3.82, and 3.27 for HRT values of 20, 30 and 60 s, respectively. Examination of the solution pH may provide a reason for the decreased production of flocs relative to electrode consumed. With aluminium electrodes, it is well known that at a pH of *ca.* 9 or greater soluble $Al(OH)_4^-$ species can form. When the HRT was increased to 30 s the pH was

elevated to 9.89 and 60 s HRT further raised the pH to 10.81. Therefore, some of the floc was expected to have transformed to soluble $Al(OH)_4^-$ species. In fact, at high pH, Al^{3+} may simply form aluminate ions in the solution below the solubility of $Al(OH)_3$ [178] and subsequently the recorded floc mass relevant to electrode mass consumed was reduced as HRT increased. In harmony with this interpretation of the data was the corresponding increase in residual aluminium detected in the treated effluent.

Additional information regarding the electrode mass loss can be gained from the inspection of the wear profiles of each electrode in the EC unit [Figure 5-3]. The general trend was that increasing HRT promoted the dissolution of each electrode in the electrocoagulation unit. In all cases, the mass loss recorded for the outermost electrodes was approximately 50 % of the value for other electrodes. This observation reflected the fact that one half of the electrode was adjacent to the wall of the EC unit and not in contact with the electrolyte. Similar to the data reported by Wellner *et al.* [132] the greatest mass loss occurred for electrodes 2 and 12 which presumably incurred the highest electrical loads due to the bipolar configuration employed. The heterogeneous distribution of electrode wear has also been reported by Cesar Lopes Geraldino *et al.* [179] and has significance in terms of the practical consumption of electrode material. If all the electrode cannot be consumed due to loss of structural integrity then the amount of electrode required to treat the water sample may be substantially greater than estimated from laboratory tests.
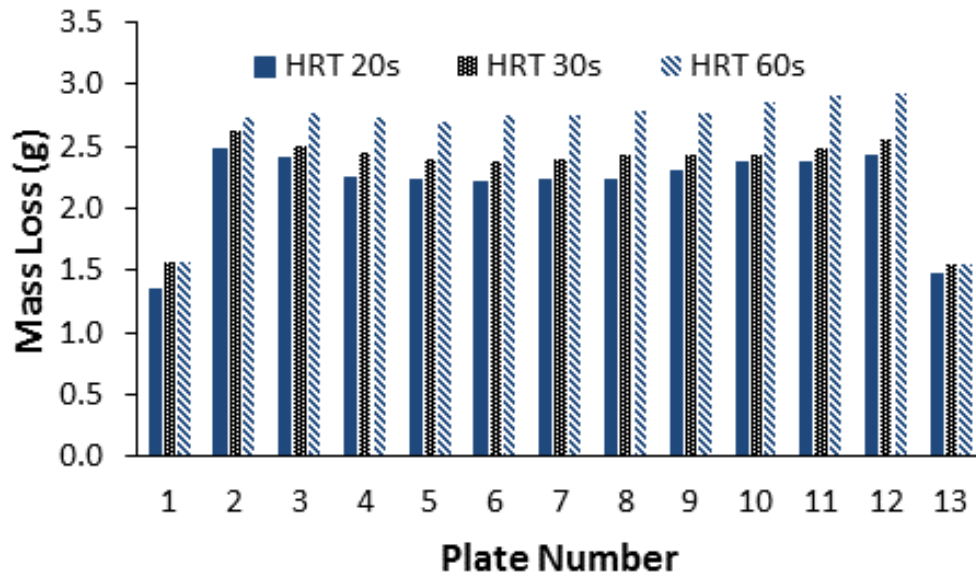
Figure 5-3: Electrode mass loss as a function of hydraulic retention time

A relationship between electrode loss and calculated theoretical mass loss from the Faraday expression was apparent in Table 5-1. As the HRT value increased the excess of electrode consumed also increased (15 % for HRT 20 s; 21 % for HRT 30 s; 36 % for HRT 60 s). Mechelhoff *et al.* [180] reported that amounts of aluminium dissolved into solution exceeded that estimated from the amount of electrical current supplied (termed super-Faradaic behaviour). The quantity of excess aluminium released into solution was related at least in part to the concentration of sodium chloride present; with higher concentrations promoting the chemical dissolution of the electrodes. Enhancement of pitting on the electrode surface by chloride ions was envisaged as one possible reason for the acceleration of the chemical dissolution process. Sari and Chellam [181] observed super-Faradaic phenomena when they treated hydraulic fracturing water with an EC unit equipped with aluminium electrodes. Again the influence of the substantial amount of chloride ions present in solution was proposed to promote chemical dissolution at the electrode surface. From

our data, it was revealed that extending the HRT increased the extent of chemical dissolution. This behaviour suggested that a certain time was required for the reaction of chloride ions with oxide/hydroxide species on the electrode surface to occur.

Table 5-1 Summary of experimental data CSG produced water was treated by electrocoagulation using aluminium electrodes and continuous run for 40 min (PRT 3 min)

HRT	20 s	30 s	60 s
Flow Rate (L/min)	1.540	1.072	0.577
Floc Mass (g/L)	1.85	2.69	4.79
Average Electrode Loss (g/L)	0.46	0.70	1.46
Theoretical Mass Loss (g/L)	0.40	0.58	1.07
Average Current (A)	9.17	9.3	9.17
Average Voltage (V)	30.29	31.07	30.29
Power consumption/Volume of Water Treated (kWh/kL)	3.01	4.49	8.02
Average Current Density (mA/cm^2)	5.09	5.17	5.09
Residual Aluminium (mg/L)	28.52	45.51	86.35

The recorded pH of the effluent can be revisited at this stage in light of the finding that the chemical dissolution process was facilitated by increasing HRT values. It was evident in Figure 5-2 that the increase in solution pH between for example 30 s HRT (pH = 9.89) and 60 s HRT (pH = 10.81) could not simply be explained on the basis of production of greater floc quantities. Doubling the floc quantity resulted in an order of magnitude increase in effluent pH. Thus an explanation for the additional

hydroxyl species required to be present was necessary. As outlined by Sari and Chellam [181] the dissolution process can be summarized as shown in Equation 5-1.

Equation 5-1 $\qquad 2\,Al^o\,(s) + 6\,H_2O \leftrightarrow 2\,Al^{3+}\,(aq) + 3\,H_2\,(g) + 3\,OH^-\,(aq)$
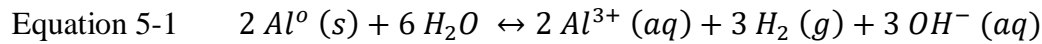
Importantly, it can be seen that the more chemical dissolution which happens the greater the solution pH will be due to the evolution of hydroxide ions.

5.2.1.3 Variation in Alkaline Earth Ions, Boron, and Silicates

As per the findings of previous researchers the removal of singly charged ions such as sodium, potassium, and chloride was not found to be significant when applying electrocoagulation to CSG associated water [34]. Therefore, Figure 5-4 shows only the data for species which were recorded to decrease when EC tests were conducted on the CSG associated water sample.

It was apparent that electrocoagulation using aluminium electrodes was effective for the removal of alkaline earth ions in the presence of turbidity causing materials. For the alkaline earth ions and silicates, the HRT value generally promoted the degree of removal. Brahmi *et al.* [182] noted comparable behaviour when they studied the electrocoagulation of phosphate mining process water using aluminium electrodes. As the HRT increased in this study, magnesium removal was 95.3, 98.4, and 99.2 % for HRT of 20, 30, and 60 s, respectively. As already mentioned, Figure 5-1 showed that pH increased from 8.58 to 10.81 with the increase of HRT. It is known that magnesium hydroxide precipitates at a pH of *ca.* 10.2 [183]; hence, this process may at least partially explain why magnesium ions were removed from the solution. However, as discussed by Jagati *et al.* [184] precipitated aluminium hydroxide

material can also effectively remove dissolved magnesium ions by sweep flocculation at lower pH values (such as 7.5). Similarly, calcium ions were also effectively removed from the CSG associated water using electrocoagulation [Figure 5-4]. As a general observation, the removal of calcium ions from the CSG associated water was actually slightly less than that recorded for magnesium ions (highest removal efficiency 97.5 %). This result indicated that simple precipitation of either calcium carbonate or magnesium hydroxide was not the only mechanism involved for remediation of these species (calcium carbonate can precipitate at a pH of *ca.* 9.4 [24, 185]). Therefore the concept of sorption of alkaline earth species on flocs *via* sweep flocculation phenomena such as electrostatic interaction was reinforced.
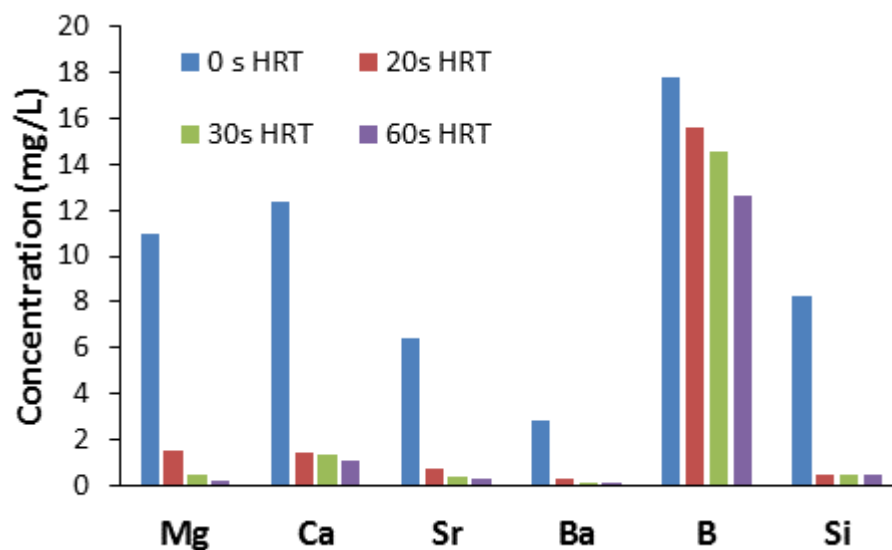
Figure 5-4: Concentration of dissolved species in CSG associated water before and after EC treatment; polarity reversal period 3 min; test time 40 min

Strontium was also majorly removed using electrocoagulation, with the degree of remediation increasing with greater HRT (93.6 % at a HRT of 60 s). In harmony, Parga *et al.* [186] observed almost complete removal of strontium ions from solution

when using iron electrodes in an EC unit. Murthy and Parmar [187] reported strontium removal values which were significantly less than recorded in this study. However, it was noted that the inter-electrode distance was 6 cm whereas this investigation had an electrode separation of 0.3 cm. Kamaraj and Vasudevan [188] found that the smaller the inter-electrode distance the greater the removal efficiency of strontium measured. Comparable to this study these authors reported *ca.* 97 % elimination of strontium from solution using electrocoagulation at an inter-electrode distance of 0.2 cm. Barium removal was always above 96.6 % and again positively influenced by increasing HRT. de Oliveira da Mota *et al.* [189] applied an electroflotation method to treat water contaminated with heavy metals ions resultant from washing soil samples. In excess of 90 % removal of barium ions was reported in the pH range 6 to 10, albeit no mechanism for this phenomena was provided.

Boron removal efficiency was 12, 18 and 29 % for HRT of 20, 30 and 60 s, respectively. Dolati *et al.* [190] reported that EC using aluminium electrodes could remove up to 70 % of boron species from solution, which was significantly greater than the values obtained in this study. However, it was noted that the removal efficiency was influenced by the initial concentration of boron in the sample. As the boron concentration was reduced from the optimal value of 100 mg/L the effectiveness of electrocoagulation was diminished (*ca.* 50 % reduction when initial boron concentration was 10 mg/L). In addition, if sodium carbonate was present in solution further inhibition was recorded (*ca.* 25 % reduction in boron removal). Furthermore, solution pH has also been demonstrated to impact the extent of boron removal from solution. As summarized by Millar *et al.* [136] a pH of 9 or greater results in the formation of negatively charged tetrahydroxyborate species which may not sorb to

negatively charged aluminium hydroxide flocs. Therefore, boron remediation would again be inhibited. In the CSG associated water sample not only was the pH highly alkaline (>8.3) in all cases which meant that carbonate species would be prevalent but also the initial concentration of boron was only 16.9 mg/L. Hence, the relatively low efficiencies determined for boron removal from CSG associated water were in line with the physical parameters of the solution. The enhancement in boron removal as a function of HRT needs to be considered carefully. The increase in solution pH as HRT was extended may have been expected to inhibit boron removal (yet, boron remediation was improved). Dolati *et al.* [190] found that another parameter was important with respect to boron removal using electrocoagulation, namely reaction time. These authors discovered that the degree of boron removal could be increased by *ca.* 300 % by tripling the reaction time in the EC cell. This data was consistent with our data which also indicated that increasing reaction time was not only critical but also could minimize the negative effect of increased solution pH.

In contrast to the data collected for the alkaline earth ions and boron, silicate removal from the CSG associated water was not significantly impacted by a change in HRT (*ca.* 98.2 % for all samples) [Figure 5-4]. This result inferred that the silicate removal mechanism was inherently different from that for the alkaline earth ions and boron. Recently, Hafez *et al.* [191] also noted that silica removal efficiency using EC was relatively independent of reaction time, in contrast to alkaline earth ion removal which was promoted to a greater degree when the reaction time was increased. Den and Wang [192] suggested that in neutral solutions, silicates were removed in the form of aluminosilicates [Equations 5-2 & 5-3].

Equation 5-2: $2 \, Al \, (III) + 2 \, Si(OH)_4 + H_2O \leftrightarrow Al_2Si_2O_5(OH)_3{}^{2+} + 6H^+$

Equation 5-3: $Al \, (III) + Si(OH)_4 + H_2O \leftrightarrow AlOSi_2O_5(OH)_3{}^{2+} + H^+$
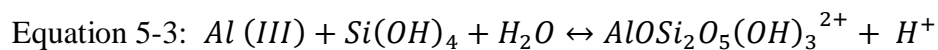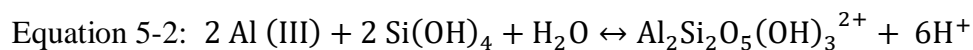
However, in this case, the treated CSG associated water samples had a pH in the range of 8.58 to 10.81. Cheng *et al.* [152] indicated that at a pH less than 9.5 the dominant silica species was silicic acid ($Si(OH)_4$) and that above this critical pH the transformations illustrated in Equations 5-4 & 5-5 occurred. Interestingly, despite the change in the chemical form of the silicate species as a function of HRT (increasing solution pH), the degree of silicate reduction did not vary.

Equation 5-4: $Si(OH)_4 \leftrightarrow H_3SiO_4{}^- + H^+$

Equation 5-5: $H_3SiO_4{}^- \leftrightarrow H_2SiO_4{}^{2-} + H^+$
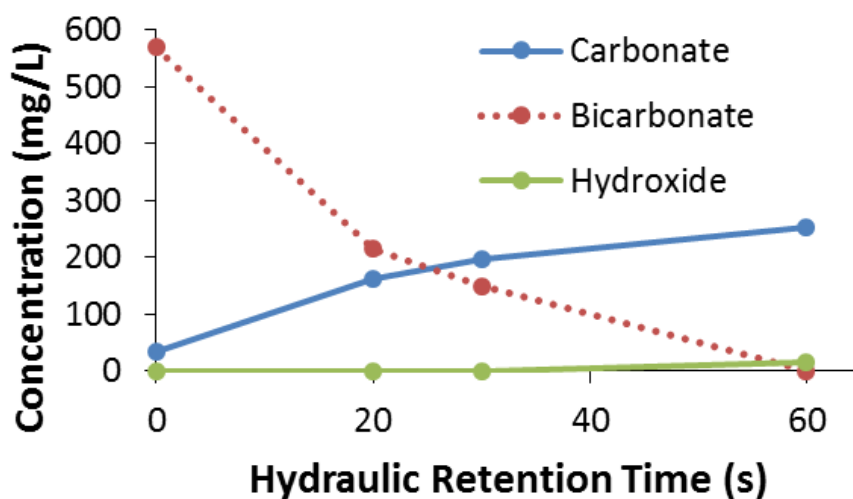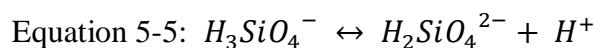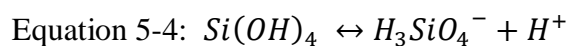
Figure 5-5: Impact of HRT on the alkalinity of CSG associated water treated using electrocoagulation

Figure 5-5 shows that the alkalinity composition was contact time dependent, with the general trend being that as HRT increased the concentrations of carbonate and hydroxide species increased. This observation correlated with the increasing pH of the solution and was consistent with the well-known stability of bicarbonate, carbonate and hydroxide species as a function of pH [193].

5.2.1.4   Floc Settling Behaviour and Characterization

The CSG associated water prior to EC treatment was white in colour due to the presence of suspended kaolin. In contrast, the treated water was light grey in colour and comparatively more viscous in character. Figure 5-6 displays the settling behaviour of the various effluents produced after the EC process operating with various HRT values. An important aspect of electrocoagulation was revealed, namely, the challenge associated with the settling of flocs produced.
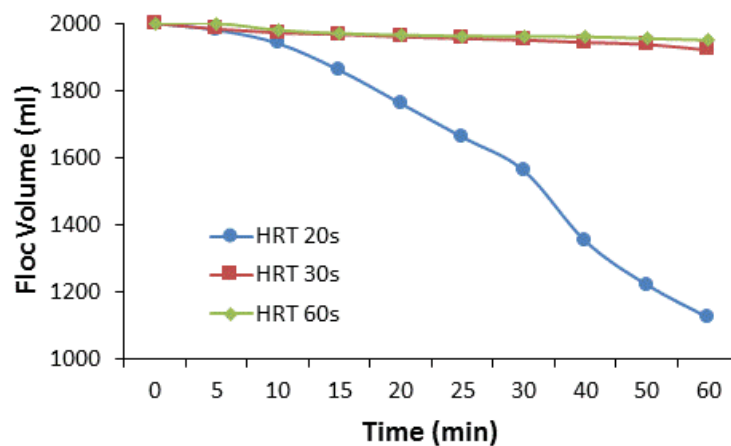
Figure 5-6: Floc sedimentation rate as a function of HRT applied during electrocoagulation of CSG associated water

Notably, only the flocs formed at a retention time of 20 s displayed significant settling within the one hour test period. Flocs formed at longer residence times, in contrast, exhibited minimal settling which suggested that the physical properties of

these materials were different from those created with a shorter HRT value. Brahmi *et al.* [194] indicated that a drawback of the electrocoagulation method was not only the production of relatively large sludge volumes but also issues with extended settling time periods. Hence, these authors advocated the use of a ballasted electroflotation method involving the addition of micro-sand and polymer to aid settling of the flocs.

Flocs formed during electrocoagulation have been shown to be different than those which are created from a conventional coagulation process. Lee and Gagnon [195] concluded that flocs from chemical coagulation were relatively bigger and denser than those created by EC. Therefore, if sedimentation was the desired means of solid/liquid separation then it could reasonably be expected that EC derived flocs may be relatively problematic. In relation to this argument further insight was gained by examination of the flocs by optical microscopy [Figure 5-7]. In general, the flocs appeared of low density when an HRT of 20 s was used in the electrocoagulation tests. Capture of the kaolin particles in the floc structure was apparent as seen by the darker areas superimposed on the lighter floc material. The flocs formed at 30 s HRT were similar to those for the 20 s HRT test, albeit there was some evidence for a "ridge-like" structure beginning to develop. This structure was considerably more visible for the floc material generated with a 60 s retention time. Not only was the floc denser in accord with the greater mass of floc produced but also the "ridge-like" material was more prevalent. The floc materials have also coalesced into a network construction. In terms of the differences in settling behaviour of the flocs created as a function of HRT, some features were noted. Firstly, the flocs generated at 20 and 30 s were broadly similar in appearance yet the 20 s HRT material settled substantially faster than that created with a 30 s HRT value. In the case where flocs were discernibly

different (30 s and 60 s HRT products) neither material exhibited any significant settling.

20 s HRT

30 s HRT

60 s HRT

Figure 5-7: Optical microscopy images of flocs formed as a function of HRT when CSG associated water treated with electrocoagulation

It appears that an alternate factor is influencing the settling rate of the flocs other than floc shape/density. The impact of hydrogen bubbles formed at the cathode during electrocoagulation of aqueous solutions should also be considered. Hakizimana *et al.* [196] described the use of electrocoagulation to pre-treat seawater prior to a desalination stage. The produced hydrogen bubbles (*ca.* 50 to 100 µm in size) were found to aid the separation of flocs from the seawater by means of the electroflotation process: wherein flocs attached themselves to the bubble surface. In contrast, for the flocs formed at 30 and 60 s in this study the hydrogen bubbles did not separate the flocs from the liquid, instead, they remained dispersed throughout the settling vessel. This behaviour suggested several possible factors may be important with regards to the solid/liquid separation process. First, the EC cell design used in this study was different in configuration from that employed by Hakizimana *et al.* [196], albeit both were operated in continuous mode. Hakizimana *et al.* [196] provided images which indicated that the hydrogen bubbles were distributed across the entire electrode surface in their EC unit. It may be that the serpentine electrode arrangement used by these authors was more beneficial than the parallel plates used in this study. In addition, the density/shape of the flocs produced when treating CSG associated water may differ from those formed when treating seawater using EC. In relation to this idea, the turbidity of the CSG associated water was relatively high (434 NTU) and the trapped kaolin particles could plausibly have made the flocs sufficiently dense to resist flotation. Moreover, an extension of the HRT value inherently increased not only the concentration of flocs but also evolved hydrogen bubbles. Hence, the 20 s HRT flocs were buoyed by the least amount of hydrogen bubbles and evidently, the floc density/shape was conducive to settling overriding the flotation phenomenon. In contrast, hydrogen bubble concentration was such for the 30 and 60 s flocs that the

driver for settling was overcome by the buoyant force of the hydrogen bubbles (regardless of floc structure).

5.2.2 Impact of Polarity Reversal Time (PRT) upon Electrocoagulation Performance

5.2.2.1 Variation in Effluent pH, Residual Aluminium, Floc Mass, Electrode Consumption and Turbidity of Treated CSG Associated Water

Figure 5-8 shows the variation in treated CSG associated water pH and turbidity after EC treatment as a function of PRT. Overall, the pH of the treated water increased with the increase of PRT, from an initial pH of 8.58 to 9.68 for 5 min PRT. Wellner *et al.* [132] also found that the solution pH was greater as the PRT was increased, as did the magnitude of the pH oscillation recorded.

Concomitantly the cell resistance (as evidenced by the trend in voltage required at the approximately same current conditions) was slightly increased when the PRT was changed from 1 to 5 min which suggested that the surface became slightly more passivated by an oxide/hydroxide layer. As the PRT value increased the super-Faradaic excess of electrode consumed decreased until a PRT value of 5 min and then slightly increased (34 % for PRT 1 min; 21 % for PRT 3 min; 19 % for PRT 5 min). Notably, the cell resistance (power consumption) trend was the mirror image of super-Faradaic electrode consumption. Therefore, it appeared that the less passivated the electrodes were the more chemical dissolution of the electrodes occurred.

A cleaner electrode surface was expected to result in the production of more floc material as oxide layers inhibit dissolution of the electrode and as a result electron flow [179]. Indeed, Cesar Lopes Geraldino *et al.* [179] employed polarity reversal in

their EC process and promoted electrode consumption as the passivated layer was eradicated. Similarly, Yu *et al.* [197] reported that a polarity reversal time of 10 to 15 min was sufficient to reduce electrode passivation when treating chromium contaminated water with EC. In line with the greater cell resistance when changing PRT from 1 to 5 min the amount of floc produced was indeed reduced.
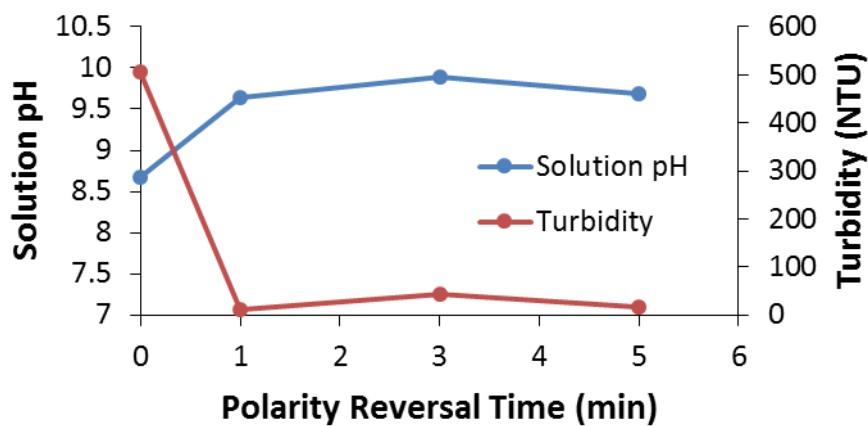
Figure 5-8: Impact of polarity reversal time upon effluent pH and turbidity of EC treated CSG water sample; HRT 30 s; test time 40 min

The turbidity removal was very high (> 96.0 %) regardless of PRT value. Slight variances in the turbidity recorded may have reflected the presence of fine aluminium hydroxide flocs in the samples as settling behaviour was relatively limited. The presence of residual aluminium was relatively stable with only a minor decrease in value as PRT extended from 1 to 5 min. From Section 5.2.1.2 it was expected that residual aluminium may have reduced in value as PRT was increased (less floc produced). However, the increasing solution pH may have compensated for the lesser amount of floc present by creating more soluble $Al(OH)_4^-$ species. When Wellner *et*

al. [135] studied EC treatment of CSG associated water they found that the amount of residual aluminium was impacted by the salinity of the water tested. The higher the total dissolved solids content of the CSG associated water the less aluminium remained in the effluent.

Table 5-2: Summary of experimental data CSG produced water was treated by EC using aluminium electrodes and continuous run for 40 min (HRT 30 s)

PRT	1 min	3 min	5 min
Flow Rate (L/min)	1.154	1.072	1.072
Floc Mass (g/L)	2.73	2.69	2.40
Average Electrode Loss (g/L)	0.71	0.70	0.69
Theoretical Mass Loss (g/L)	0.53	0.58	0.58
Average Current (A)	9.15	9.3	9.33
Average Voltage (V)	30.86	31.07	31.31
Power consumption/Volume of Water Treated (kWh/kL)	4.08	4.49	4.54
Average Current Density (mA/cm^2)	5.08	5.17	5.18
Residual Aluminium (mg/L)	45.99	45.51	45.19

5.2.2.2 Variation in Alkaline Earth Ions, Boron, and Silicates

The influence of PRT upon the removal of dissolved species from CSG associated water is shown in Figure 5-9. As before [Figure 5-4] alkaline earth ions, boron, and silicates were all reduced in concentration due to the EC treatment. Broadly, the degree of removal of these outlined contaminants was similar to that shown in Figure 5-4.
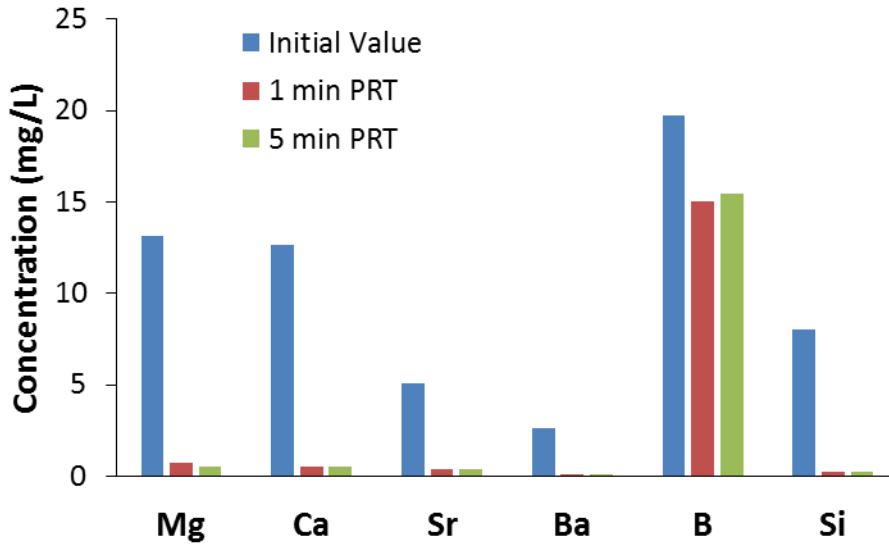
Figure 5-9: Concentration of dissolved species in CSG associated water before and

after EC treatment; PRT from 1 to 5 min; test time 40 min; HRT 30 s

5.2.2.3   Floc Settling Behaviour and Characterization

Figure 5-10 shows the floc settling rates of EC treated CSG associated water with different PRT applied. As a general observation, the PRT did not appear to change the settling properties of the flocs to any discernible extent.
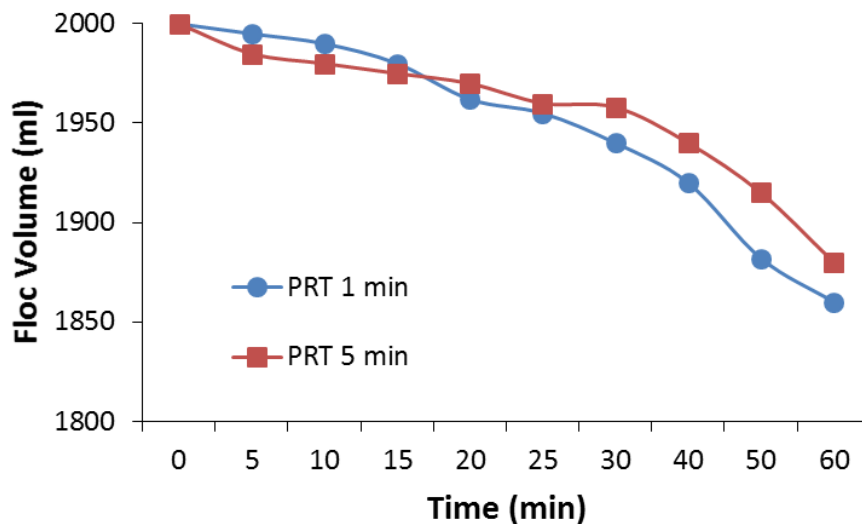
Figure 5-10: Floc sedimentation rate as a function of polarity reversal time; test time
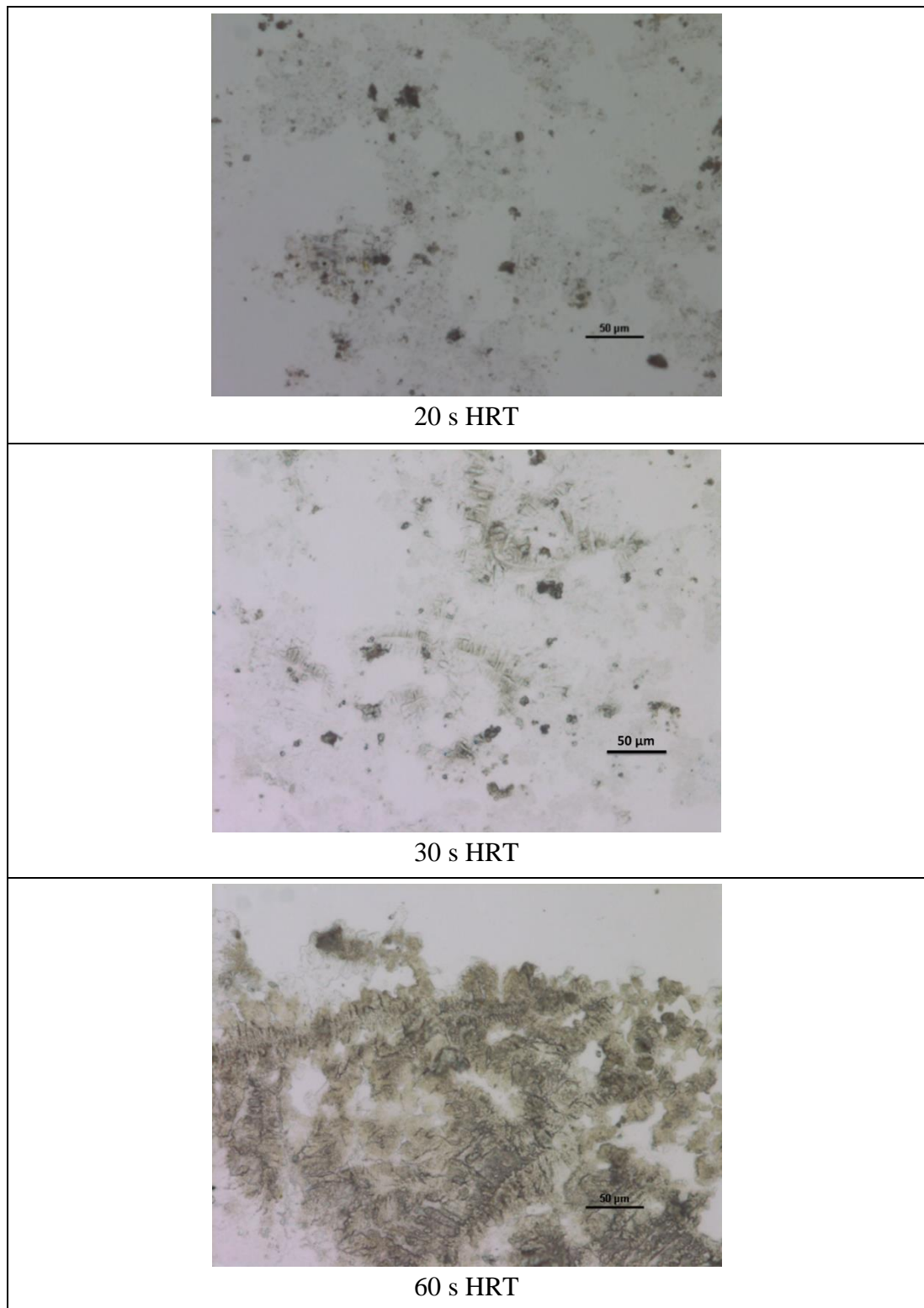
40 min; HRT 30 s

| 30 s HRT; 1 min PRT | 30 s HRT; 5 min PRT |
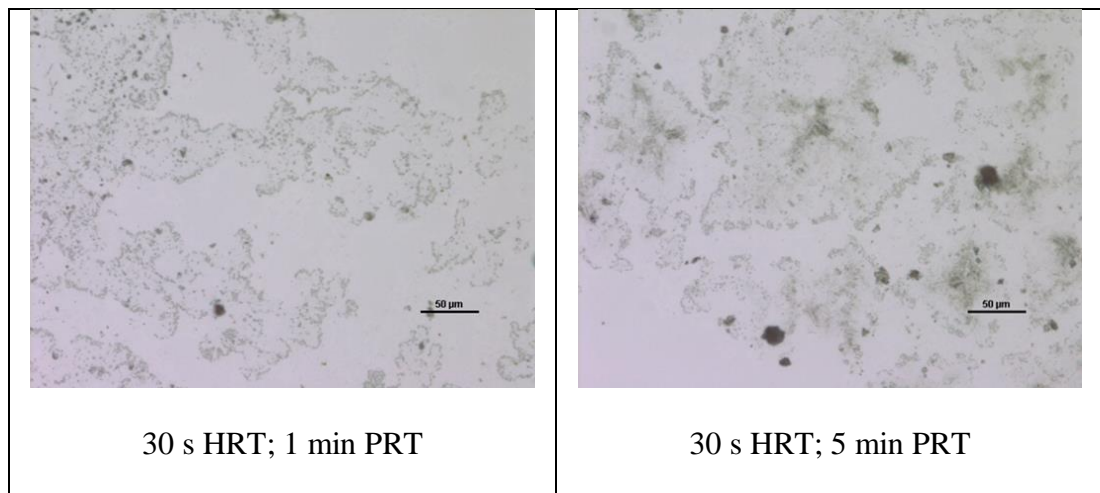
Figure 5-11: Optical microscopy images of flocs formed as a function of HRT when CSG associated water treated with electrocoagulation

The lack of differences in the settling behaviour of the flocs was reflected in the corresponding optical microscopy images [Figure 5-11]. The flocs formed at PRT times of 1 min and 5 min were both relatively "open" with signs of networking. Again, one must assume that the buoyancy forces of the evolved hydrogen bubbles did not allow the flocs to settle in a reasonable timeframe.

5.3 CONCLUSIONS

This study demonstrated that electrocoagulation with aluminium electrodes can reduce the concentrations of suspended solids, dissolved alkaline earth ions and silicates from highly turbid CSG associated water. Alkaline earth ions and dissolved silicates were removed by at least 90 %, albeit the removal mechanism for alkaline earth ions and dissolved silicates in the EC cell was determined to be different. Formation of aluminosilicates was postulated to explain the substantial reduction in dissolved silicate in solution. Suspended kaolin which can cause solution turbidity, from CSG associated water was effectively removed at low values of hydraulic

retention time. However, longer HRT values resulted in the fine flocs being suspended in the treated solution and thus minimizing the HRT was concluded as being more beneficial in terms of turbidity control.

Hydraulic retention time was also a critical parameter in terms of capital and operating costs for electrocoagulation of CSG associated water. The benefit in terms of removal efficiency of dissolved species such as alkaline earth ions and when increasing HRT from 20 to 60 s was minimal in relation to the extra electrode and power consumption required. Use of relatively short residence times for the feedwater in an EC unit is beneficial in terms of reducing not only the footprint of the EC unit required for industry operation but also electricity cost and electrode consumption.

Polarity reversal time did not significantly influence EC treatment performance in terms of reduction of solution turbidity and dissolved species. However, the power consumption was reduced due to the lesser presence of a passivation layer on the electrode surface.

The recommended conditions for application of electrocoagulation to pre-treat CSG associated water prior to a reverse osmosis desalination stage were a HRT value of 20 s or less and a PRT value of 1 min or less. The results from this study indicate that electrocoagulation remains a potentially valuable method for pre-treatment of CSG associated water prior to a central desalination stage such as reverse osmosis.

Chapter 6: Electrocoagulation with Iron Electrodes for High-turbidity CSG Water Treatment

6.1 INTRODUCTION

In the coal seam gas (CSG) industry, depressurization of the coal seams by extraction of water is required to release the entrapped gas [1]. Accordingly there are large volumes of associated water which may be used for applications such as crop irrigation [13]. The quality of CSG associated water depends upon the depth of the coal bed, the formation profiles of the coal and basin characteristics [5]. CSG associated water is saline in nature and the concentrations of the individual salts present are highly variable (total dissolved solids from hundreds to tens of thousands of mg/L) [37]. Nevertheless, sodium chloride and sodium bicarbonate species always comprise the major fraction of the impurities found in the CSG associated water [1, 13, 19, 144]. Salts of calcium, magnesium, barium, strontium, and iron in addition to dissolved silicates may be in lesser quantities, but they can be problematic in terms of their impact upon desalination technologies employed to make the water suitable for beneficial reuse [198, 199]. Another factor which impacts the performance of desalination methods for purification of CSG associated water is turbidity. Rebello *et al.* [21] analysed 150 CSG associated water samples from three different fields in the Surat basin for a range of water quality parameters. Notably, these authors reported that the total suspended solids (TSS) content varied between 5 and 7560 mg/L. The suspended solids probably comprised of a mixture of sand, silt, clay and other solids from bore operation [69].

Typically the associated water is not suitable for direct release to the environment [15, 16, 19]. Therefore, a range of technologies has been implemented to make the CSG associated water compliant with discharge and reuse regulations. One of the simplest strategies is to pH adjust the CSG associated water with acid and then to adjust the sodium adsorption ratio with micronized gypsum (to make it suitable for irrigation purposes). However, as shown by Vedelago and Millar [145] this process is limited to relatively low salinity CSG associated water to avoid inhibition of plant growth and degradation of soil quality. Ion exchange has also been employed for desalination of CSG associated water particularly in regions where the water is dominated by dissolved sodium bicarbonate species [200]. Use of a cation resin not only removed the sodium ions but also reduced solution alkalinity as the water became highly acidic under operating conditions. Alternatively, reverse osmosis (RO) is the most popular CSG associated water treatment method in Australia due to its proven performance for a range of water desalination applications [74].

However, as RO is a membrane based technique the challenge is always to minimize fouling by species such as sulphates/carbonates of alkaline earth ions, silicates and organic matter [192, 201, 202]. Consequently, several pre-treatment methods have been implemented or considered for CSG associated water in order to stabilize the performance of the central desalination stage [1]. Generally, pre-treatment technologies can be classified as coarse filtration, fine filtration, softening and chemical adjustment operations [1]. Coagulation using iron and aluminium based salts has been shown to remove some dissolved species such as alkaline earth ions and silicates under laboratory testing conditions using simulated CSG associated water samples [22, 23]. However, when real CSG associated water samples were evaluated

the removal performance was inhibited by the presence of organic species. Le *et al.* [82] also described the application of a coarse disc filter as a coarse filtration stage prior to a microfiltration system prior to an RO unit used for CSG associated water desalination. As algae were also present in the CSG associated water several biocides were also added in the pre-treatment stage to protect downstream membranes and equipment from fouling.

Recently, electrocoagulation (EC) has been evaluated as an alternative method to chemical coagulation for CSG associated water treatment [135, 136]. Using aluminium electrodes, Millar *et al.* [136] found that alkaline earth ions and dissolved silicate species were significantly removed from the CSG associated water (>85 % effectiveness). Lesser amounts of dissolved organic carbon (<55 %), boron (<13.3 %) and fluoride (<44 %) were also removed by the EC process. Wellner *et al.* [135] also investigated the influence of CSG associated water composition upon the effectiveness of EC equipped with either aluminium or iron (mild steel) electrodes. Higher salt concentrations limited the reduction in alkaline earth ion content, whereas silicate removal was not significantly inhibited by solution salinity. Notably, iron electrodes were discovered to be less effective than aluminium electrodes for low and medium salinity CSG associated water samples; but potentially more effective at high salinity conditions. Iron based flocs were also recorded to settle faster than aluminium derived flocs which was an important issue with respect to the practical operation of an EC system. Moreover, with aluminium electrodes, the production of residual aluminium was found. This species may have a detrimental impact upon downstream membrane performance as precipitates may form which increase solution turbidity [203].

EC process optimization depends on critical factors such as hydraulic retention time (HRT), polarity reversal time (PRT), electrode characteristics, and current density. Xu *et al.* [204] found that the flow rate in the EC cell was critical in relation to removing copper from a salt solution. If the flow was too fast (*i.e.* short HRT value) the removal effectiveness was decreased. Alternatively, if the HRT value was too long then no significant gain in performance was recorded, yet inherently power/electrode consumption would be expected to increase per kL of water treated. Polarity reversal has been successfully employed by Timmes *et al.* [205] when using electrocoagulation to pre-treat seawater prior to an ultrafiltration stage. The fundamental premise was to alleviate issues associated with surface passivation of electrodes during EC operation which can increase the cost of power required. For example, Mao *et al.* [206] applied an alternating pulse current when treating simulated wastewater with an EC unit equipped with aluminium electrodes. Up to 30 % energy reduction was stated for equivalent removal rates for chemical oxygen demand and notably, the electrodes were discovered to wear more evenly. Iron (mild steel) and aluminium electrodes are the most common materials using in EC studies. Panikulam *et al.* [207] applied EC to remove kaolin turbidity from a sodium chloride solution and discovered that iron electrodes removed turbidity (> 95 %) in a wider pH range relative to Al electrodes. Pertinently, alkaline conditions were not conducive to turbidity reduction with aluminium electrodes; thus for CSG associated water samples which are normally pH >8, iron electrodes may be beneficial. Increasing current density is universally agreed to improve electrocoagulation performance as more floc is formed as the current density is increased [208].

This investigation addressed the research gap relating to the impact of hydraulic retention time and polarity reversal time upon the performance of an EC unit equipped with iron electrodes for CSG associated water pre-treatment. The hypothesis was that iron electrode performance during EC operation may be optimized by judicious choice of HRT and PRT. Research questions which were considered to support the hypothesis included: (1) What is the impact of HRT upon electrocoagulation performance when treating CSG associated water; (2) Which species are removed from the CSG associated water and to what extent? ; (3) What is the effect of turbidity on the removal of dissolved ions? (4) Does polarity reversal time influence EC performance? To answer these research questions a bench top electrocoagulation unit was employed which was operated in continuous mode. Multiple iron (mild steel) electrodes were used in parallel and produced flocs were analysed for settling ability. A simulated coal seam gas water was treated which comprised mainly of sodium chloride and sodium bicarbonate species.

6.2 RESULTS AND DISCUSSION

6.2.1 Impact of Hydraulic Retention Time (HRT) upon Electrocoagulation Performance

Three different flow rates were examined which corresponded to hydraulic retention times of 20, 30 and 60 s for the CSG associated water. The aim of these tests was to evaluate the effect of HRT on the performance of an electrocoagulation unit equipped with iron electrodes for dissolved ions removal efficiency in presence of turbidity causing species.

6.2.1.1 Variation in Effluent pH and Turbidity of Treated CSG Water

Figure 6-1 shows the change in pH and turbidity level as a function of HRT. The final pH value was higher than the initial value and clearly depended upon the HRT value employed. The pH of the treated CSG associated water was raised to 9.58, 9.82 and 10.24 when HRT was 20, 30 and 60 s, respectively. Ciblak *et al.* [209] indicated that the pH rise in solution (up to pH 10.5) when iron was an anode in an EC cell was due to the dominance of the oxidation of iron metal to ferrous ions [Equation 6-1] and inhibition of the oxidation of water [Equation 6-2]. This conclusion was inferred from the considerably lower standard potential for dissolved ferrous iron production compared to that for water oxidation. Thus, protons would not be available to neutralize hydroxyl ions produced at the cathode due to the process shown in Equation 6-3.

Equation 6-1: $$Fe^o \rightarrow Fe^{2+} + 2e^-$$

Equation 6-2: $$2\,H_2O \rightarrow 4\,H^+ + H_2 + 4\,e^-$$

Equation 6-3: $$2\,H_2O + 2\,e^- \rightarrow 2\,OH^- + H_2$$
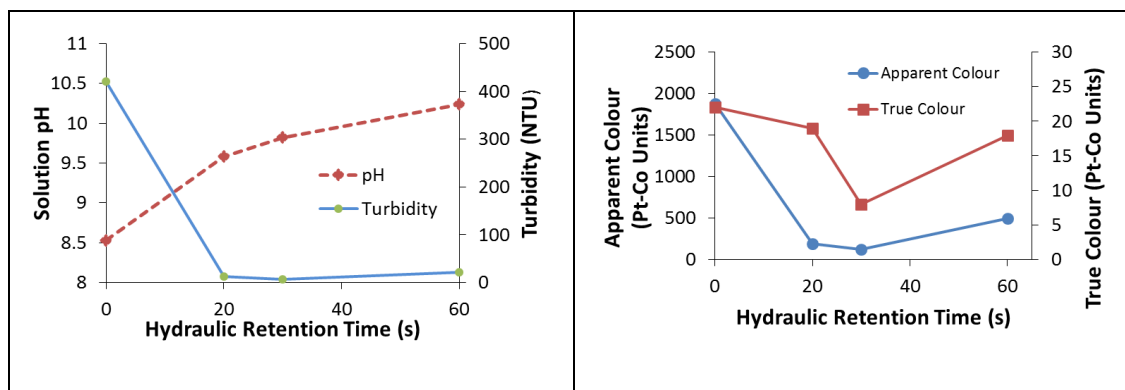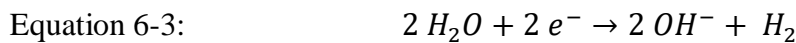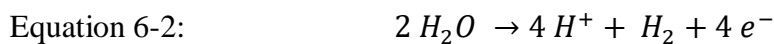
Figure 6-1 Impact of HRT upon effluent pH and turbidity of EC treated CSG associated water; PRT 3 min; test time 40 min

The highest turbidity reduction (98.5%) was achieved by 30 s HRT; albeit an HRT value of 20 s was already sufficient to remove 97 % of turbidity from solution. Increasing HRT to 60 s induced a slight inhibition of turbidity reduction with 95 % removed under these conditions. The presence of suspended flocs in the solution may have been the cause of such turbidity [See Section 6.2.1.4]. Similarly, the apparent colour of the feedwater was 1880 Pt-Co units and this decreased to 188, 117 and 495 Pt-Co units for HRT values of 20, 30 and 60 s, respectively. Concomitantly, the true colour which was initially 22 Pt-Co units decreased to 19 and 8 Pt-Co units when HRT was 20 and 30 s, respectively. However, the true colour increased to 18 Pt-Co units for a retention time of 60 s. The apparent colour was the result of both iron compounds and kaolin particles suspended in solution. Whereas, the true colour measurements may reflect the presence of iron species in solution because the treated water was initially "green" in colour (Fe^{2+}) and this then turned to dark orange (Fe^{3+}) once the solution was removed from the reactor. During electrocoagulation with iron electrodes, the primary dissolution of the anode proceeds via Equation 6-1 and then Fe^{2+} species can further oxidise to form Fe^{3+} ions as illustrated in Equation 6-4 [210].

Equation 6-4: $\qquad Fe^{2+} \leftrightarrow Fe^{3+} + e^-$

Van Genuchten *et al.* [211] noted that the dissolved oxygen content of an iron electrode based EC cell was undetectable after electrocoagulation of arsenic contaminated groundwater. Upon exposing the treated solution to air the dissolved oxygen content returned to a similar value of the initial feedwater. Thus, oxidation of the Fe^{2+} ions to Fe^{3+} ions could proceed under aerobic conditions. During corrosion of iron the formation of "green rust" has also been reported. In solutions where there

are bicarbonate/carbonate species present (such as is the case with CSG associated water) the iron hydroxyl carbonate of the general formula $Fe_{x1}^{III} Fe_{x2}^{II} (OH)_{y1} (CO_3)_{z1}$ can be created [212]. Oxidation of this "green rust" material can also occur upon air exposure to form $Fe_{x1+x2}^{III} (OH)_y (CO_3)_z$. Further support for "green rust" was provided by Legrand *et al.* [213] who identified the presence of carbonate green rust $[Fe_4^{II} Fe_2^{III} (OH)_{12}][CO_3 . 2H_2O]$ when they employed iron electrodes in a solution of sodium bicarbonate/carbonate. Legrand *et al.* [213] also discovered that the green rust oxidised when exposed to oxygen and in this case ferrihydrite was characterized.

From this interpretation of the behaviour of iron species in the electrocoagulation process, a critical aspect is that the EC cell under operating conditions must have been anaerobic in character. The vigorous evolution of hydrogen bubbles at the cathode according to Equation 6-3 could displace the oxygen from the water sample. Dubrawski *et al.* **[214]** demonstrated that with various solutions of sodium sulphate, sodium chloride and sodium bicarbonate with iron electrodes that anaerobic conditions were indeed possible in the EC cell and that "Green Rust" was produced if carbonate was present.

6.2.1.2   Variation in Floc Mass and Electrode Consumption

Table 6-1 shows the change in floc mass and electrode consumption as a function of HRT. In general, as the residence time increased the floc mass produced and electrode mass consumed increased with an increasing residence time of the CSG associated water in the EC cell. Power consumption per kL of water treated was also greater as HRT was extended. The ratios of floc mass to electrode mass lost were 1.64, 1.58 and 1.28 for HRT values of 20, 30 & 60 s, respectively. If we assume that the iron floc had the formula $Fe(OH)_2$ then the predicted mass ratio of floc produced to

electrode loss would be 1.61. This latter calculation was in excellent agreement with the amount of floc determined when HRT was 20 & 30 s. However, there was a notably lesser quantity of floc measured for 60 s HRT compared to theoretical estimates. The experimental data also suggested that the presence of "green rust" was relatively minimal as the mass ratio of floc to iron consumed would be *ca.* 1.90 if this material dominated the floc composition (significantly higher than the recorded value of 1.28). Wei *et al.* [215] found that the formation of ferrite polymers was promoted at higher pH values when adding poly-ferric-acetate coagulant to wastewater containing kaolin and phosphate. If it was assumed that bridging Fe – $(OH)_2$ – Fe species were created [216], the ratio of floc to iron loss was calculated to be 1.30 which was very similar to the experimental value of 1.28. Hence, we can conclude that the iron species present in solution changed from monomeric to polymeric as the HRT was increased.

In all cases, the measured mass loss of the iron electrode was significantly lower than the mass predicted from the Faraday expression [Equation 3-1]. The discrepancy in electrode loss was calculated as 9.6, 13.2 & 14.8 % for HRT values of 20, 30 & 60 s, respectively. Typically, a super-Faradaic loss of metal from the anodes in an EC test has been described due to the chemical dissolution of the surface [180, 217]. Dissolution of iron electrodes at a pH in excess of 9 typically produces soluble $Fe(OH)_4^-$ ions [171] (albeit, minimal dissolved iron was recorded in the treated effluent). However, competing with this process was the formation of carbonate species on the electrode surface which inhibited dissolution of iron ions and instead formed a passivated surface [218]. It is accepted that the less the degree of passivation (*i.e.* less resistance) of the electrode surface the greater the consumption of electrode

occurs. Increasing the HRT decreased the resistance of the iron electrode surface from 3.47 to 3.30 to 3.28 ohms for HRT values of 20, 30 & 60 s, respectively. Hence an explanation was required for why the cleanest electrode surface displayed the least mass loss.

Table 6-1 Summary of experimental data CSG produced water was treated by electrocoagulation using iron electrodes and continuous run for 40 min (PRT 3 min)

HRT	20 s	30 s	60 s
Flow Rate (L/min)	1.66	1.16	0.60
Floc Mass (g/L)	1.71	2.29	3.89
Average Electrode Loss (g/L)	1.04	1.45	2.53
Theoretical Mass Loss (g/L)	1.15	1.67	2.97
Average Current (A)	9.17	9.28	8.54
Average Voltage (V)	31.81	30.61	27.97
Power consumption/Volume of Water Treated (kWh/kL)	2.93	4.08	6.63
Average Current Density (mA/cm^2)	5.09	5.15	4.74

It was visually noted that a coating had formed on the electrode surface due to the EC tests. Timmes *et al.* [134] observed substantial accumulation of precipitate on the iron plates after pilot plant use which was consistent with the idea that passivation of the iron electrodes increased with time. van Genuchten *et al.* [130] also found a significant build-up of an oxide/hydroxide layer on iron electrodes used in the field for extended periods of time. The analysis suggested that the surface of the electrodes was majorly composed of a mixture of Fe_3O_4 and $FeOOH$. Therefore, although iron was lost from the anode to form the flocs, there was also an accumulation of a material

such as iron carbonate or iron oxyhydroxide [219] which would explain the apparent net reduction in mass loss from the electrodes (balance between loss of iron and gain of carbonate or oxyhydroxide species).

6.2.1.3   Variation in Alkaline Earth Ions, Boron, and Silicates

All alkaline earth ions were reduced in concentration by application of electrocoagulation [Figure 6-2].   Albeit, it was found that magnesium ions were preferentially removed from the CSG associated water (60.1, 81.7 and 96.9 % magnesium removal for HRT values of 20, 30 and 60 s, respectively). The promotion of magnesium removal corresponded to the raising of solution pH to 9.58, 9.82 and 10.24 as HRT values were increased from 20 to 60 s. Magnesium precipitation as brucite ($Mg(OH)_2$) is favoured by pH approaching 10 or greater

According to Malakootian *et al.* [220], a pH of 10 was very favorable in removing calcium (>97 %) from solution as calcium carbonate; which was significantly higher than the reduction in calcium ion concentration in this study. A potential explanation was the difference in initial calcium concentration in the solution and overall solution salinity. Wellner *et al.* [135] treated CSG associated water by EC using Fe electrodes and found that calcium was removed efficiently when the feed water contained low TDS (5290 µS/cm) and high TDS (15690 µS/cm). Surprisingly, calcium removal efficiency was relatively low from medium TDS water (9550 µS/cm). Likewise, the initial calcium concentrations were 1.47, 7.63 and 36.26 mg/L in the low, medium and high TDS CSG associated water, respectively. In this study, the initial calcium concentration was 12.69 and conductivity was 9940 µS/cm, which is comparable to the medium TDS water studied by the latter authors. Wellner *et al.* [135] noted that magnesium removal efficiency was 44.6 % compared to 24.9 % for

calcium ions, which was similar in trend to the data in this study. A precise reason for the superior magnesium removal performance was not provided, however, it was noted that precipitation of insoluble carbonate and hydroxide species was not the only mechanism for contaminant remediation from CSG associated water. Hafez *et al.* [191] recently found that magnesium ions were removed to a greater extent than calcium ions when using electrocoagulation to treat cooling tower blowdown water. However, no information was given regarding the mechanism which preferred removal of magnesium ions over calcium ions.
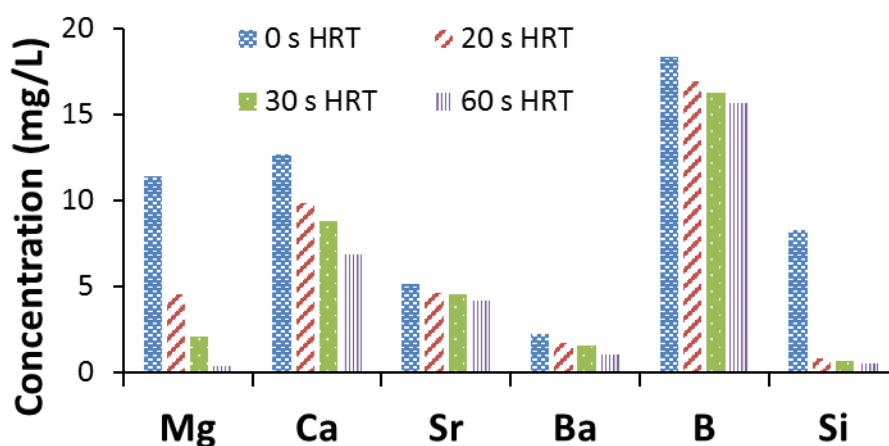
Figure 6-2: Concentration of dissolved species in CSG water before and after EC treatment; polarity reversal period 3 min; test time 40 min

The relatively low percentage of strontium removed (10.0, 12.6 and 18.7 % at HRT values of 20, 30 and 60 s, respectively) was consistent with the established view that strontium removal is favored at an optimum pH of 7 to 8 [188]. In this study, the solution pH was from 9.58 to 10.24 after EC treatment which was not favorable for removal of strontium ions. Further inhibiting the removal of strontium ions was the fact that the initial strontium concentration was relatively low (5.48 mg/L); whereas

concentrations up to 100 mg/L were reported as enhancing the percentage reduction in strontium present in solutions treated using EC [187]. In this study, the highest barium removal (53.61%) was achieved for 60 s HRT. Notably, previous studies of CSG associated water treatment typically reported higher removal rates for barium ions, albeit one must again consider the influence of varying CSG associated water composition and physical properties such as pH.

Boron removal efficiency was not substantial in this study (7.95, 11.27 and 12.67 % for HRT of 20, 30 and 60 s, respectively). Widhiastuti *et al.* [221] achieved 70.3 % removal of boron using iron electrocoagulation to treat 10 mg/L boron in a sodium chloride solution. Notably, the solution pH was only 8.5 which was considerably lower than the pH values in this study [Figure 6-1] and the residence time in the EC cell was 60 minutes. Notably, the point of zero charge on the surface of the iron based sludge was pH 8.2. Hence, increasing the solution pH would result in a negatively charged surface which could be expected to repel negatively charged $B(OH)_4^-$ ions. Another factor responsible for lowering the effectiveness of EC for boron removal from CSG associated water was the relatively low concentration of boron species present. Sayiner *et al.* [222] demonstrated that the greater the boron concentration the higher the percentage of boron removed from solution by iron electrodes in an EC process. These authors examined solutions with up to 1000 mg/L which was substantially greater than the initial amount of 18 mg/L in this study. Hence, the relatively low EC performance for reduction of the amount of boron species in CSG associated water correlated with previous literature. In terms of the impact of HRT, Isa *et al.* [27] found that increasing the contact time of boron in an EC unit promoted the removal performance from *ca.* 75 % to greater than 95 %. Sorption

studies suggested that the boron was bound to the flocs by a chemical bond and that intra-particle diffusion at least in part explained the rate limitations recorded.

Silica removal efficiency was excellent (89.9, 92.1 and 93.0 % at HRT of 20, 30 and 60 s, respectively). Electrocoagulation has been demonstrated to be very effective at removing dissolved silicates when using aluminium electrodes [136] with the primary mechanism involving the reaction of aluminium with silicates to make insoluble aluminosilicate materials. Den *et al.* [223] conducted a mechanistic study of silica removal from polishing wastewater by means of an electrocoagulation unit equipped with iron electrodes. It was concluded that silicate species were removed due to two possible processes. The first involved destabilization of the charge on the silicate species by Fe^{2+} ions liberated from the anode, thus allowing them to floc. The second mechanism was postulated to be enmeshment of silicates in iron oxide/hydroxide flocs.

We note that irrespective of HRT iron was not present in a significant amount during any of our tests (*ca.* 0.02 mg/L). Mohora *et al.* [224] employed bipolar iron electrodes for EC treatment of arsenic in groundwater and they measured not only some residual iron species (< 0.5 mg/L) but also a distinct relationship to HRT. As the flow rate was increased (*i.e.* the HRT decreased) the amount of residual iron present reduced. However, we note that Ciblak *et al.* [209] discovered that the identity of the electrolyte exerted a significant impact upon the electrode dissolution. Indeed, solutions with bicarbonate species present such as CSG associated water actually had essentially no residual iron in solution.

It was illuminating to compare the performance of iron electrodes with aluminium electrodes used for electrocoagulation of CSG associated water. Data presented by Millar *et al.* [136] revealed that dissolved silicate removal was majorly removed when applying aluminium electrodes (up to 98.3 %) which was slightly greater than the removal rates measured in this study. Furthermore, the reduction of calcium, strontium, and barium was greater than 99 % when using aluminium electrodes which was significantly higher than the values recorded in this investigation. A more recent study by Wellner *et al.* [135] has shown that the TDS of the CSG associated water is important and that when high concentration CSG associated water is treated (*ca.* 10,000 mg/L) iron electrodes actually perform better than aluminium electrodes. In agreement with Wellner *et al.* [135] when medium and low TDS CSG associated water was treated using EC (as in this investigation), aluminium electrodes performed more adequately. Economic considerations indicated that iron electrodes were less expensive in terms of both material and electricity consumption [225].

6.2.1.4 Floc Settling Behaviour and Characterization

Figure 6-3 shows the sedimentation rates of iron flocs produced during EC treatment as a function of HRT employed. In general, the higher the HRT value the slower the sedimentation rate measured. When extending the contact time of the fluid in the EC reactor the production of hydrogen gas from the cathodic oxidation of water can promote a floc flotation process [226]. Consequently, a correlation was evident between the increasing amount of gas evolved and the settling rate of the flocs produced.

In terms of practical application, Figure 6-3 suggested that a 60 s HRT value may be problematic due to the slow settling rate recorded. However, from Figure 6-2 the removal rates of dissolved species were generally enhanced when HRT was increased from 20 to 60 s; hence, a strategy to operate with 60 s HRT may be valuable. One possible option to facilitate the use of the extended HRT value is the use of the ballasted electrocoagulation process described by Brahmi *et al.* [194]. These authors added a combination of micro-sand and polyethyleneimine to enhance the settling properties of the flocs and noted a significant promotion of dissolved species removal could also be achieved by their approach.
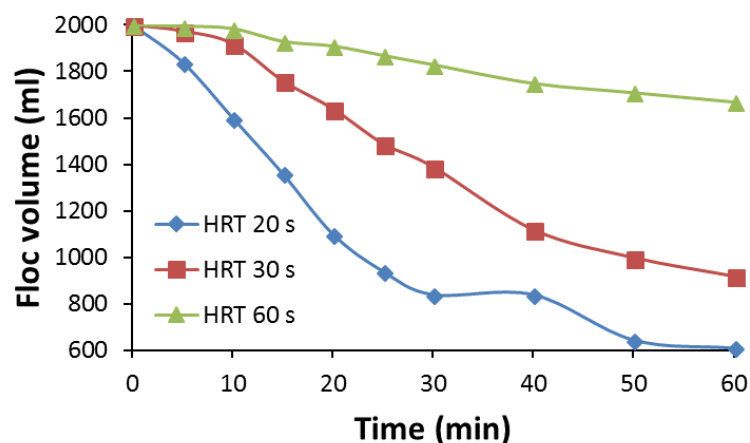
Figure 6-3: Floc sedimentation rate as a function of HRT; test time 40 min; PRT 3 min

It was noted that the settling rates of iron based flocs were improved compared to aluminium electrodes if the HRT value was carefully chosen. For a medium TDS CSG associated water such as the one examined herein, the floc volume decreased by no more than 45 % with aluminium electrodes [135]. With an HRT value of 20 s and iron electrodes the settled volume after one hour decreased by 70 % [Figure 6-3].

Figure 6-4 illustrates the physical appearance of flocs produced during EC treatment at 20, 30 and 60 s HRT values, respectively. The flocs were orange-red in colour which inferred the presence of iron (III) oxides/hydroxides, a portion of which may have been formed from the oxidation of Fe (II) species by oxygen in the air. Wellner *et al.* [135] characterized flocs from the EC treatment of CSG associated water with iron electrodes and identified both magnetite (Fe_3O_4) and goethite ($FeO(OH)$). The CSG associated water was initially white in colour due to kaolin addition and turned dark green immediately after EC treatment. This dark green colour denoted the presence of iron (II) species. It was observed that the flocs were networked to each other and that the floc density increased as the HRT was extended.

(a) HRT 20 s   (b) HRT 30 s   (c) HRT 60 s
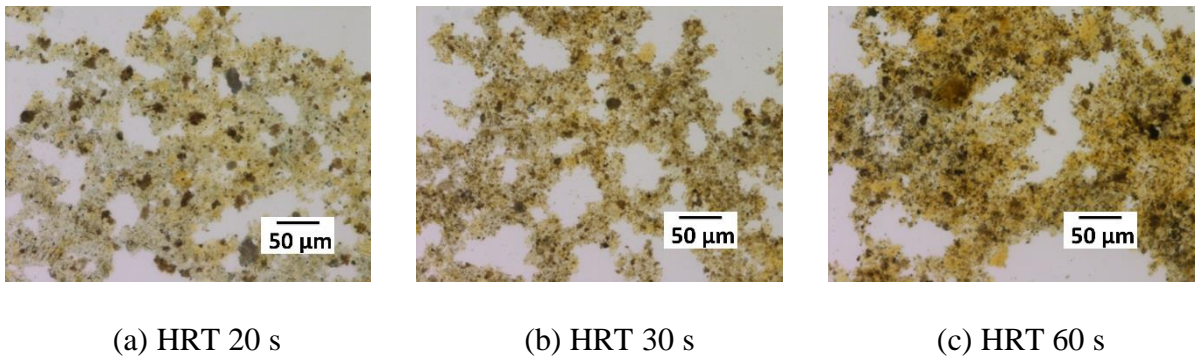
Figure 6-4: Optical microscopy images of flocs from electrocoagulation of different HRT; PRT 3 min

The optical images of the flocs supported the conclusion that greater gas production in the EC cell resulted in floatation of the flocs and inhibition of sedimentation. The denser flocs formed at 60 s HRT may have been expected to settle faster than those more porous flocs at 20 s HRT. As the opposite situation was the

case another factor such as floatation was necessary to explain the sedimentation rate in Figure 4-3.

6.2.2 Impact of Polarity Reversal Time (PRT) upon Electrocoagulation Performance

To evaluate the influence of PRT on EC performance experiments were conducted at three different PRT values, either 1, 3 or 5 min while the HRT value was constantly 30 s.

6.2.2.1 Variation in Effluent pH and Turbidity of Treated CSG water

Figure 6-5 shows the change in pH and turbidity as a function of PRT. It was observed that the solution pH increased during EC treatment compared to the initial pH of the CSG associated water (*c.f.* 8.55 to *ca.* 9.82). However, pH did not vary significantly whether PRT was 1, 3 or 5 min. Similarly, the effect of PRT on turbidity removal was negligible as >94.5 % reduction was recorded in all instances.
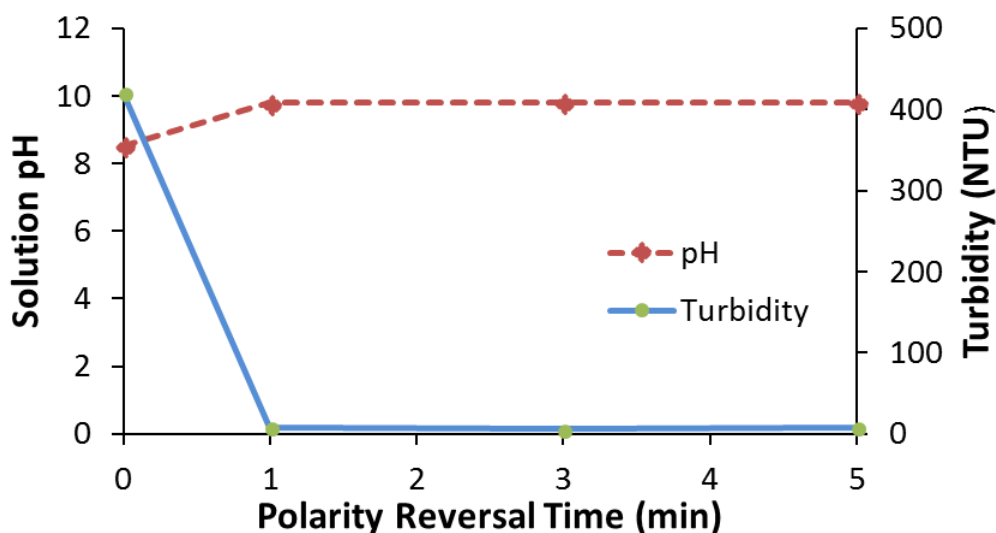
Figure 6-5: Impact of PRT upon effluent pH and turbidity of EC treated CSG water sample, HRT 30 s; test time 40 min

6.2.2.2 Variation in Floc Mass, and Electrode & Power Consumption

Table 6-2 shows that power consumption reduced gradually with the increase of PRT. Initially, power consumption was 4.12 kWh/kL for 1 min PRT and this diminished to 3.88 kWh/kL when PRT was increased to 5 min.

Table 6-2: Summary of experimental data of CSG water treated by EC equipped with Fe electrodes; HRT 30 s; test time 40 min.

PRT	PRT 1 min	PRT 3 min	PRT 5 min
Flow Rate (L/min)	1.17	1.16	1.16
Floc Mass (g/L)	2.26	2.29	2.30
Average Electrode Loss (g/L)	1.41	1.45	1.48
Theoretical Mass Loss (g/L)	1.65	1.67	1.57
Average Current (A)	9.28	9.28	8.71
Average Voltage (V)	31.2	30.61	30.98
Power consumption/Volume of Water Treated (kWh/kL)	4.12	4.08	3.88
Average Current Density (mA/cm^2)	5.15	5.15	4.84

As with the case when HRT was varied, the mass loss recorded of the electrode was less than predicted by the Faraday expression [Equation 3-1]. In this instance, the discrepancy in electrode amounts was 14.5, 13.2 & 5.7 % for PRT values of 1, 3 & 5 min respectively. Ciblak *et al.* [209] suggested that polarity reversal when using iron electrodes for electrocoagulation of saline solutions promoted the formation of reducing conditions in the EC unit. Hence, removal of passivating oxide/hydroxide films was accelerated. Pertile and Birriel [225] evaluated EC treatment of a wastewater solution from galvanic processing. Application of polarity reversal was

found to increase the consumption of the electrodes used and this was again correlated with less oxide formation on the electrode surface and greater pitting of the electrode material. Therefore, we can infer that the increasing PRT value decreased passivation of the electrode surfaces. The data also suggest that PRT value in excess of 5 min may be beneficial as a balance between theoretical and recorded mass loss had not yet been achieved. Timmes *et al.* [134] discovered that the polarity reversal time when employed in an electrocoagulation pilot-plant for seawater treatment required the PRT be increased as the test time was lengthened. The basis of this variation in PRT was to ensure a constant dose rate for iron into the seawater. No mention of why the PRT value was required to be increased during the study by Timmes *et al.* [134] was given. However, the study of Fekete *et al.* [133] demonstrated that a certain minimum time was required for the de-passivation of electrode surfaces to occur when polarity reversal was applied during electrocoagulation. If the size of the passive layer increased then it is logical that the PRT required to remove the passivating oxide/hydroxide layer would also increase.

6.2.2.3 Variation in Alkaline Earth Ions, Boron, and Silicates

Figure 6-6 presents the change in dissolved ions before and after EC treatment. Overall, it was observed that the removal of dissolved species was not substantially influenced by PRT. Application of a 3 min PRT was slightly superior in terms of EC performance with removal rates of: magnesium (81.7 %); calcium (30.7 %); strontium (12.6 %); barium (32.3 %), boron (11.3 %) and silica (92.1 %).

The relatively stable removal of the species outlined in Figure 6-6 as a function of PRT was not expected based upon the study of Pertile and Birrie [225]. These authors reported in excess of 20 % increase in the degree of removal of cyanide, zinc

and nickel species from galvanic effluent which was attributed to the lesser passivation of the aluminium electrodes. From this data and that recorded in this study, the extent of the promotional effect of the polarity reversal period upon removal of dissolved species in solution can be inferred to relate to the degree of surface passivation present in that system. It would thus appear that the passivation of electrodes in this investigation was significantly less than that in the study of Pertile and Birrie [225]. This conclusion was in agreement with the study of Wellner *et al.* [132] which revealed that the overall salinity of a solution and identity of the salts present had a significant impact upon the passivation of the electrodes in an EC process. A point of interest was the fact that PRT 3 min appeared to be slightly better than PRT 5 min for reducing the concentration of the species denoted in Figure 6-6. From Table 6-2 the cleanest surface was created by using a PRT value of 5 min and this may have then be expected to give the highest removal performance.
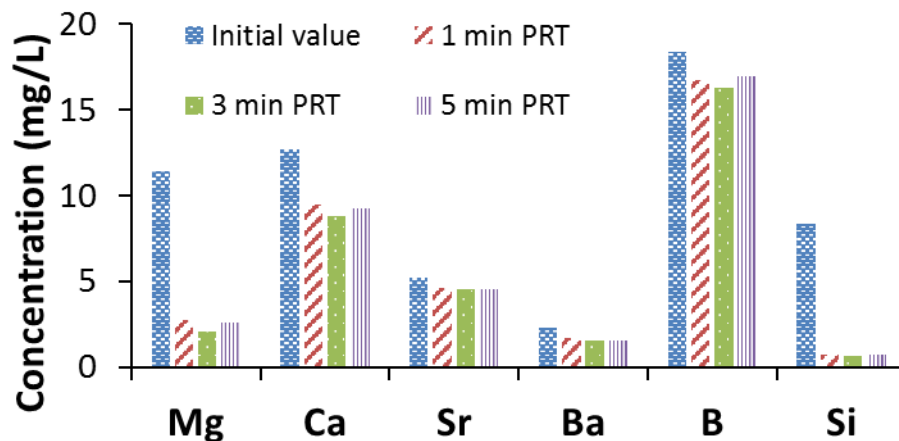
Figure 6-6: Concentration of dissolved species in CSG associated water before and after EC treatment as a function of PRT; test time 40 min; HRT 30 s

6.2.2.4 Floc Settling Behaviour and Characterization

Figure 6-7 reveals the impact of PRT upon the sedimentation rates of EC produced flocs. There appeared to be a slight reduction in floc settling rate when a PRT value of 1 min was employed, whereas for 3 min and 5 min PRT the floc settling rate were similar.
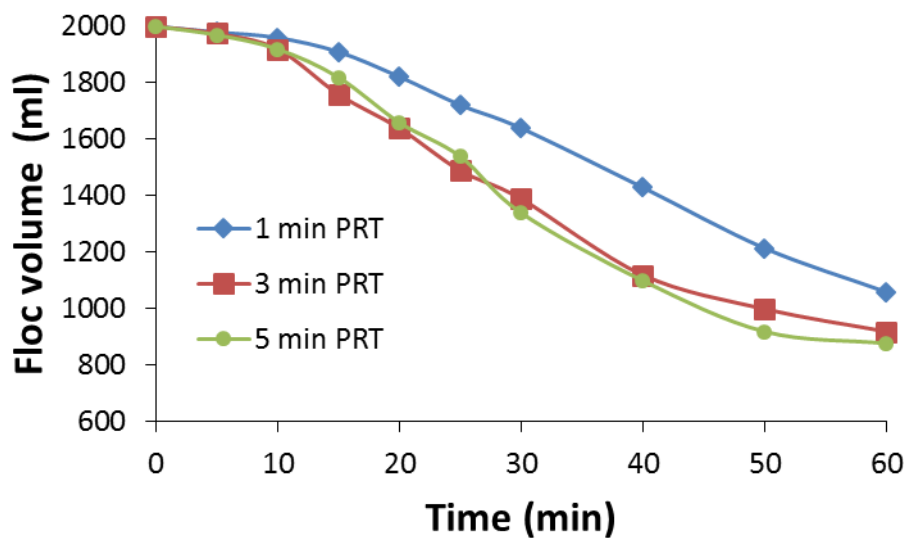
Figure 6-7: Floc sedimentation rate as a function of PRT: test time 40 min; HRT 30 s
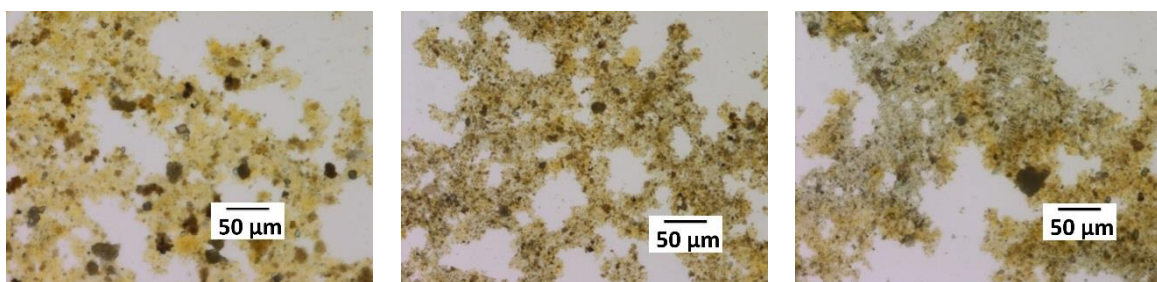
(a) 1 min PRT   (b) 3 min PRT   (c) 5 min PRT

Figure 6-8: Optical microscopic images of flocs produced during EC at different PRT; HRT 30 s; test time 40 min

When an anode is passivated this can promote the oxidation of water [Equation 6-2] which results in greater hydrogen production. Thus, it can be postulated that the anode surface was most passivated at a PRT value of 1 min; as in this situation, the excess hydrogen gas could "float" the produced flocs. This conclusion was in agreement with the data discussed in Table 6-2.

Figure 6-8 shows the optical microscopic images of flocs from EC treatment of the CSG associated water as a function of PRT. In general, the flocs all appeared to exhibit a network structure and evidence for entrapment of kaolin particles was observed. From the optical images, it was difficult to ascertain any major differences in floc structure. Thus, the settling behaviour would be expected to be similar, apart from the importance of the quantity of hydrogen bubbles produced in the EC unit.

6.3 CONCLUSIONS

Electrocoagulation with mild steel (iron) electrodes has been demonstrated to be of interest for pre-treatment of CSG associated water. Solution turbidity and dissolved silicates were readily reduced by application of EC to very low residual levels. Alkaline earth ions which are known to potentially cause scaling problems with downstream equipment and membranes were also removed with magnesium being favoured.

Selection of appropriate hydraulic retention times was determined to exert a profound influence upon electrocoagulation performance when treating CSG associated water. Increasing HRT promoted the removal of dissolved alkaline earth ions, silicates, and boron. However, the corresponding substantial increase in

electricity consumption may outweigh any performance gains. This is a matter for further techno-economic evaluation.

Polarity reversal time was found to be an important factor in relation to the operation of an EC unit. Optimization of the PRT value could reduce surface passivation of the electrode surface and interestingly this value may be tailored to control the extent of anode dissolution. As the electrode surface became cleaner a slight, general improvement in removal performance of dissolved species in the CSG associated water could occur. In this instance, the PRT was required to be at least 5 min and it was recommended to explore longer timeframes in future studies.

Chapter 7: Electrocoagulation with Aluminium and Iron Combined Electrodes for High-turbidity CSG Water Treatment

7.1 INTRODUCTION

Electrocoagulation has been widely researched in relation to water and wastewater treatment for many years [171, 227]. EC involves the electrochemical dissolution of anodic materials (commonly aluminium or iron) with resultant floc formation which can remove a variety of suspended and dissolved species [228]. A benefit of EC appears to be the ability to reduce the concentration of a range of water contaminants in one unit operation [226]. For example, Xu *et al.* [229] removed zinc, cadmium, and manganese simultaneously from real smelting wastewater while Dhadge *et al.* [230] removed fluoride, iron, arsenic and microorganisms from contaminated drinking water.

Recently, the ability of EC to remove problematic species such as alkaline earth ions, dissolved silicates, fluoride, and boron has been demonstrated for coal seam gas (CSG) associated water [135]. The CSG, also known as coal bed methane (CBM) in the USA has become more popular in recent years due to the advent of better technologies for extracting unconventional gas resources [231-234]. However, substantial volumes of associated water which is mainly brackish in character are inherently produced due to the need to depressurize the coal seams to allow gas to flow to the surface. As such as desalination technology such as reverse osmosis (RO) [74] or ion exchange (IX) [200] is often required to purify the water to the extent it is

suitable for beneficial reuse. Reverse osmosis, in particular, has been the major technology employed in this industry sector as it has a proven track record. However, membranes are susceptible to degradation in performance due to factors such as fouling, scaling, and chemical degradation [26, 235]. Hence, a range of processes has been implemented to protect the membranes including coarse filtration (coagulation), fine filtration (microfiltration; ultrafiltration), biocide addition, softening and anti-scalant dosing [1]. In the CSG associated water which is dominated by sodium chloride and sodium bicarbonate, the species of concern include alkaline earth ions, turbidity causing moieties and dissolved silicates [21]. Silica has been shown to be especially difficult in terms of mitigating scale formation [236]. Therefore, there is a need to develop a technology which can not only substantially reduce silica concentrations in CSG associated water but also reduce the prevalence of alkaline earth ions and reduce turbidity.

As alluded to above, initial studies by Wellner *et al.* [135] using either aluminium or iron electrode materials for CSG associated water evaluated the ability of electrocoagulation to remediate solutions of low, medium and high total dissolved solid (TDS) concentration. These authors found that aluminium electrodes were more effective for low and medium TDS solutions, whereas for the high TDS sample iron electrodes were preferred. In all cases levels of silicates, alkaline earth ions and boron were diminished significantly. Although aluminium electrodes performed well with regards to EC treatment of CSG associated water, there were some disadvantages to using this material. First, the flocs produced were difficult to settle [237] which meant that more costly dewatering technologies such as a filter press may be required [238, 239]. Secondly, the use of aluminium electrodes resulted in the formation of residual

aluminium species in the treated water which could potentially precipitate and cause problems downstream [132]. Third, aluminium is normally significantly more expensive than iron [135] and thus optimization of process economics dictated that iron would be preferred if performance could be improved.

One strategy to reduce electrode costs may be the use of both aluminium and iron electrodes in the same EC unit. Potentially, this situation could maintain the performance of aluminium electrodes but take advantage of the lower cost of iron. For example, Phalakornkule *et al.* [240] studied textile water treatment by EC and discovered that individual Al or Fe electrodes consumed approximately 40 to 50 % more energy compared to a situation where combined electrodes were employed. Heidmann *et al.* [241] reported that 52 % Ni, 90 % Cu and 99 % Cr were removed from galvanic wastewater by an Al-Fe electrode combination (which was higher compared to individual Al or Fe electrodes).

Although electrode material selection is an important operational parameter, there are other factors which can impact EC performance such as current density, solution pH, temperature & composition, hydraulic retention time (HRT), polarity reversal time (PRT) and electrode history [132, 242, 243]. Millar *et al.* [34] studied EC treatment of CSG associated water and showed that greater HRT values enhanced removal efficiency albeit this came at a cost in terms of additional consumption of electricity and electrode material. During EC operation a complication arises due to the formation of oxidic layers on the electrode surfaces which can promote passivation [130, 244]. This passivation layer obstructs or stops the normal rate of the EC process which can elevate power consumption and reduce removal efficiency [245].

Suggested methods to minimize the impact of passivation include ultrasonic processing, the addition of chloride ions, or application of polarity reversal [179, 244, 246]. Addition of chloride ions changes the composition of Al or Fe oxide film and forms transitory compounds which initiate pitting in the passivation layer [247, 248]. Though chloride ions addition may work effectively, this process contaminates the water and increases the costs of chemicals [249]. Therefore, application of polarity reversal is preferred [246, 250, 251]. For instance, Ciblak *et al.* [252] recommended a polarity reversal time (PRT) of 5 h to control pH and to maintain a proper environment for removal performance in an EC unit. Whereas, other authors have indicated that PRT should be progressively increased from 30 s to 250 s during extended tests using EC [253]. Wellner *et al.* [132] experimented with 0.5, 1 and 3 min PRT values when conducting EC of NaCl and NaHCO$_3$ solution. They found that applying polarity reversal impacted the rate of electrode erosion, thus potentially increasing the cost of EC operation. It is noted that Fekete *et al.* [254] suggested a minimum duration existed for PRT to be effective as time was required to remove the passivation layer.

From the above literature review it can be concluded there was a significant knowledge gap in relation to the applicability of EC using mixed iron-aluminium electrodes to treat CSG associated water. The hypothesis was that optimisation of EC equipped with Al-Fe combined electrodes can not only be an efficient pre-treatment method for CSG associated water but also more cost effective than aluminium electrodes. Therefore, the aim of this study was to develop an improved understanding of the benefits and drawbacks of the influence of HRT and PRT on a continuous EC unit. To achieve this aim, the following research questions were addressed: (1) what

is the performance of Al-Fe combined electrodes as a function of hydraulic residence time? (2) How do the water quality and consumption of electrodes/electricity compare to individual Al or Fe electrodes? (3) Can the selection of appropriate HRT values maintain purification efficiency while minimizing consumable cost? (4) Does the application of different polarity reversal times provide process improvement (PRT)? (5) What is the settling behaviour of produced flocs? To answer these questions, a benchtop, continuous EC unit equipped with Al-Fe combined electrodes was used to treat simulated CSG water of moderate TDS content.

7.2 RESULTS AND DISCUSSION

7.2.1 Impact of Hydraulic Retention Time (HRT) upon Electrocoagulation Performance

The freshly prepared simulated CSG associated water was treated by the continuous EC system at HRT values of 20, 30, and 60 s (which equated to flow rates of 1.59, 1.13, and 0.58 L/min, respectively).

7.2.1.1 Variation in Effluent pH and Turbidity of Treated CSG Associated Water

Initially, the solution turbidity was 468 NTU and this decreased to 2.46, 11.9, and 145 NTU with HRT of 20, 30, and 60 s, respectively [Figure 7-1]. It was noted that apparent colour removal also followed the trend of turbidity reduction. Initially, the apparent colour was 2230 Pt-Co units, which was then reduced to 25, 110 and 650 Pt-Co units for the HRT values of 20, 30, and 60 s, respectively. In contrast, true colour did not change significantly (10 - 15 Pt-Co unit) when HRT was varied.
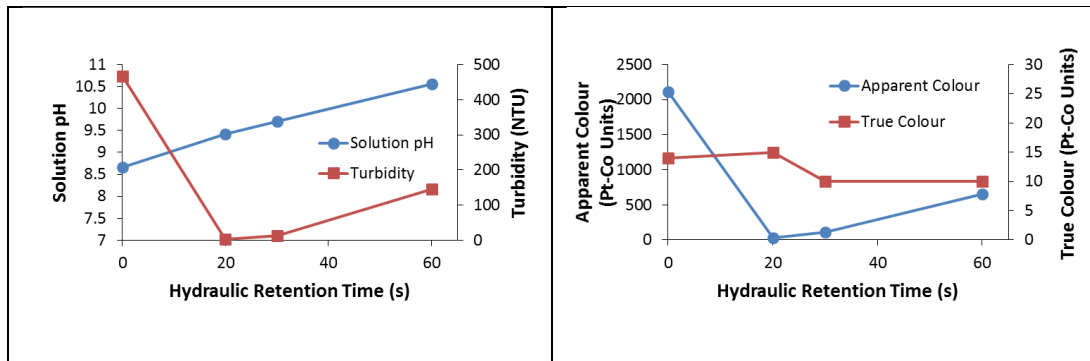
Figure 7-1: Impact of HRT upon effluent pH and turbidity of EC treated CSG associated water sample: PRT 3 min; test time 40 min

From these results, it was deduced that the apparent colour was mostly due to the presence of suspended kaolin in the solution. True colour may have related to the presence of iron species which are known to be coloured. Analysis of the treated water sample indicated that there were no detectable amounts of dissolved iron, hence the colour could not be ascribed to these species. Instead, it was assumed that particulate material was the cause of the discolouration. As the sample was filtered through a 0.45 micron syringe filter for the true colour measurement it can be inferred that colloidal particles less than the aforementioned size were present. This conclusion was in accord with the fact visual observations indicated that as the HRT value was increased the amount of suspended flocs in the treated CSG associated water became greater. Hence, a rise in solution turbidity was recorded after HRT was increased to 30 and 60 s. Essentially the suspended flocs interfered with the turbidity measurement. The overall recorded effectiveness of EC to substantially reduce turbidity levels was in harmony with previous studies. For example, Bellebia *et al.* [173] investigated the feasibility of EC over chemical coagulation to reduce contaminants from paper mill effluents. The time-dependent turbidity removal efficiency of EC was measured using Al or Fe electrodes. In both cases removal efficiency increased with time and highest

removal (> 99.9%) of turbidity was achieved after 10 min HRT and the removal efficiency was constant beyond that time. Wang *et al.* [255] applied EC to oxide chemical mechanical polishing wastewater using Fe-Al and Al-Fe combination as anode and cathode. They recorded 95 % turbidity removal at 12 min HRT from Fe-Al (anode-cathode) combination and 28 min HRT for Al-Fe (anode-cathode) combination. The reason behind these results was explained as a factor of the electrochemical equivalent mass of Al (335.6 mg/Ah) and Fe (1041 mg/Ah). Theoretically, more coagulant was produced from Fe electrodes relative to Al electrodes for the same electric charge; thus greater reduction in turbidity due to more flocs formed could be expected.

The behavior of pH in an EC process can be complex because it is a combination of chemical and electro-chemical reactions [242, 256]. Figure 7-1 showed a gradual increase in pH value from 8.66 to 9.41, 9.71, and 10.56 for HRT of 20, 30, and 60 s, respectively. Canizares *et al.* [256] studied pH variation in a NaCl solution during electrocoagulation and found that pH may increase up to 2 units during the EC process depending on the cation dose. It was discovered that when the initial pH was below 9 it increased after EC treatment and decreased if the pH was above 9 prior to treatment. An increase in pH after EC treatment has been described by Mores *et al.* [139] for aluminium electrodes. They postulated that aluminium hydroxide production increased the pH level in the solution. Similarly, Ciblak *et al.* [252] and Sengil and Ozacar [257] proposed that iron hydroxide production also increased the pH level. Principally, the longer the water was retained in the reactor the more flocs were produced; thus contributing to higher pH values. Moreover, Zhi and Zhang [258] reported that aluminium hydroxide can further react with chloride ions if the

electrolyte contains sodium chloride. This reaction formed OH$^-$ species and as such increased the alkalinity of the solution.

7.2.1.2   Variation in Alkaline Earth Ions, Boron, and Silicates

The concentration of sodium and potassium did not change noticeably after the EC treatment which was consistent with the fact that a plausible removal mechanism was absent for singly charged cations [34]. Therefore, Figure 7-2 shows only those species which were changed in concentration due to the EC process. Overall, the removal of alkaline earth ions and silicates was relatively high with a distinct increase in performance as HRT was extended.
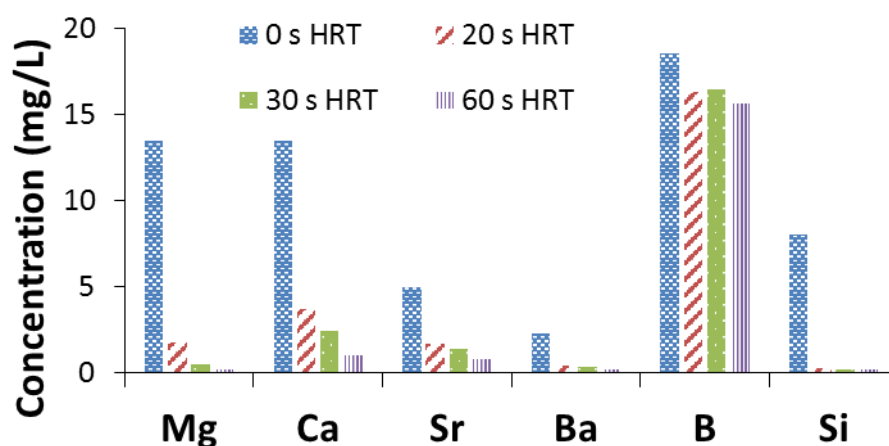
Figure 7-2: Concentration of dissolved species in CSG associated water before and after EC treatment; polarity reversal period 3 min; test time 40 min

As a general observation, increasing the HRT primarily promoted the removal of alkaline earth ions and boron. Whereas, silicate removal was less dependent upon HRT value. The ease of removal for the alkaline earth ions was in the order Mg > Ba > Ca > Sr [Table 7-2].

Table 7-1: Summary of removal performance for dissolved species in CSG water before and after EC treatment: polarity reversal period 3 min; test time 40 min (concentrations are in mg/L, % removal in brackets)

Aluminium & Mild Steel (Iron) Electrodes			
	Initial	HRT 20 s	HRT 30 s	HRT 60 s
Mg	13.52	1.77 (86.9 %)	0.47 (96.5 %)	0.02 (99.9 %)
Ca	13.48	3.71 (72.5 %)	2.46 (81.3 %)	1.02 (92.3 %)
Sr	5.013	1.67 (66.6 %)	1.41 (71.6 %)	0.81 (84.3 %)
Ba	2.29	0.41 (82.1 %)	0.37 (83.8 %)	0.21 (91.1 %)
B	18.6	16.31 (12.3 %)	16.45 (12.1 %)	15.66 (18.3 %)
Si	8.06	0.23 (97.1 %)	0.17 (97.9 %)	0.19 (97.6 %)
Al	0	20.35	34.89	68.63

Comparison of the performance of the mixed Al-Fe electrodes with either pure aluminium or pure iron electrodes revealed some interesting information. In the study of Wellner *et al.* [135] the water designated "medium TDS" was similar to the one tested in this investigation. For Al electrodes the removal order for alkaline earth ions was Ba > Sr > Mg > Ca and for Fe electrodes the corresponding order was Ba > Mg > Sr > Ca. In terms of the absolute percentage of alkaline earth species removed, the mixed electrodes considerably outperformed pure iron electrodes and were similar in magnitude to pure aluminium electrodes. Promotion of magnesium removal (96.5 % *c.f.* 83.6 and 44.6 % for Al & Fe, respectively) with the Al-Fe electrode combination (compared to aluminium or iron [135]) cannot simply be attributed to the elevated pH conditions as similar values were obtained with Al & Fe electrodes. One means of removing magnesium is thought to be as precipitated $Mg(OH)_2$ species according to Equation 7-1 at a pH around 10.2 [259].

Equation 7-1: $$Mg^{2+} + 2\,OH^- \leftrightarrow Mg(OH)_2$$

Malakootian *et al.* [220] found that increasing solution pH facilitated the removal of hardness from drinking water using EC equipped with iron electrodes. This result essentially agreed with the data in Table 7-1 where increasing HRT caused the pH to rise. At a pH of *ca.* 9.5 magnesium is present in solution as a mixture of Mg^{2+} and $Mg(OH)^+$ ions and it is reasonable to assume they can interact with the surface of negatively charged flocs [260]. It is therefore suggested that the co-presence of iron and aluminium based flocs generated material with enhanced properties for coagulation. This idea was in agreement with the investigation of Gomes *et al.* [261] who studied the removal of arsenic species from solution using an EC unit with Fe-Al electrodes along with polarity reversal every 15 min. Compared to Fe-Fe electrodes the Al-Fe derived flocs were more amorphous in character and Mössbauer spectroscopy analysis suggested that there was novel interaction between the iron and aluminium phases. Moreover, evidence was provided for the substitution of some aluminium ions in the iron material.

Similarly, the highly alkaline environment of the EC treated CSG associated water coupled with the substantial concentration of carbonate/bicarbonate species present would promote the formation of insoluble calcium carbonate [185]. Yet again though, the mixed electrode EC unit outperformed either Al or Fe electrodes (81.3 % *c.f.* 73.9 and 24.9 % Ca reduction for aluminium and iron electrodes [135]. Both strontium and barium removal were not promoted with the mixed electrodes but the extent of the reduction in their concentration was still favourable as it was only slightly less than pure aluminium electrodes. According to Kamaraj and Basudevan [188], EC

using Fe and Al electrodes achieved > 90 % strontium removal with an optimum pH of 7. Hence, it appears that the removal mechanism for strontium and barium may differ from that for calcium and magnesium ions.

Boron was removed to the least extent by the electrocoagulation process which was in agreement with previous studies of CSG associated water treatment with EC [135, 172]. Reasons for the relatively small reduction in boron content included too high a solution pH which inhibited uptake of borates by a negatively charged floc [262].

Remediation of dissolved silicates was practically independent of the HRT value [Table 7-1] which inferred that the mechanism for removal was different from that for alkaline earth ions. Den and Wang [192] were of the opinion that the formation of aluminosilicates was the explanation for high rates of silica removal when an aluminium coagulant was present. For iron, this avenue was not possible and instead, Den et $al.$ [223] postulated that silicate species were reduced by two means (1) destabilization of the charge on the silicate species by Fe^{2+} ions, and (2) enmeshment of silicates in iron oxide/hydroxide flocs (sweep flocculation). It appears that with the mixed electrodes the amount of aluminium species present was sufficient to make aluminosilicates and remove silica to high levels.

7.2.1.3 Variation in Residual Aluminium, Floc Mass, and Electrode Consumption

Analysis of the EC treated CSG associated water revealed that the amount of residual aluminium ion steadily increased as the HRT was extended [Figure 7-3].

There was no detectable trace of iron in the treated water, which indicated that this species was either completely hydrolysed to ferrous/ferric hydroxide or precipitated as insoluble iron oxide/oxyhydroxide. Recently, Fu [263] used mixed Fe-Al electrodes when applying EC to remove a dye from solution. When using polarity reversal the concentration of dissolved iron ions was not detectable. Whereas dissolved aluminium ions were present and the quantity steadily increased as the treatment process was lengthened. These observations were in accord with this study. Zaroual *et al.* [264] treated textile effluent by EC using Fe electrodes at a pH above 8 and concluded that electrolysis potentials above 0.7 V resulted in an effluent which was completely exempt from iron. In the experiments detailed here, the potential was typically above 2.5 V per cell on average and effluent pH was always above 9. Therefore, the experimental conditions in this study may be expected to contain no iron. Residual metal ions can lead to contamination of post-treated water to an unacceptable level. In this case, the residual aluminium concentration was relatively high (ranging from 20.35 to 68.63 mg/L at HRT of 20 and 60 s, respectively). In comparison, He *et al.* [176] demonstrated that aluminium based coagulants at pH 6.5 used to remove fluoride from drinking water produced up to 16 mg/L residual aluminium in the treated water. Jimenez *et al.* [265] experimented with both Fe and Al electrodes separately with a NaCl solution as an electrolyte. They found above pH 9 precipitate formation decreased for Al (presumably due to the presence of soluble $Al(OH)_4^-$ and increased for Fe); which was consistent with our findings.

Notably, the mass lost from the iron electrodes was significantly greater than from the aluminium electrodes [Figure 7-4]. The mass ratio of iron to aluminium was measured as 2.28, 2.27, and 2.00 for HRT values of 20, 30, & 60 s, respectively. The

predicted ratio of atomic mass Fe: Al was 3.10 which was substantially higher than the measured values. However, this ratio was estimated using the assumption that Al^{3+} and Fe^{2+} species were ideally formed at the anodes due to the electrochemical process. In reality, it was noted in Table 7-2 that there appeared to be an excess mass of Al electrode consumed which was attributed to a chemical process and not an electrochemical pathway [181, 266]. Interestingly, a reduced amount of iron was consistently released from the electrodes compared to the theoretical prediction [Table 7-2]. This behaviour suggested that instead of anodic dissolution of iron occurring that instead, some oxidation of water occurred [Equation 7-2].

Equation 7-2: $2\,H_2O \rightarrow 4\,H^+ + O_2 + 4\,e^-$
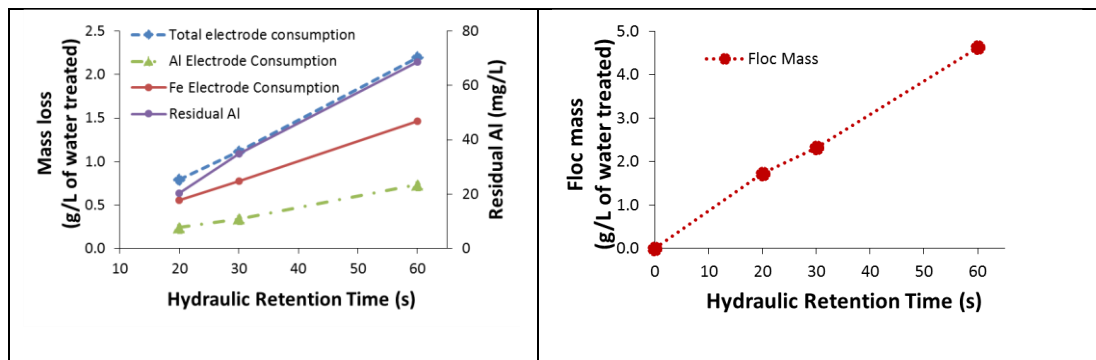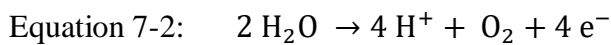
Figure 7-3: Impact of HRT upon residual aluminium, floc mass formed and electrode consumption for CSG associated water sample; PRT 3 min; test time 40 min

Floc mass increased from 1.71 to 4.63 g/L with the same variation in HRT [Figure 7-3 & Table 7-2]. Theoretically, if all aluminium dissolved from the electrodes was hydrolysed to aluminium hydroxide ($Al(OH)_3$) then the ratio of floc mass to electrode consumed would be 2.89. Similarly, if all iron from the electrodes was hydrolysed to $Fe(OH)_2$ or $Fe(OH)_3$ then the ratio of floc to electrode would be 1.61 or

1.91, respectively. Hence, a calculation was made to estimate the amount of floc that should have been found based upon the measured mass loss of electrodes [Table 7-2].
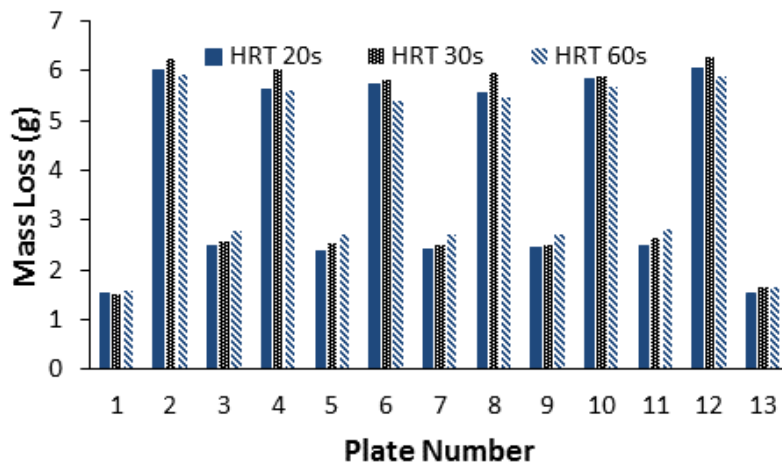
Figure 7-4: Electrode mass loss as a function of hydraulic retention time (aluminium "odd number" and iron "even number")

It was apparent that a close correspondence between recorded electrode mass loss and recorded floc mass was achieved if it was assumed that $Al(OH)_3$ and $Fe(OH)_3$ were the major components of the EC flocs when the HRT was 20 s. For longer HRT values an explanation for the relationship of floc mass to electrode mass loss was only possible if it was assumed that a mixture of $Fe(OH)_2$ and $Fe(OH)_3$ was present. As the HRT was extended the production of hydrogen was also increased thus purging the solution and making it anaerobic in character. An iron electrode based EC investigation of arsenic removal by Van Genuchten $et~al.$ [211] found that the dissolved oxygen concentration essentially zero, thus confirming that anaerobic conditions are probable in an EC unit. Dubrawski $et~al.$ [214] evaluated electrocoagulation equipped with iron electrodes to treat solutions of sodium chloride, sodium sulphate, and sodium bicarbonate. These authors noted that under anaerobic conditions in the EC cell "green rust" was formed in the presence of carbonate.

Bicarbonate/carbonate species were present in substantial amounts in the CSG associated water and thus species such as $[Fe_4^{II} Fe_2^{III}(OH)_{12}][CO_3.2H_2O]$ may form part of the floc composition [213].

Table 7-2: Summary of current, voltage, power consumption, and electrode consumption when treating CSG associated water by EC at various HRT values

	HRT 20 s	HRT 30 s	HRT 60 s
Average Voltage (V)	31.84	30.68	28.84
Average Current (A)	9.36	9.46	9.16
Average Current Density (mA/cm^2)	5.20	5.26	5.09
Flow Rate (L/min)	1.59	1.17	0.58
Power Consumption (kWh/kL)	3.12	4.13	7.59
Theoretical Al electrode loss (g/L)	0.20	0.27	0.53
Actual loss Al electrode loss(g/L)	0.24	0.34	0.73
Theoretical Fe electrode loss (g/L)	0.61	0.84	1.65
Actual loss Fe electrode loss (g/L)	0.55	0.77	1.46
Measured Floc Mass (g/L)	1.72	2.32	4.63
Predicted Floc Mass (g/L) (assuming Al(OH)$_3$ + Fe(OH)$_2$)	1.58	2.22	4.46
Predicted Floc Mass (g/L) (assuming Al(OH)$_3$ + Fe(OH)$_3$)	1.75	2.46	4.90

From the wear profile of the electrodes, the electrode dissolution of the two Al end-plates was approximately half of the other Al electrodes. The reason behind this observation was the fact that the two end electrodes were adjacent to the EC unit walls and thus did not participate in reactions. Wear of electrodes 2 and 12 was higher compared to inner electrodes due to the bipolar configuration delivering the biggest electrical load to these elements [171].

It was seen in Table 7-2 that electrode dissolution increased gradually with the increase of HRT for aluminium electrodes. The percentage excess of Al consumed by a chemical pathway was 20, 26, & 38 % for HRT values of 20, 30 & 60 s, respectively. Therefore it was inferred that the chemical reaction was favoured by increased residence time. With iron electrodes, the percentage consumed relative to theoretical predictions was 90, 92, & 88 % for HRT values of 20, 30 & 60 s, respectively. A correlation between current density and Fe electrode loss was present; namely, a higher current density corresponded to a greater amount of iron released from the anodes. Higher current density means that the surface was less passivated by oxide/oxyhydroxide species [132]. The less passivation of the anode the less water oxidation according to equation 3-1 which occurred (and hence more release of Fe^{2+} species).

7.2.1.4 Floc Settling Behaviour and Characterization
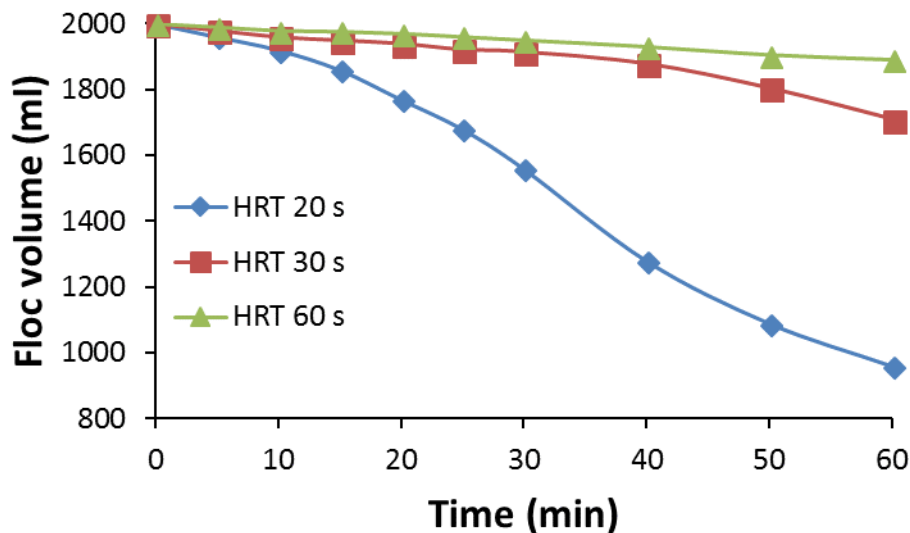
Figure 7-5: Floc sedimentation rate as a function of HRT; test time 40 min; PRT 3 min

The floc settling rate is very important in relation to the practical use of EC. In an industrial situation, floc settling within 60 min is preferred in order to be cost-effective [267]. Consequently, floc sedimentation rates were recorded for the EC tests as a function of HRT [Figure 7-5]. It was apparent that only at the shortest HRT value of 20 s that the flocs exhibited settling behaviour. A point of relevance as mentioned in Section 7.2.1.2 was the fact that more hydrogen bubbles are produced from the cathodic reduction of water as residence time increased. This hydrogen gas gets trapped in the aggregated flocs and thus can induce the electroflotation effect which keeps the flocs suspended in the solution for a longer period [268].

(a) HRT 20 s   (b) HRT 30 s   (c) HRT 60 s
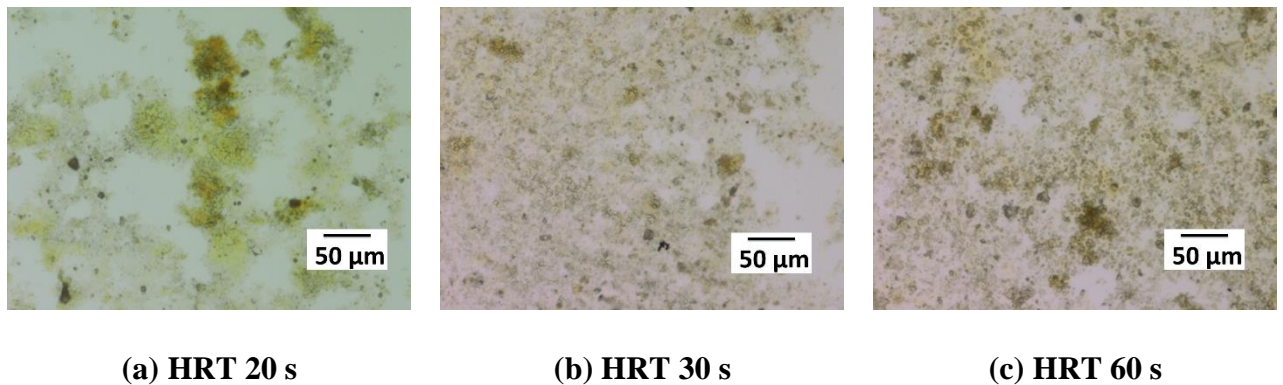
Figure 7-6: Optical microscopic images of flocs for various HRT values

Figure 7-6 illustrated the general structure of the flocs produced as a function of hydraulic residence time. The most notable aspect was that the flocs formed at 20 s HRT were remarkably different from those at 30 & 60 s. This observation was consistent with the conclusions in Section 7.2.1.2 which indicated that at 20 s HRT the floc was comprised of $Al(OH)_3$ and $Fe(OH)_3$ and that for 30 & 60 s HRT values the flocs were comprised of $Al(OH)_3$ and perhaps "green rust" or other species which comprise of Fe^{2+} and Fe^{3+} species.

7.2.2 <u>Impact of Polarity Reversal Time (PRT) upon Electrocoagulation</u>

    <u>Performance</u>

In this section, results from EC experiments for 1, 3 and 5 min PRT periods are presented and a 30 s HRT value was maintained throughout these experiments.

7.2.2.1 <u>Variation in Effluent pH and Turbidity of Treated CSG Associated</u>

    <u>Water</u>

Figure 7-7 showed a slight difference in solution pH with the change of polarity reversal time (9.64, 9.71, and 9.65 for PRT values of 1, 3, & 5 min, respectively.
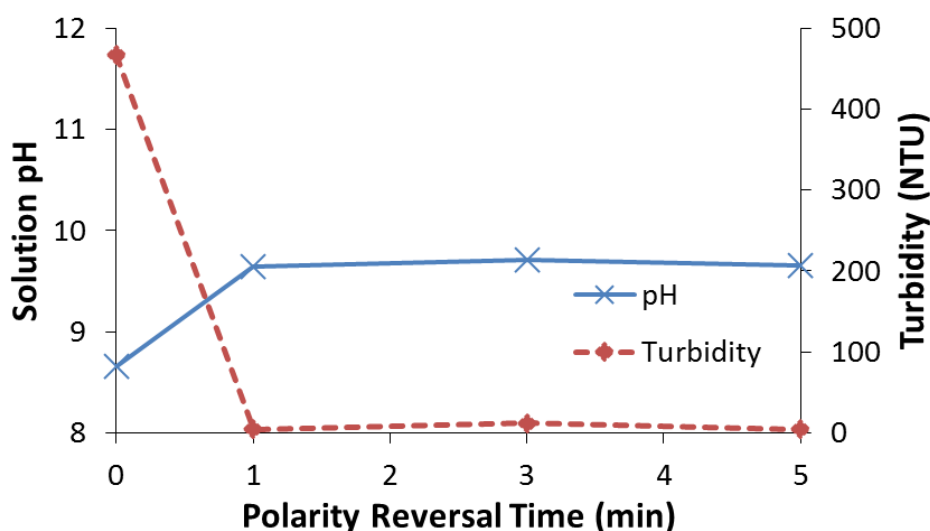
Figure 7-7: Impact of PRT upon effluent pH and turbidity of EC treated CSG water sample; HRT 30 s; test time 40 min

Figure 7-7 also revealed that turbidity was removed > 99 % for 1 and 5 min PRT periods and 97 % for 3 min PRT. The small difference in turbidity removal efficiency may reflect the presence of some suspended floc matter in the treated CSG associated water after EC treatment.

7.2.2.2 Variation in Alkaline Earth Ions, Boron, and Silicates

Figure 7-8 displays the impact of EC treatment using variable PRT periods upon the removal of alkline earth ions, boron, and silicates. Overall, PRT did not sifgnificanly impact the removal of either alkaline earth ions, boron or dissolved silicates. There was a trend in that a 3 min PRT seemed to produce a cleaner solution than the other PRT values. One example to illustate this observation was the removal of calcium ions. The initial concentration was 13.80 mg/L which reduced to 2.89, 2.46, and 2.81 mg/L for 1, 3 and 5 min PRT periods, respectively.
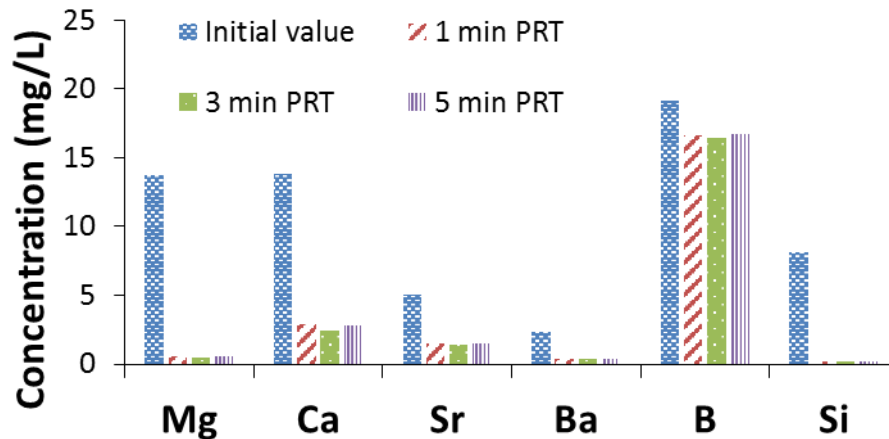
Figure 7-8: Concentration of dissolved species in CSG associated water before and after EC treatment; polarity reversal time from 1 to 5 min; test time 40 min; HRT 30s

Residual aluminium showed a similar trend as noted for the alkaline earth ions, boron, and silicates. The presence of dissolved aluminium in the treated water sample was not significantly influenced by PRT value as with the other species measured, and the greatest amount of aluminium was present at 3 min PRT (34.89 mg/L compared to 33.62 mg/L for 1 min PRT and 34.81 mg/L for 5 min PRT).

7.2.2.3   Variation in Floc Mass and Electrode Consumption

Table 7-2 revealed that the greatest current in the EC unit occurred at a PRT of 3 min. This behaviour indicated that the resistance of the electrode surface was least with this operational parameter. Conversely, this situation resulted in greater power consumption which may be compensated for by the enhanced pollutant removal recorded in Figure 7-8. As with the HRT experiments as the excess of aluminium consumption was evident (31, 26, & 30 % for PRT periods of 1, 3, & 5 min, respectively). As before the quantity of iron released from the anodes was less than predicted by the Faraday expression for all PRT values (86, 95, & 92 %). This data indicated that the degree of passivation was impacted by PRT with the 3 min PRT indicated as having the cleanest surface.

Table 7-3: Summary of current, voltage, power consumption, and electrode consumption when treating CSG associated water by EC at various polarity reversal time (PRT) periods

	PRT 1 min	PRT 3 min	PRT 5 min
Average Voltage (V)	30.7	30.7	30.7
Average Current (A)	9.15	9.46	9.35
Average Current Density (mA/cm^2)	5.08	5.26	5.19
Power Consumption (kWh/kL)	4.00	4.13	4.09
Theoretical Al electrode loss (g/L)	0.26	0.27	0.27
Actual loss Al electrode loss (g/L)	0.34	0.34	0.35
Theoretical Fe electrode loss (g/L)	0.81	0.83	0.84
Actual loss Fe electrode loss (g/L)	0.70	0.79	0.77
Measured Floc Mass (g/L)	2.53	2.62	2.60

In harmony with the fact that a PRT time of 3 min provided the cleanest electrode surfaces the formation of floc was greatest with this condition.

7.2.2.4 Floc Settling Behaviour and Characterization

Figure 7-10 represents the sedimentation behavior of flocs produced during the EC process as a function of PRT. It was observed that floc produced for 1 min PRT settled more rapidly than those formed at 5 min and 3 min PRT. A potential reason for this phenomenon may be the relatively cleaner nature of the electrodes with PRT 3 min (Section 7.2.2.3). Increased electrocoagulation activity, in turn, promotes the evolution of hydrogen gas from the cathodes which lead to the flotation of the flocs and thus reduced sedimentation rate.
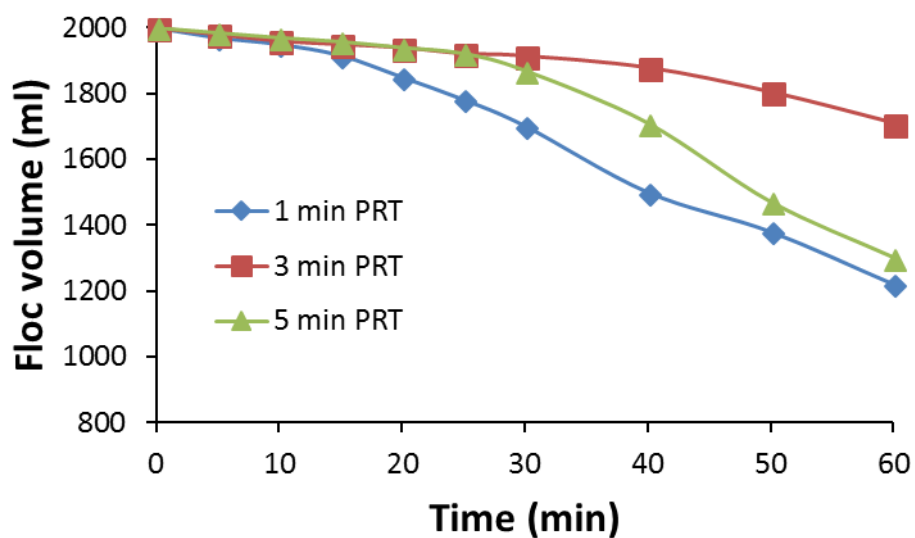
Figure 7-9: EC produced floc sedimentation rate as a function of PRT; test time 40 min; HRT 30 s

Figure 7-10 shows the optical microscopic images of flocs produced during EC for different PRT periods. Variation of the PRT did not cause a significant change in

the floc structure. Instead, increased hydrogen production seems the preferred explanation for variation in settling rate as a function of PRT.
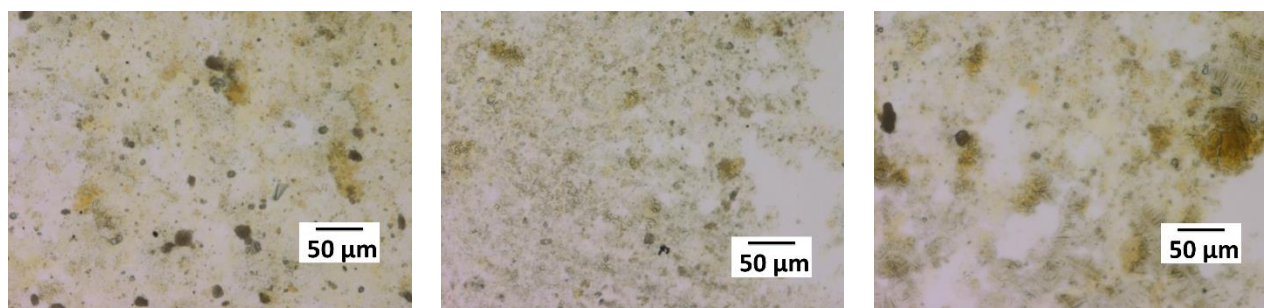
(a) PRT 1 min   (b) PRT 3 min   (c) PRT 5 min

Figure 7-10: Optical microscopy images of flocs produced during EC with various PRT periods

7.3 CONCLUSIONS

Electrocoagulation of CSG associated water with a mixed aluminium-iron electrode system has been shown to effectively remove turbidity, dissolved alkaline earth species and silicates (and to lesser extent boron). Residual aluminium was found in the effluent whereas no residual iron was evident. A strategy for eliminating aluminium species from the treated water needs to be found with future work suggested to focus on pH adjustment to convert soluble $Al(OH)_4^-$ into $Al(OH)_3$.

The mixed electrode system was particularly advantageous in terms of calcium and magnesium removal from solution. Overall, use of Fe-Al electrodes was better than with pure Fe-Fe electrodes and almost equivalent to pure Al-Al electrodes.

Hydraulic retention time was a key factor in terms of optimizing the EC treatment of CSG associated water. Extending the HRT did promote the removal of alkaline earth ions and boron (with a lesser impact on silicate removal) but the electrode and electricity consumption were at the same time greatly enhanced. Exploration of HRT values less than 20 s appears warranted as does an evaluation of the trade-off between performance and cost.

On the other hand, treatment efficiency was not strongly influenced by polarity reversal time but it was important with regards to electrode and electricity consumption. A 3 min PRT was deemed beneficial in terms of reduction in the presence of water contaminants. However, the electrode surfaces which were now less passivated consumed more power and electrode material.

Electrocoagulation is an attractive method for pre-treating water prior to a central desalination stage. Further refinement of this technology in terms of minimizing costs and understanding the relationship between water quality and performance is recommended.

Chapter 8: Applicability of Electrocoagulation to Treat High Efficiency Reverse Osmosis (HERO) Brine from CSG water

8.1 INTRODUCTION

Purification of associated water produced by the coal seam gas (CSG) industry has received considerable attention in recent years due to the need to make it suitable for beneficial reuse options [1, 19]. The CSG associated water is universally saline in character with total dissolved solids concentrations ranging from only a few hundred mg/L to in excess of 50,000 mg/L (depending upon geographical location) [21, 269]. Regardless of the source of the CSG associated water, the major species present are sodium, chloride and bicarbonate ions along with lesser amounts of alkaline earth ions, dissolved silicates, fluoride, sulphate and dissolved organic carbon [1, 51].

Reverse osmosis [74, 270] is the primary desalination method employed to reduce salt content in CSG associated water and make it suitable for uses such as crop irrigation, dust suppression, and re-injection. Despite the success of reverse osmosis for the CSG industry, brine management remains of concern, with several strategies suggested to resolve this issue [100, 271-275]. Typically, the brine is stored in a double lined brine storage dam which is relatively expensive to construct. Hence, efforts have been focussed on the recovery of greater quantities of water from the CSG associated water to maximise the lifetime of the storage dams. For example, Le [82] described the implementation of a "brine squeezer" technology developed by Osmoflo which was used to treat CSG associated water from the Santos Narrabri project in New

South Wales. Water recovery was said to increase from *ca.* 70 to 75 % from the first reverse osmosis system to 92 to 95 % after application of the "brine squeezer". Nghiem *et al.* [53] related the results from a pilot plant study of a CSG associated water treatment system incorporating an ultrafiltration unit, reverse osmosis plant and a multi-effect distillation process to improve water recovery rates. It was intimated that 95 % water recovery could be achieved over a one week operational period; albeit, there was evidence that some scaling due to calcium, magnesium, and silica may have occurred. Kim *et al.* [276] described the integration of a fertilizer drawn forward osmosis process to further recover water from reverse osmosis brine derived from desalination of CSG associated water. Not only were water recovery rates improved to in excess of 85 % but also a concomitant reduction in energy required to treat the water was noted. Membrane distillation (MD) has also received attention for recovering high quantities of water from CSG associated water. For instance, Duong *et al.* [277] applied a direct contact MD system to concentrate CSG reverse osmosis brine and reported stable operation when the water recovery rate was up to 90 %.

Another option for high percentage water recovery is the High Efficiency Reverse Osmosis (HERO) process. As described by Mukhopadhyay [278] the essence of the HERO process design was to firstly soften the feed water and simultaneously reduce alkalinity using a H^+- weak acid cation (WAC) resin. Subsequently, the carbon dioxide evolved during the initial softening stage was removed by degassing. Then the solution pH was raised to between 10 and 11 as this reduced the solubility of problematic silicates and also eliminated the potential for microbiological growth. Using the outlined approach it has been reported that water recovery can be in excess of 90 %. Moftah [279] provided further insight into the HERO approach and the

process variations which included lime softening, softening with strong acid cation resins or zeolites, acidification following sodium cycle softening and use of hydrophobic membrane contactors for carbon dioxide removal. Demonstration of the HERO process for cooling tower water supply in a power station confirmed that 92 % recovery of water was possible. Long *et al.* [280] also used a HERO system for wastewater treatment and stable operation was demonstrated when the feed solution pH was in the range 10.5 to 10.8.

Ideally, the recovery of the salts present in the concentrated brines from the RO process is desirable as part of a zero liquid discharge strategy [281]. However, Chen *et al.* [33] indicated that the main issue with highly concentrated brines, such as those produced from the application of the HERO process, was the presence of dissolved silica at levels up to 1500 mg/L. When the brine samples were acidified prior to a final salt crystallization stage fouling of equipment due to precipitation of silicates becomes a challenge.

One potential technological solution is the use of electrocoagulation (EC) which has been reported as being able to remove up to 89 % of silica species from brine produced after nanofiltration of Arizona Project Water [33]. Notably, the use of mild steel (iron) electrodes limited the operational pH of the EC unit due to extensive passivation of the electrode surface at a pH of 10 or above. In terms of the application of electrocoagulation to CSG associated water, Wellner *et al.* [135] treated simulated CSG produced water using an EC unit equipped with aluminium or iron electrodes. These authors recorded 89.5 to 98 % dissolved silica removal irrespective of salt content and electrode type and also noted that alkaline earth ions were significantly

removed from the feed sample (albeit aluminium electrodes appeared more effective than steel electrodes in this instance). The question arises as to whether EC can remove dissolved silicates from concentrated brine samples. Canizares *et al.* [282] indicated that electro-dissolution of the anodes during electrocoagulation occurs *via* both electrochemical and chemical pathways. Alkaline pH values such as those expected for HERO brine samples could substantially accelerate chemical dissolution of anodes; thus increasing operational costs. Additionally, the presence of pitting promoters such as chloride ions is also well known to enhance the dissolution of electrode materials and potentially result in super-Faradaic charge yields [180].

Critical analysis of current literature has revealed that these exists a research gap relating to the evaluation of electrocoagulation for the purification of highly concentrated brines produced by reverse osmosis treatment of CSG associated water. Therefore, the aim of this study was to investigate the applicability of EC to treat concentrated brine and determine optimum conditions for EC operation. The hypothesis was that electrocoagulation units equipped with aluminium or mild steel (iron) or combined aluminium and iron electrodes may be a promising technology to treat HERO brine resultant from CSG produced water treatment. To support this hypothesis the following questions were addressed: (1) can EC effectively treat HERO brine? (2) which combination of electrodes enhances the performance of EC? (3) what is the effect of hydraulic retention time (HRT) upon contaminant removal efficiency? (4) how does polarity reversal time (PRT) influence EC performance? (5) what are the settling properties of the flocs produced? To answer these questions a laboratory-scale EC unit was used, which not only operated in a continuous mode but was also equipped

with a polarity reversal facility. Electrodes studied were aluminium, mild steel and a combination of aluminium and mild steel.

8.2   RESULTS AND DISCUSSION

8.2.1 Impact of Hydraulic Retention Time (HRT) upon Electrocoagulation Performance

To investigate the effect of hydraulic retention time on EC performance three different HRT values of 20, 30, and 60 s were used with each combination of electrodes (Al, Fe, and Al-Fe). As the retention time was increased the pH was slightly elevated regardless of the electrode material employed [Figure 8-1]. This behaviour was in contrast to EC studies of CSG associated water where the pH significantly increased to *ca.* 10 [34, 135].

Figure 8-1 Impact of hydraulic retention time upon treated brine pH using either aluminium, mild steel (iron) or combined aluminium-mild steel (iron) electrodes

However, it was noted by Wellner *et al.* [135] that the final solution pH of the EC treated CSG associated water trended to lower values as the TDS of the sample was increased. In addition, the HERO brine was buffered by bicarbonate/carbonate

species similar to other high salinity solutions such as soda lakes in central Asia where the pH is stabilized in the range 9 to 11 due to high salt content (up to 600 mS/cm) and high alkalinity (up to 0.55 M total carbonate alkalinity) [283].

8.2.1.1 Variation in Alkaline Earth Ions, Boron, Silicates, and Residual Aluminium/Iron

Figure 8-2 Impact of hydraulic retention time upon treated brine composition using either aluminium, mild steel (iron) or combined aluminium-mild steel (iron) electrodes

Chapter 8: Applicability of Electrocoagulation to Treat High Efficiency Reverse Osmosis (HERO) Brine from CSG water

In terms of alkaline earth ion removal, application of iron electrodes appeared to be more effective in general than either aluminium electrodes or mixed aluminium/iron electrodes [Figure 8-2]. This observation was consistent with the study of Wellner *et al.* [135] who noted that iron electrodes more effectively removed alkaline earth ions for high TDS CSG associated water (compared to aluminium). This observation was in contrast to low and medium TDS content water samples where aluminium electrodes performed better than iron. The performance of aluminium and iron combined electrodes was majorly in between that of aluminium and iron electrodes.

Another general conclusion from the EC tests was that extending the HRT promoted the reduction in alkaline earth ions for all electrode configurations [Table 8-1]. More specifically, for every electrode combination the percentage of alkaline earth ions removed was in the order Ba > Sr > Ca > Mg. Previous studies also concluded that barium ions were in most instances the alkaline earth ion removed to the greatest extent from CSG associated water [135]. Esmaeilirad *et al.* [259] examined the softening of flowback water from a shale oil & gas operation in the USA both before and after EC treatment. Investigation of the solubility product constant for a variety of carbonate, sulphate, and hydroxide salts of alkaline earth ions suggested that barium sulphate was the least soluble salt under process conditions followed by strontium carbonate and calcium carbonate. If the solution pH had been higher than 10 then magnesium hydroxide species would have been the least soluble; however, in this study, the solution pH was ca. 9.6 or less hance magnesium was removed to the least extent [Figure 8-1]. As the brine comprised of a large excess of sulphate species compared to barium ions the formation of $BaSO_4$ was strongly favoured. Calcium

carbonate can precipitate at a pH of 9.4 [24, 185] which was less than the effluent pH of *ca.* 9.5 in this study. The promotion of alkaline earth ion removal as a function of increasing HRT [Table 8-1] may reflect the fact that a greater amount of floc species were created in the EC cell [Table 8-2] in addition to a slight raising of solution pH [Figure 8-1].

The question arose as to why iron electrodes appeared to be more effective at reducing the concentration of alkaline earth ions relative to aluminium electrodes. Inspection of Figure 8-1 revealed that the solution pH was highest for iron electrodes, less for mixed aluminium-iron electrodes and least for aluminium electrodes. Consequently, the ability of EC to remove alkaline earth ions appeared directly related to the solubility of corresponding salts in agreement with Esmaeilirad *et al.* [259]. Notably, the solution pH reported by Wellner *et al.* [135] for CSG associated water characterized by high TDS content was *ca.* 10 to 11 for iron electrodes and only *ca.* 9 when aluminium electrodes were employed. In harmony with the data from this current study of CSG brines, the removal percentage of alkaline earth ions was greater with the iron electrodes. As a caveat, it is emphasised that solution pH although highly important in relation to the reduction of alkaline earth ions in solution is not the only factor which must be considered. The study of Wellner *et al.* [135] measured the highest levels of removal with aluminium electrodes with solution pH values (9 to 10) less than when iron electrodes were used at higher pH values (10 to 11). One possible influencing factor was the solubility of the flocs formed.
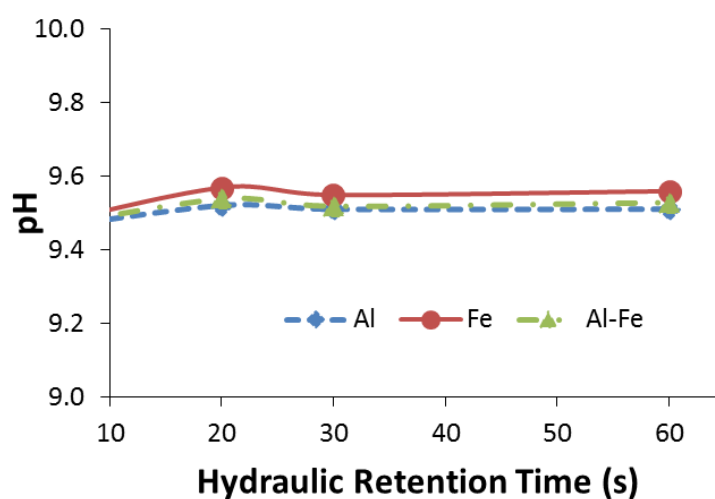
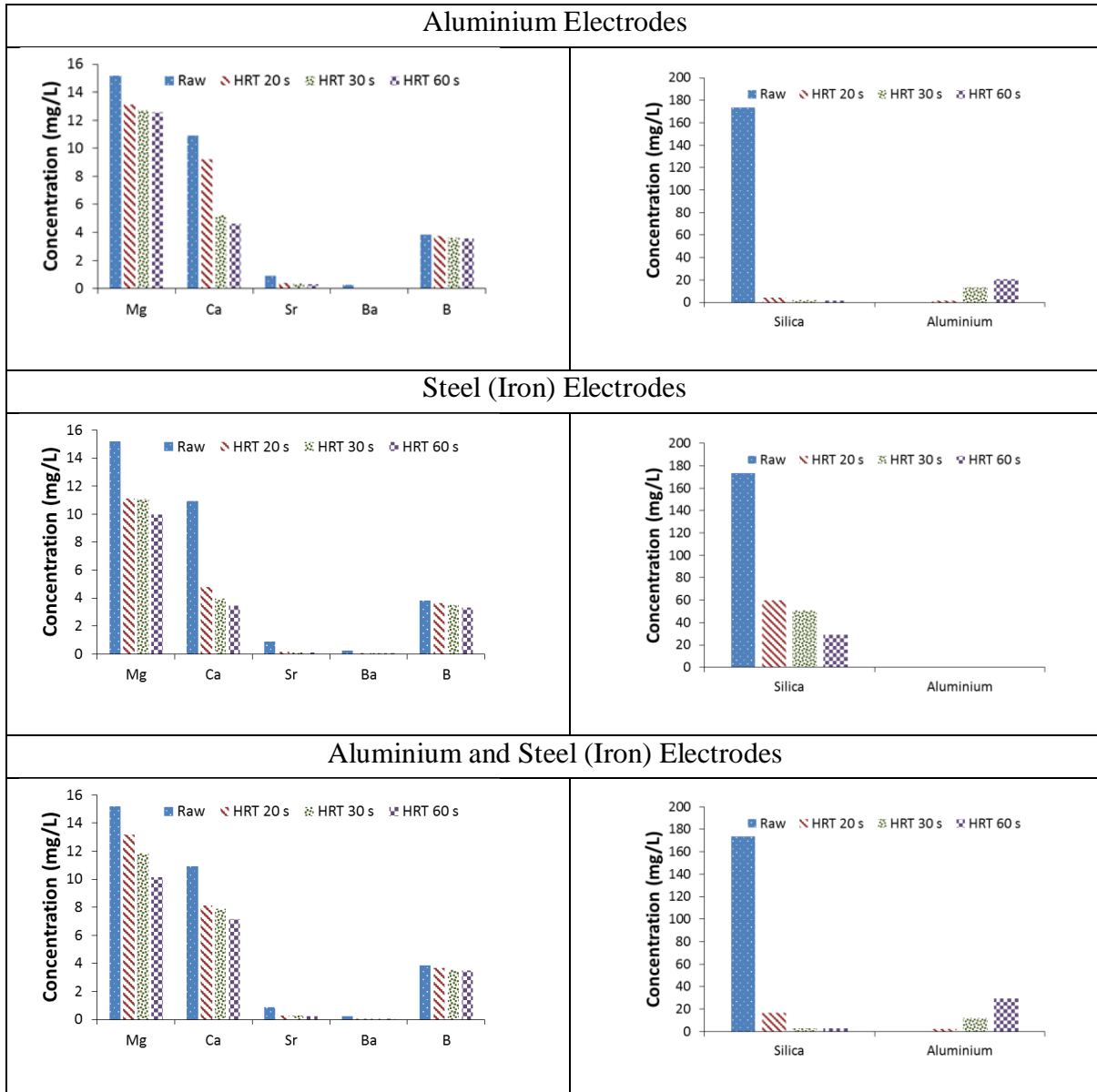Table 8-1 Data for Impact of hydraulic retention time upon treated brine composition using either aluminium, mild steel (iron) or combined aluminium-mild steel (iron) electrodes (concentrations are in mg/L, % removal in brackets)

Aluminium Electrodes				
	Initial	HRT 20 s	HRT 30 s	HRT 60 s
Mg	15.2	13.1 (13.7%)	12.7 (16.2 %)	12.5 (17.4 %)
Ca	10.9	9.2 (15.4%)	5.2 (52.2%)	4.6 (57.7 %)
Sr	0.89	0.39 (56.3%)	0.34 (61.5 %)	0.31 (64.6%)
Ba	0.25	0.03 (89.0%)	0.02 (90.7 %)	0.02 (91.5 %)
B	3.8	3.7 (2.53%)	3.6 (5.2 %)	3.6 (6.6 %)
Si	82.2	2.1 (97.5%)	0.91 (98.9%)	0.87 (98.94%)
Al	0	1.7	13.3	20.9
Mild Steel (Iron) Electrodes				
	Initial	HRT 20 s	HRT 30 s	HRT 60 s
Mg	15.2	11.1 (26.8%)	11.1 (27.2%)	10.0 (34.4%)
Ca	10.9	4.8 (56.0%)	4.0 (63.6%)	3.4 (68.5%)
Sr	0.89	0.17 (81.3%)	0.10 (88.7%)	0.09 (89.8%)
Ba	0.25	0.02 (93.9%)	0.01 (95.1)	0.01 (95.1%)
B	3.8	3.6 (5.2%)	3.5 (8.8%)	3.3 (14.0%)
Si	82.2	28.2 (65.7%)	24.2 (70.7%)	13.7 (83.3%)
Al	0	0	0	0
Aluminium & Mild Steel (Iron) Electrodes				
	Initial	HRT 20 s	HRT 30 s	HRT 60 s
Mg	15.2	13.2 (13.2%)	11.9 (21.9%)	10.1 (33.2%)
Ca	10.9	8.1 (25.7%)	7.9 (27.7%)	7.2 (34.4%)
Sr	0.89	0.28 (68.5%)	0.26 (70.9%)	0.21 (76.5%)
Ba	0.25	0.022 (91.1%)	0.021 (91.5%)	0.017 (93.1%)
B	3.8	3.7 (4.1%)	3.53 (8.0%)	3.5 (8.7%)
Si	82.2	7.9 (90.4%)	1.4 (98.3%)	1.2 (98.5%)
Al	0	2.2	11.9	29.5

Kamaraj and Vasudevan [188] discussed the pH dependence of strontium ion removal when using an EC system equipped with either aluminium or iron electrodes. Optimal reduction in dissolved strontium species was observed at neutral pH values. This phenomenon was attributed to the formation of soluble species such as Al^{3+} ions at low pH and $Al(OH)_4^-$ at elevated pH. The same authors also noted that iron electrodes outperformed aluminium electrodes under their test conditions which simply involved the addition of a strontium salt to pure water. This study also highlighted the need to carefully consider solution chemistry when inferring mechanisms for alkaline earth ion removal. In this investigation, we employed a complex brine for EC evaluation containing species such as sulphate, bicarbonate, and carbonate which all react with alkaline earth ions. Murthy and Parmar [187] similarly found maximum Sr removal by iron electrodes (93.49 %) and aluminium electrodes (78.57 %) around neutral pH as again they only used a very simple solution of strontium chloride.

In all instances boron was not removed to a substantial degree (< 15 %) which suggested EC was not the preferred technique for reducing the content of this species in CSG brine. Nevertheless, there are numerous publications which indicate that boron can be eliminated from contaminated water samples using EC to a high degree. For example, Widhiastuti *et al.* [221] achieved 70.3 % removal of boron using iron electrodes to treat 10 mg/L boron in a sodium chloride solution. Introduction of nickel electrodes to the EC unit further promoted boron uptake. A key finding was that the pH corresponding to the point of zero charge (pzc) was important with respect to boron sorption. These authors postulated that a positive surface was required to sorb boron and that iron based flocs had a pH_{pzc} value of only 8.2. Hence, for CSG brine the pH

values induced a negative charge on the floc surface and thus limited boron uptake. This view was in accord with the EC study of Millar *et al.* [34] relating to CSG associated water treatment with aluminium electrodes. A pH of 9 or greater was said to result in the formation of negatively charged tetrahydroxyborate species, which may not sorb to negatively charged aluminium hydroxide flocs. Interestingly, the pH_{pzc} value for $NiFe_2O_4$ materials of 10.2 [221] made this system of interest for future work on boron remediation in CSG brine as it was in excess of the pH values of *ca.* 9.5. The increase in boron removal with longer HRT may be related to the increasing amounts of flocs generated which can potentially remove the boron species by sweep flocculation. Isa *et al.* [27] found that increasing the contact time of boron in an EC unit promoted the removal performance from *ca.* 75 % to greater than 95 %, and Dolati *et al.* [190] also found that HRT was an important parameter with respect to boron removal using electrocoagulation. Hence, the benefit of HRT in terms of boron removal is an accepted result. Nevertheless, consideration of this situation on process economics is a topic that should also be addressed in future studies.

Silicate removal from the HERO brine was dependent upon not only electrode choice but also HRT [Table 8-1]. When aluminium or aluminium-iron electrode configuration was adopted, a very high percentage of silicate removal was recorded (> 90 %). This finding was significant in terms of the main aim of this study to determine if silicates could be effectively removed from CSG brine to facilitate salt crystallization. What was also apparent was that iron electrodes were not as effective as aluminium electrodes with silicate removal ranging from 65.7 to 83.3. Recently, Hafez *et al.* [191] noted that silica removal efficiency from cooling blowdown water using EC was favoured by aluminium electrodes rather than iron electrodes. A critical

observation was enhanced removal of silicates occurred when current density was increased. If solution pH became too high it was mentioned that a slight reduction in silicate remediation was recorded due to the formation of soluble species from the produced flocs such as Al(OH)$_4$$^-$. XRD analysis indicated the produced flocs were mainly amorphous thus it was difficult to assess the removal mechanism for silicates. Den and Wang [192] previously suggested that in neutral solutions, silicates were removed in the form of aluminosilicates. Obviously, this route to silicate removal is not applicable to EC systems with iron electrodes. Instead, Den *et al.* [223] suggested that silica removal from polishing wastewater by means of an electrocoagulation unit equipped with iron electrodes proceeded by two processes. The first involved destabilization of the charge on the silicate species by Fe^{2+} ions liberated from the anode, thus allowing them to floc. The second mechanism was postulated to be enmeshment of silicates in iron oxide/hydroxide flocs. In relation to the form of silica Cheng *et al.* [152] indicated that at a pH less than 9.5 the dominant silica species was silicic acid (Si(OH)$_4$) and that above this critical pH the transformations illustrated in Equations 8-1 & 8-2 occurred.

Equation 8-1: $Si(OH)_4 \leftrightarrow H_3SiO_4{}^- + H^+$

Equation 8-2: $H_3SiO_4{}^- \leftrightarrow H_2SiO_4{}^{2-} + H^+$
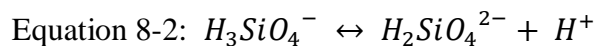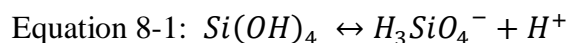
Notably, based upon the assumption that iron based flocs had a pH$_{pzc}$ value of 8.2 and the pH of the brine was typically *ca.* 9.5, removal of silicate species was expected to be more challenging with iron electrodes.

Residual material from the electrodes in the effluent may be a concern when applying EC to treat contaminated water. For example, aluminium ions in the treated water can lead to problems associated with precipitation of aluminosilicate species on reverse osmosis membranes [284]. Additionally, the presence of aluminium ions in solution can significantly limit the effectiveness of commercial anti-scalant chemicals used to protect reverse osmosis membranes [285, 286]. Aluminium species in drinking water can also lead to health implications such as the promotion of Alzheimer's disease [287]. Residual iron was not detected in the EC studies which was in agreement with the study by Ciblak *et al.* [209] which indicated residual iron formation was inhibited when bicarbonate/carbonate species were present. Hence discussion will only focus on residual aluminium. The concentration of aluminium species in the EC treated brine increased as a function of HRT for both aluminium and aluminium-iron electrodes [Table 8-1]. The recorded range of values was 1.7 to 20.9 mg/L for aluminium electrodes and 2.2 to 29.5 mg/L for aluminium-iron electrodes. These values were in harmony with reported residual aluminium concentrations produced when treating CSG associated water with EC. Wellner *et al.* [135] found that the amount of aluminium was related to the solution TDS and ranged from 4.6 to 39 mg/L. The observation that greater residual aluminium was formed with aluminium-iron electrodes rather than pure aluminium electrodes can be related to the solution pH. As shown in Figure 8-1 the solution pH was slightly higher when iron/aluminium electrodes were employed. Thus, the formation of $Al(OH)_4^-$ species was accelerated.

8.2.1.2 Variation in Floc Mass, Power, and Electrode Consumption

The values for floc mass produced, electricity and electrode consumption during the EC tests are displayed in Table 8-2. General trends included an increase in electrode & power consumption with increasing HRT and a corresponding greater

generation of floc. Specifically, the power consumption was least for the Al-Fe electrode configuration.

Table 8-2: Summary of EC performance when using aluminium electrodes to treat CSG brine for 3 min PRT

	Aluminium			Iron			Aluminium & Iron		
	20 s	30 s	60 s	20 s	30 s	60 s	20 s	30 s	60 s
Average Voltage (V)	17.64	17.89	18.69	13.58	16.11	16.98	13.95	15.67	15.27
Average Current	4.89	5.03	5.06	4.93	4.97	5.01	4.46	4.91	5.03
Average Current Density (mA/cm^2)	2.72	2.79	2.81	2.74	2.76	2.78	2.48	2.73	2.79
Treatment volume (L)	17.70	13.50	5.46	17.70	13.50	5.46	17.70	13.50	5.46
Specific Power Consumption	0.81	1.11	2.89	0.63	0.99	2.60	0.59	0.95	2.34
Theoretical Al electrode loss (g/L)	0.19	0.25	0.62	-	-	-	0.085	0.122	0.309
Actual Al electrode loss (g/L)	0.06	0.08	0.21	-	-	-	0.044	0.070	0.161
Theoretical Fe electrode loss (g/L)	-	-	-	0.58	0.77	1.91	0.26	0.38	0.96
Actual Fe electrode loss (g/L)	-	-	-	0.20	0.24	0.70	0.06	0.10	0.26
Measured floc mass (g/L)	0.35	0.38	0.4	0.22	0.59	0.78	0.34	0.58	0.76

An unusual aspect of this study was that the measured electrode loss was always less than the theoretical prediction based on the Faraday expression [Equation 8-2]. Electrocoagulation of CSG associated water with aluminium or iron electrodes has been reported to consume greater quantities of electrode compared to theoretical calculations [34, 135]. This behaviour was rationalized in terms of chemical dissolution of the aluminium or iron surface due to the presence of chloride ions.

However, the brine was significantly different than the CSG associated water in that there was a substantial concentration of carbonate anions present. Carbonate species can interact with the surface of electrodes and result in passivation by the formation of siderite ($FeCO_3$) and ferric hydroxycarbonates [212]. An investigation of arsenic removal by electrocoagulation with iron electrodes revealed the presence of an "orange layer" on the electrode surface [130]. Notably, the overall electrode mass loss was suggested to be significantly less than would occur with a clean surface. Analysis using XRD indicated that Fe_3O_4 was the main phase present at the electrode surface, a material comprising of 33 % Fe^{2+} species. This discovery suggested that the EC unit was anaerobic in character as the complete oxidation of Fe^{2+} to Fe^{3+} was inhibited. The possibility of anaerobic conditions existing in an EC cell has been confirmed by Dubrawski *et al.* [214] when using iron electrocoagulation with various salt solutions. Formation of a passivated anode surface was expected to promote oxidation of water [Equation 8-3] instead of electrochemical dissolution of aluminium/iron.

Equation 8-3: $\quad 2\,H_2O \rightarrow 4\,H^+ + O_2 + 4\,e^-$
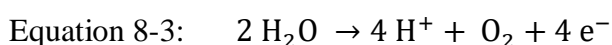
Fundamental investigations of electrocoagulation of sodium chloride and sodium bicarbonate solutions have shown that pH oscillations occurred which related to the degree of electrode passivation. The evolution of H^+ ions was detected by a dramatic decrease in the effluent pH and application of polarity reversal was demonstrated to exert significant influence on the nature of the pH oscillations. An estimate of the severity of surface passivation can be deduced from inspection of the ratio of electrode consumed predicted consumption based upon Equation 3-2. For aluminium electrodes the ratio was 0.32, 0.32, & 0.34 for HRT values of 20, 30, & 60

s, respectively. Similarly, for iron electrodes the ratio was 0.34, 0.31, & 0.37 for HRT values of 20, 30, & 60 s, respectively. Finally for the mixed electrode EC unit the ratio was 0.52, 0.57, & 0.52 (aluminium electrodes) and 0.23, 0.26, & 0.27 (iron electrodes) for HRT values of 20, 30, & 60 s, respectively.

Aluminium flocs are mainly $Al(OH)_3$ and iron flocs are commonly thought to be comprised of $Fe(OH)_2$ and $(Fe(OH)_3$. Therefore floc quantity can, in theory, be predicted from the actual consumption of the iron anodes (ratio floc/iron = 1.61 for $Fe(OH)_2$ and 1.91 for $Fe(OH)_3$) and aluminium anodes (ratio floc/aluminium = 2.89). In this case, calculations indicated that an excess of floc was mainly detected relative to anode material consumed; albeit, there were exceptions when electrode loss was substantially greater than the amount of floc created. A possible explanation related to the observation that the electrode surfaces at the end of the test period appeared heavily fouled by a gel like coating. Timmes *et al.* [134] recorded extensive formation of deposits on the surface of iron electrodes during pre-treatment of seawater. Similarly, van Genuchten *et al.* [130] observed a coating on iron electrodes which was difficult to remove. Thus it is plausible that a portion of the floc material released has been included into the passivating film on the electrode surface.

8.2.1.3 Floc Settling Behaviour and Physical Characteristics

Figure 8-3 displays the settling behaviour of flocs as a function of HRT values and electrode material. Notably, all flocs settled within the 60 min period of evaluation. This behaviour was not seen when aluminium electrodes were employed in an EC unit for treatment of CSG associated water [135]. Indeed, aluminium based flocs were particularly difficult to settle and this was ascribed to the fact these materials were amorphous with the consistency of "gel-like cotton wool" similar to reported

studies by Mahesh *et al.* [176] and Lee and Gagnon [288]. In line with the view of Kim *et al.* [289], it was evident that the structure of the flocs when treating CSG brine were changed due to the difference in water composition relative to CSG associated water.
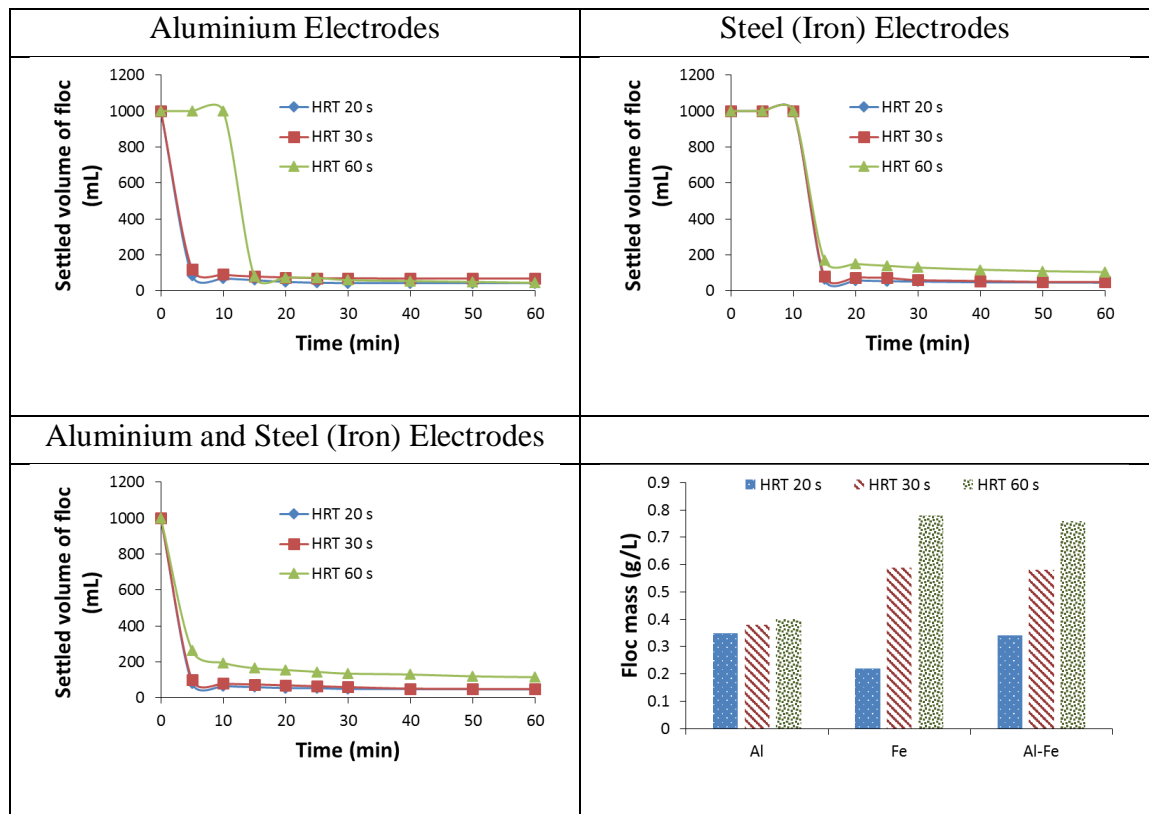
Figure 8-3: EC produced floc properties at various HRT for various electrode combinations (PRT 3 min; test time 10 min).

In all instances, flocs produced at the highest HRT value of 60 s were the most difficult to settle (particularly for aluminium electrodes) [Figure 8-3]. During the electrocoagulation process, hydrogen bubbles are evolved at the cathode and these can be entrapped in the flocs thus causing them to float [290]. Therefore, the longer the residence time of the brine in the EC unit the more bubbles produced and the greater

the chance of flotation occurring. This phenomenon was most notable when aluminium electrodes were present in the EC unit. Overall, the flocs settled well which was in contrast to the opinion of Brahmi *et al.* [182] who indicated that a drawback of the electrocoagulation method was not only the production of relatively large sludge volumes but also issues with extended settling time periods. Again, the importance of solution chemistry in relation to electrocoagulation application is stressed as being critical in terms of treatment performance.
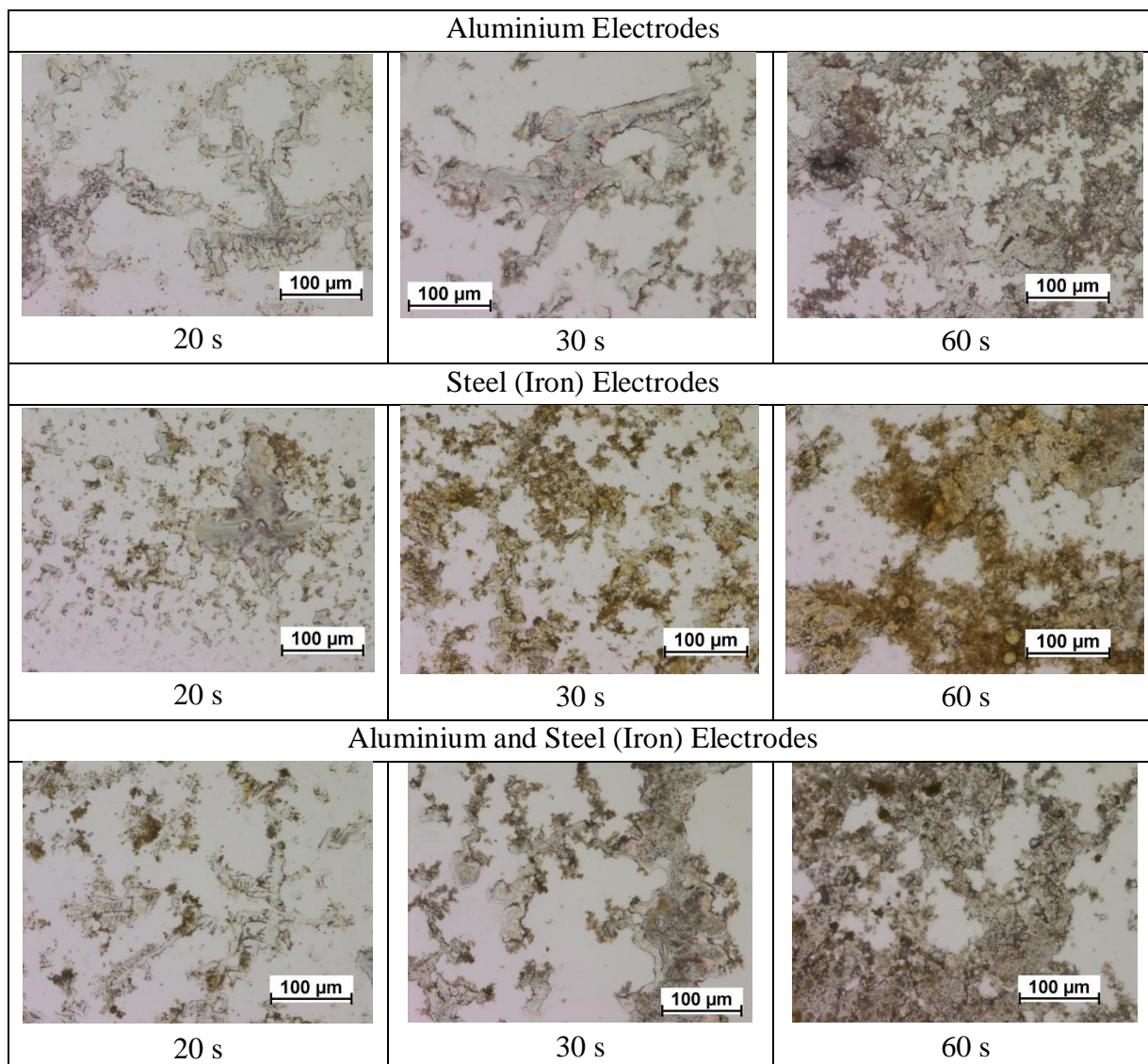
Figure 8-4: Optical microscopic images of EC produced flocs at various HRT for

various electrode combinations (PRT 3 min; test time 10 min)

In relation to this argument further insight was gained by examination of the produced flocs by optical microscopy [Figure 8-4]. In general, the flocs appeared to attain greater density when HRT was extended from 20 to 60 s in the electrocoagulation tests. In addition, the flocs generated from Al and Al-Fe combined electrodes were broadly similar in appearance.

8.2.2 Impact of Polarity Reversal Time (PRT) upon Electrocoagulation Performance

Figure 8-5 shows the variation in treated CSG brine pH after EC treatment as a function of PRT. Initial pH was 9.44 which slightly increased during EC testing, with aluminium electrodes exhibiting the lowest pH, iron the highest and the combined Fe-Al electrodes in between the pH for the individual electrodes.
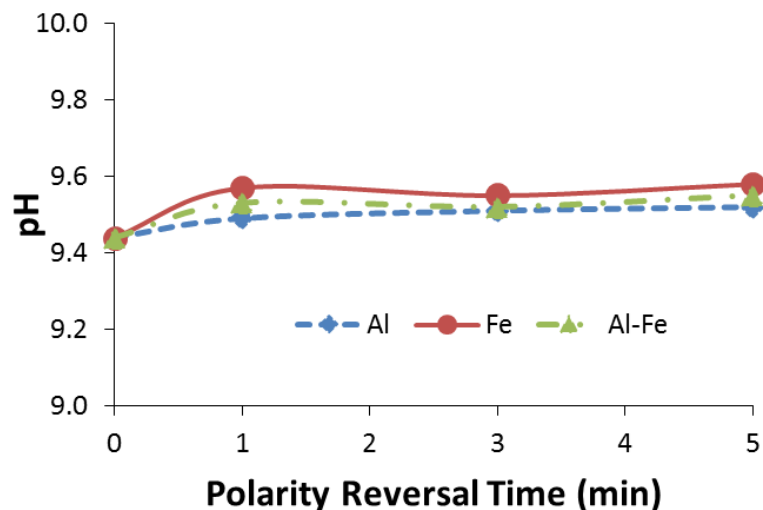
Figure 8-5: Impact of polarity reversal time (PRT) upon treated brine pH using either

aluminium, mild steel (iron) or combined aluminium-mild steel (iron) electrodes

8.2.2.1 Variation in Alkaline Earth Ions, Boron, Silicates, and Residual Aluminium/Iron

The influence of PRT upon the removal of dissolved species from HERO brine is shown in Figure 8-6.

Chapter 8: Applicability of Electrocoagulation to Treat High Efficiency Reverse Osmosis (HERO) Brine from CSG water
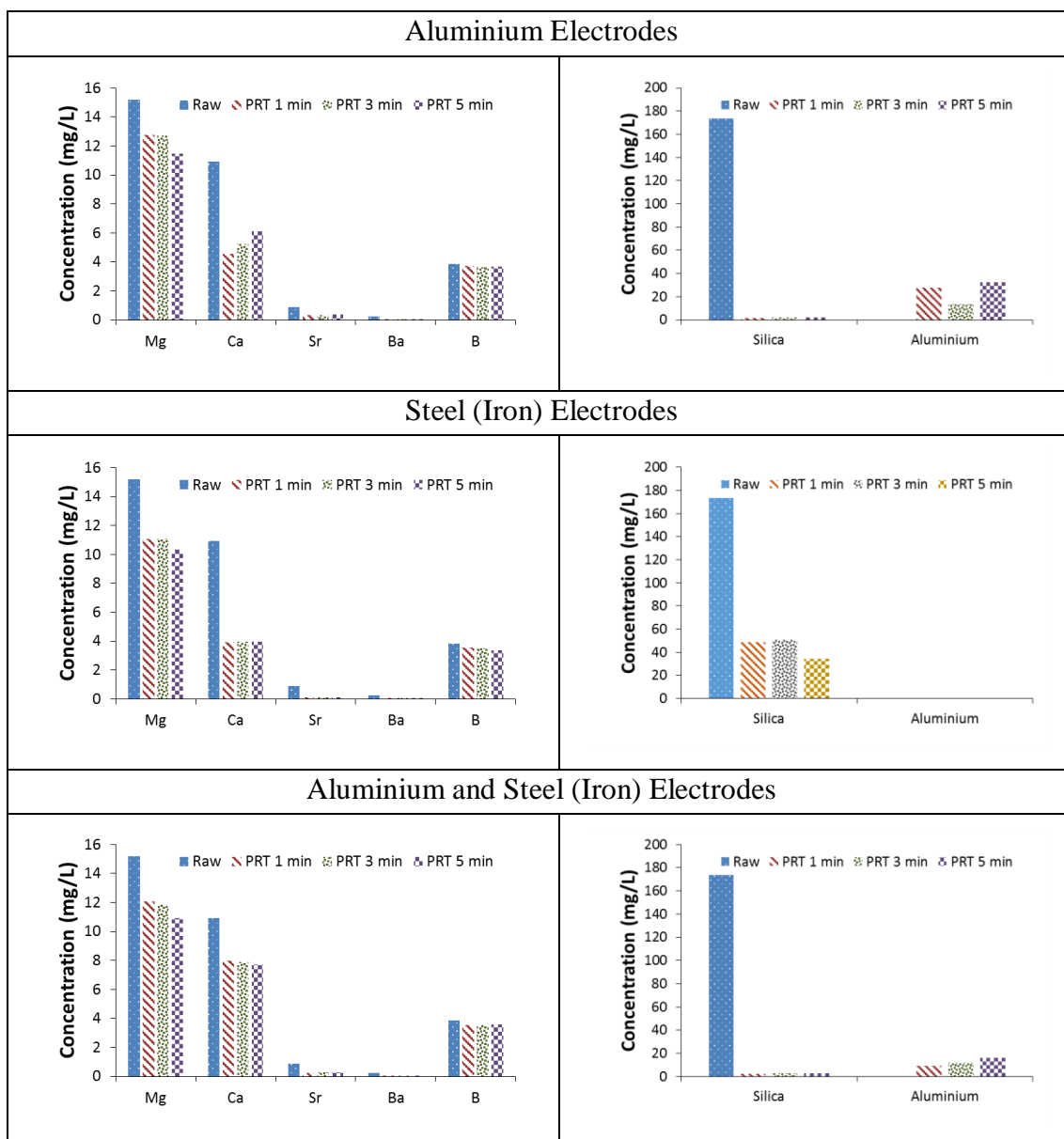
Figure 8-6: Impact of polarity reversal time upon treated brine composition using either aluminium, mild steel (iron) or combined aluminium-steel electrodes

Table 8-3: Data for Impact of polarity reversal time upon treated brine composition using either aluminium, mild steel (iron) or combined aluminium-mild steel (iron) electrodes (concentrations are in mg/L, % removal in brackets)

Aluminium Electrodes				
	Initial	PRT 1 min	PRT 3 min	PRT 5 min
Mg	15.2	12.86 (16.0 %)	12.72 (16.3 %)	11.45 (24.7 %)
Ca	10.9	4.54 (58.4 %)	5.212 (52.2 %)	6.11 (43.9 %)
Sr	0.89	0.34 (62.0 %)	0.341 (61.7 %)	0.348 (60.9 %)
Ba	0.25	0.025 (90.0 %)	0.023 (90.8 %)	0.02 (92.0 %)
B	3.8	3.71 (2.5 %)	3.634 (4.4 %)	3.657 (3.8 %)
Si	82.2	0.78 (99.1 %)	0.908 (98.9 %)	0.903 (98.9 %)
Al	0	27.9	13.3	32.6
Mild Steel (Iron) Electrodes				
	Initial	PRT 1 min	PRT 3 min	PRT 5 min
Mg	15.2	11.07 (27.2 %)	11.05 (27.3 %)	10.31 (32.2 %)
Ca	10.9	3.92 (64.0 %)	3.969 (63.6 %)	3.936 (63.9 %)
Sr	0.89	0.01 (88.8 %)	0.1 (88.8 %)	0.11 (87.6 %)
Ba	0.25	0.015 (94.0 %)	0.014 (94.4 %)	0.013 (94.8 %)
B	3.8	3.56 (6.3 %)	3.497 (8.0 %)	3.379 (11.1 %)
Si	82.2	22.94 (72.1 %)	24.12 (70.7 %)	16.22 (80.3 %)
Al	0	0	0	0
Aluminium & Mild Steel (Iron) Electrodes				
	Initial	PRT 1 min	PRT 3 min	PRT 5 min
Mg	15.2	12.08 (20.5 %)	11.85 (22.0 %)	10.9 (28.2 %)
Ca	10.9	7.97 (26.9 %)	7.89 (27.6 %)	7.71 (29.3 %)
Sr	0.89	0.24 (72.7 %)	0.26 (71.0 %)	0.28 (68.8 %)

Ba	0.25	0.022 (91.2 %)	0.021 (91.6 %)	0.015 (94.0 %)
B	3.8	3.52 (7.3 %)	3.53 (7.18 %)	3.58 (5.9 %)
Si	82.2	1.06 (98.7 %)	1.39 (98.3 %)	1.26 (98.5 %)
Al	0	9.1	11.1	16.3

As before [Figure 8-2] alkaline earth ions, boron, and silicates were all reduced in concentration due to the EC treatment. Broadly, the degree of removal was not substantially altered by the change in the PRT period [Table 8-3]. However, there were some notable trends as follows: for aluminium electrodes increasing PRT promoted the removal of magnesium and decreased the removal of calcium ions. Whereas, barium, strontium, boron and silicate concentrations remained relatively stable.

For iron electrodes, the most notable change was the increase in boron removal with increasing PRT. No statistically relevant change in alkaline earth in content was noted and silica concentration varied but no in a systematic manner. Finally, for the mixed Fe-Al electrodes magnesium, calcium, and barium all displayed a slightly better removal performance as PRT increased. In contrast, strontium, boron, and silicate removal were slightly decreased as HRT increased. Formation of residual aluminium species was noted for aluminium electrodes and mixed iron-aluminium electrodes with greater quantities observed for the pure Al electrodes.

8.2.2.2 Variation in Floc Mass and Electrode Consumption of Treated HERO brine

The power consumption varied with PRT period [Table 8-4]. For aluminium electrodes, there was perhaps a minimal change in power consumption when varying PRT from 1 to 5 min. Alternatively, with iron electrodes, there was a definite increase in power consumption as PRT increased. With the mixed electrode system, the

minimum energy consumption was apparent with a PRT of 1 min and this value slightly increased as PRT was elongated.

Table 8-4: Summary of EC performance when using aluminium, iron or aluminium-iron electrodes to treat CSG brine: effect of polarity reversal time

	Aluminium			Iron			Aluminium & Iron		
	1 min	3 min	5 min	1 min	3 min	5 min	1 min	3 min	5 min
Average Voltage (V)	17.94	17.89	17.59	12.75	16.11	16.06	15.02	15.67	15.64
Average Current	5.09	5.03	5.06	5.20	4.97	5.26	5.08	4.91	5.19
Average Current Density (mA/cm^2)	2.83	2.79	2.81	2.89	2.76	2.92	2.82	2.73	2.88
Treatment volume (L)	13.5	13.5	13.5	13.5	13.5	13.5	13.5	13.5	13.5
Specific Power Consumption	1.13	1.11	1.1	0.82	0.99	1.04	0.94	0.95	1.00
Theoretical Al electrode loss (g/L)	0.25	0.25	0.25	-	-	-	0.13	0.12	0.13
Actual loss Al electrode loss (g/L)	0.07	0.08	0.11	-	-	-	0.07	0.07	0.07
Theoretical Fe electrode loss (g/L)	-	-	-	0.8	0.77	0.81	0.39	0.38	0.40
Actual loss Fe electrode loss(g/L)	-	-	-	0.22	0.24	0.3	0.10	0.10	0.12
Measured floc mass (g/L)	0.30	0.38	0.42	0.42	0.59	0.65	0.60	0.58	0.53

8.2.2.3   Floc Settling Behaviour and Characterization

Figure 8-7 showed that the settling of the aluminium and aluminium-iron based flocs was very rapid. In contrast, the iron based flocs appeared to have an initial induction time of *ca.* 15 min wherein the flocs did not settle followed by a very quick settling rate. In all cases, the final floc volume was relatively compact (< 5 % of initial

volume). Polarity reversal period did not appear to induce a notable change in floc

behaviour as the settling curves were similar whether 1, 3, or 5 min PRT was applied.

Aluminium Electrodes	Steel (Iron) Electrodes
Aluminium and Steel (Iron) Electrodes	
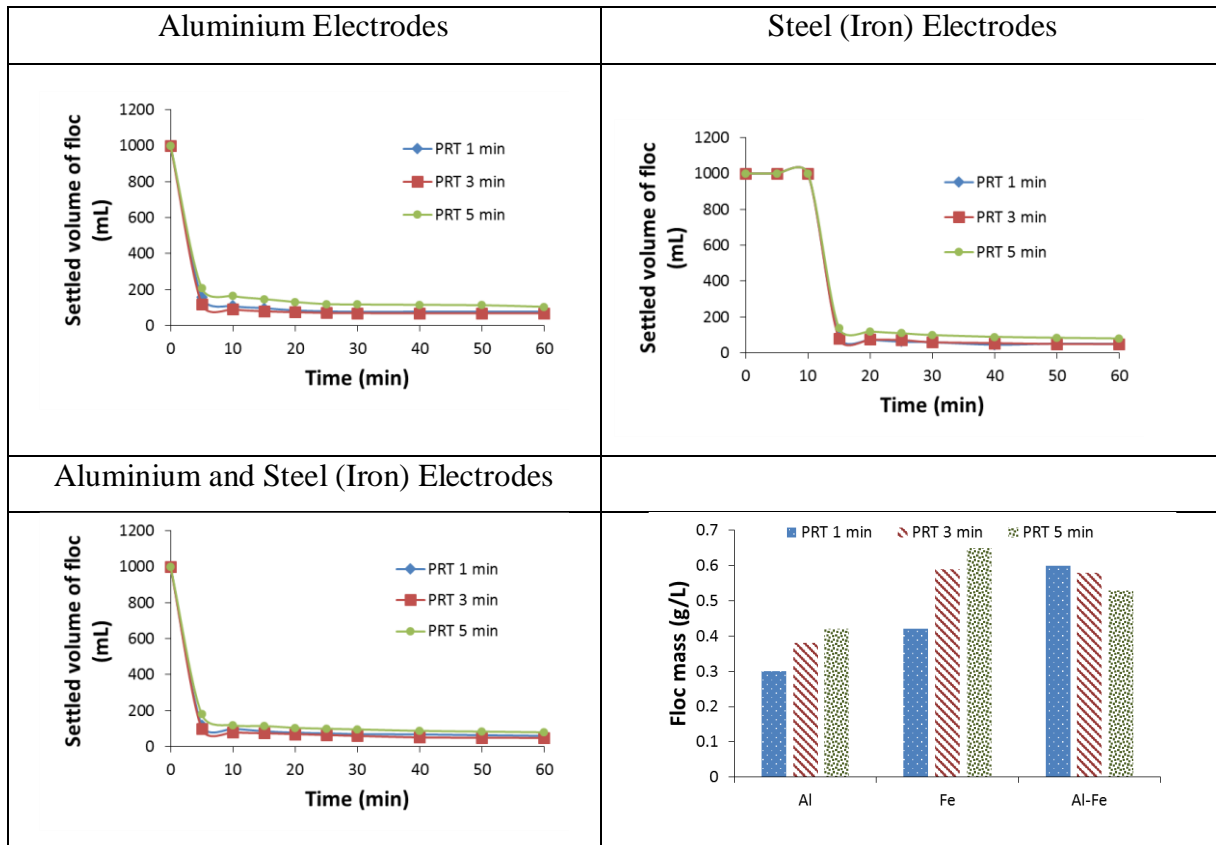
Figure 8-7: EC produced floc properties at various PRT for various electrode

combinations (HRT 30 s; test time 10 min).

Corresponding optical microscopy images [Figure 8-8] revealed that these was

no significant difference in the nature of the flocs formed. Therefore, comparable

settling behaviour not unexpected.

Aluminium Electrodes		
1 min	3 min	5 min
Steel (Iron) Electrodes		
1 min	3 min	5 min
Aluminium and Steel (Iron) Electrodes		
1 min	3 min	5 min
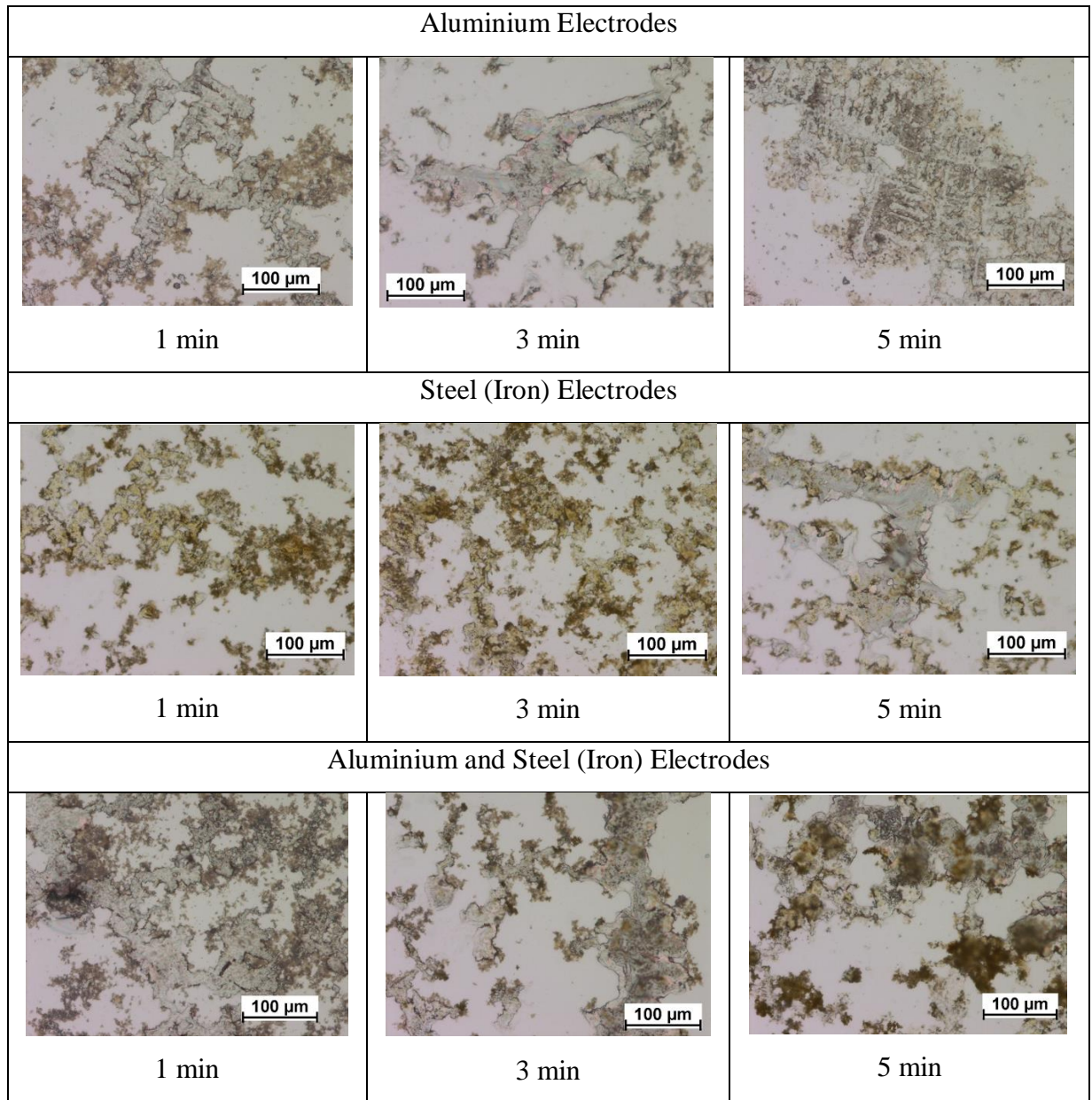
Figure 8-8: Optical microscopic images of EC produced flocs at various PRT for various electrode combinations (HRT 30 s; test time 10 min).

8.3 CONCLUSIONS

This study proved that electrocoagulation can operate successfully in highly concentrated brine produced from high pH reverse osmosis desalination of CSG associated water. Dissolved silicates which were the primary target for removal using

EC were reduced substantially in concentration when aluminium or aluminium-iron electrodes were employed.

Increasing the hydraulic retention time generally promoted the removal of contaminants present in the brine (alkaline earth ions, boron, and silicates). Economic considerations should be taken into account in detail in future studies to determine the trade-off between increased operational costs (electricity and electrode consumption) relative to better performance when HRT is increased.

Polarity reversal time was not a key parameter in relation to the removal of species such as silicates from the brine solution. Flocs settled rapidly regardless of whether they were aluminium, iron, or aluminium-iron based.

Chapter 9: Conclusions and Recommendations

9.1 CONCLUSIONS

The purpose of this research was to develop a pre-treatment process for Coal Seam Gas (CSG) to enhance the efficiency of reverse osmosis (RO) desalination unit and to remove salts from concentrated brine produced from high-efficiency reverse osmosis (HERO) operation. This study showed that coagulation technologies can reduce alkaline earth ions, boron, and dissolved silicates from both CSG water and HERO brine. Though coagulation is not a core technology in CSG water treatment it can be a potential pre-treatment technology for CSG water prior to a reverse osmosis desalination stage and for removing salts from HERO brine. The sections below show how the objectives of this study (stated in Section 1.3) was achieved;

9.1.1 Objective 1

The performance of aluminium chlorohydrate (ACH), alum and ferric chloride coagulants were evaluated to pre-treat CSG water with varying total dissolved solids (TDS) and different levels of turbidity. This study found that chemical coagulation (CC) can remove turbidity from CSG water efficiently (> 95 % removal). Among three inorganic coagulants studied aluminium chlorohydrate (ACH) was preferred because of its ability to promote the removal of silicate species by forming aluminosilicates and because of not introducing sulphate species in the CSG water, unlike alum. The floc produced from ACH settled faster than alum and ferric chloride with respect to floc sedimentation rate. A key finding of this study was that the co-presence of turbidity and organic matter promoted the formation of polymeric and colloidal species

which positively influenced the removal of contaminants. Turbidity level and salinity of the CSG water did not appear to be critical parameters with respect to coagulant performance. This observation suggested that coagulation processes may cope with the variation in CSG water quality.

9.1.2 Objective 2

Performance of electrocoagulation (EC) equipped with aluminium (Al-Al), iron (Fe-Fe) and combined (Al-Fe) electrodes to pre-treat turbid CSG water were studied. Comparison of varying hydraulic retention time (HRT) (20, 30 and 60 s) and varying polarity reversal time (PRT) (1, 3 and 5 min) were studied for the performance analysis of the EC.

Removal of turbidity from CSG water by electrocoagulation (EC) was very efficient with all combinations of electrodes. With a HRT of 20 s ca. 99 % turbidity was removed. Turbidity removal efficiency decreased with the increase of HRT because longer HRT values resulted in the fine flocs being re-suspended in the treated solution and thus minimizing the HRT was concluded as being more beneficial in terms of turbidity control. The ability of electrocoagulation to remove dissolved ions from CSG water was influenced by electrode types and HRT. Hydraulic retention time was also a critical parameter in terms of capital and operating costs for electrocoagulation of CSG associated water. The benefit in terms of removal efficiency of dissolved species such as alkaline earth ions and when increasing HRT from 20 to 60 s was minimal in relation to the extra electrode and power consumption required.

This study demonstrated that electrocoagulation with Al-Al, Fe-Fe and Al-Fe electrode combinations can reduce the concentrations of suspended solids, dissolved alkaline earth ions and silicates from highly turbid CSG associated water. Alkaline earth ions and dissolved silicates were removed by at least 90 %, albeit the removal mechanism for alkaline earth ions and dissolved silicates in the EC cell was determined to be different. Formation of aluminosilicates was postulated to explain the substantial reduction in dissolved silicate in solution. Suspended kaolin which can cause solution turbidity, from CSG associated water was effectively removed at low values of hydraulic retention time. Overall, use of Fe-Al electrodes was better in terms of removing dissolved species than with Fe-Fe electrodes and almost equivalent to pure Al-Al electrodes. The problem associated with Al-Al and Al-Fe electrodes was that residual aluminium was found in the effluent whereas no residual iron was evident. On the other hand, treatment efficiency was not strongly influenced by polarity reversal time (PRT), but it was important with regards to electrode and electricity consumption. The preferred PRT for electrocoagulation equipped with Al-Al electrodes to pre-treat CSG water prior to a reverse osmosis desalination stage was a value of 1 min or less and for Fe-Fe electrodes, the PRT was required to be at least 5 min. A 3 min PRT was found beneficial in terms of reduction in the presence of water contaminants when Al-Fe electrodes are employed. The results from this study indicate that electrocoagulation remains a potentially viable method for pre-treatment of CSG associated water prior to a central desalination stage such as reverse osmosis.

9.1.3 Objective 3

In this study, the applicability of EC to treat HERO brine was evaluated. Three different combinations of electrodes i.e., Al-Al, Fe-Fe, and Al-Fe were studied to compare the dissolved species removal efficiency. PRT did not influence the

performance of EC to treat HERO brine due to the presence of high chloride concentration, where the removal efficiency of alkaline earth ions, boron and silica increased with longer HRT. Highest alkaline earth ions and boron removal was achieved by Fe-Fe electrodes. Silicates removal was least by Fe-Fe electrodes ($< 68\%$), which was expected because silicates are easily removable as aluminosilicates by Al-Al and Al-Fe electrodes. Though Al-Fe electrodes consumed the least amount of power, the main concern in using Al-Fe electrodes was the high residual aluminium concentration (> 29 mg/L). Al-Al electrodes demonstrated the best performance regarding the amount of floc production and the electrode dissolution. However, the benefit of using Fe-Fe electrodes was that no residual iron was traced in the treated HERO brine. From the experimental results, it is evident that EC is a potential treatment method for HERO brine.

9.1.4 Summary

The experimental results advocate that EC can potentially treat both CSG water and HERO brine. EC equipped with Al-Al electrodes produces the best results for CSG water, while the performance of Fe-Fe electrodes is best in treating HERO brine by removing alkaline earth ions. In contrast, flocs produced in EC equipped with Fe-Fe electrodes settle rapidly for both CSG water and HERO brine. A significant finding is that EC can efficiently remove silicates from CSG water and HERO brine with any electrode combinations either Al-Al, Fe-Fe or Al-Fe at each studied hydraulic retention time (HRT: 20, 30 or 60 s) and each polarity reversal time (PRT: 1, 3 or 5 min).

This study suggested EC over chemical coagulation as the pre-treatment technology for CSG water. It was hypothesised that EC can replace the stages required in the CSG water process flow diagram (Figure 2-2) before RO. However, effluent

from EC was accompanied by floc which might require further treatment units such as clarifier or ballast flocculation. EC could not remove boron efficiently. Therefore, CSG water containing a considerable amount of boron should employ ion-exchange (IX) softening. EC was very efficient in removing salts from HERO brine with a fast floc sedimentation rate.

9.2 RECOMMENDATIONS FOR FUTURE RESEARCH

The following recommendations can be made for future research.

- **Novel EC configuration**

In this study, an EC reactor with multiple electrodes was connected in a bipolar configuration which resulted in non-uniform reactions in different cells. This issue probably reduced EC performance. Therefore, novel EC reactor configurations should be explored such as "pipe" reactor, fluidized bed EC reactor, horizontal plate EC and raceway type EC geometries.

- **Floc separation**

This study revealed that flocs generated by EC can be difficult to settle. Produced floc was very fine and fluffy and thus was very hard to separate from treated effluent. It is worth studying the integration of filtration steps such as centrifuges or filter presses.

- **Alternative electrodes**

This study found that aluminium electrodes can reduce alkaline earth ions efficiently but residual aluminium was a problem. On the other hand, iron electrodes were not effective in removing ions from CSG water. In that case, Ni and Zn could be

potential alternative electrodes which may provide benefits in terms of EC performance.

- **Pulsed current**

In this study, direct current was applied for EC. Alternatively, pulsed current can be studied to reduce the effect of passivation on anodes.

- **Boron Removal**

This study achieved lower removal of boron compared to silicates and alkaline earth ions. It is recommended to gain further understanding about how to optimise EC to remove boron from CSG water. Ideas include different electrodes to adjust the point of zero charge on the floc surface to be "positive" at high pH conditions.

- **Deeper Economic Evaluation:**

Hydraulic retention time was a key factor in terms of optimizing the EC treatment of CSG associated water. Extending the HRT did promote the removal of alkaline earth ions and boron (with a lesser impact on silicate removal) but the electrode and electricity consumption were at the same time greatly enhanced. Exploration of HRT values less than 20 s appears warranted as does an evaluation of the trade-off between performance and cost.

- **Feed water sample**

Simulated solutions could not adequately mimic the range of organic species such as natural organic matter which may be present in CSG water; hence, greater testing of real solutions was recommended.

- **Optimizing operation parameters**

Three different PRT (1, 3 and 5 min) were studied and it was found that in terms of removal efficiency 1 min and 5 min were best for Al-Al and Fe-Fe electrodes respectively. Therefore, it is worth studying Al-Al electrodes for less than 1 min PRT and Fe-Fe electrodes for more than 5 min PRT. Besides, the performance of electrocoagulation directly depends on electrode size and inter-electrode spacing. This study also found that the experimental results are in agreement with that observation. Different sizes of the electrodes and varying inter-electrodes spacing are also worth exploring.

Bibliography

[1] G.J. Millar, S.J. Couperthwaite, C.D. Moodliar, Strategies for the management and treatment of coal seam gas associated water, Renewable and Sustainable Energy Reviews, 57 (2016) 669-691.

[2] Meenakshi, R.C. Maheshwari, Fluoride in drinking water and its removal, Journal of Hazardous Materials, 137 (2006) 456-463.

[3] W.E. Forum, The Global Risks Report 2017, in, 2017.

[4] W.H. Organization, Progress on sanitation and drinking water: 2015 update and MDG assessment, World Health Organization, 2015.

[5] C.A. Rebello, S.J. Couperthwaite, G.J. Millar, L.A. Dawes, Understanding coal seam gas associated water, regulations and strategies for treatment, Journal of Unconventional Oil and Gas Resources, 13 (2016) 32-43.

[6] A.D. Khawaji, I.K. Kutubkhanah, J.-M. Wie, Advances in seawater desalination technologies, Desalination, 221 (2008) 47-69.

[7] S.A. Kalogirou, Seawater desalination using renewable energy sources, Progress in Energy and Combustion Science, 31 (2005) 242-281.

[8] globalwaterintel, Desalination industry enjoys growth spurt as scarcity starts to bite, in.

[9] j.Q. Protection, sector=government, E. corporateName=Department of, Heritage, Coal seam gas water, (2016).

[10] S.R. Osipi, A.R. Secchi, C.P. Borges, Cost assessment and retro-techno-economic analysis of desalination technologies in onshore produced water treatment, Desalination, 430 (2018) 107-119.

[11] O. Santiago, K. Walsh, B. Kele, E. Gardner, J. Chapman, Novel pre-treatment of zeolite materials for the removal of sodium ions: potential materials for coal seam gas co-produced wastewater, SpringerPlus, 5 (2016) 571.

[12] M. Taulis, M. Milke, Chemical variability of groundwater samples collected from a coal seam gas exploration well, Maramarua, New Zealand, Water Res., 47 (2013) 1021-1034.

[13] D. Monckton, J. Cavaye, N. Huth, S. Vink, Use of coal seam water for agriculture in Queensland, Australia, Water International, (2017) 1-19.

[14] M. Navi, C. Skelly, M. Taulis, S. Nasiri, Coal seam gas water: potential hazards and exposure pathways in Queensland, International journal of environmental health research, 25 (2015) 162-183.

[15] M. Stearns, J. Tindall, G. Cronin, M. Friedel, E. Bergquist, Effects of coal-bed methane discharge waters on the vegetation and soil ecosystem in Powder River Basin, Wyoming, Water, Air, & Soil Pollution, 168 (2005) 33-57.

[16] D. Mallants, J. Šimůnek, S. Torkzaban, Determining water quality requirements of coal seam gas produced water for sustainable irrigation, Agricultural Water Management, 189 (2017) 52-69.

[17] C. Geotechnics, Coal seam gas extraction: modelling groundwater impacts, in, Department of the Environment, Australian Government, 2014.

[18] V. Aravinthan, D. Harrington, Coal seam gas water as a medium to grow Dunaliella tertiolecta microalgae for lipid extraction, Desalination and Water Treatment, 52 (2014) 947-958.

[19] L.D. Nghiem, T. Ren, N. Aziz, I. Porter, G. Regmi, Treatment of coal seam gas produced water for beneficial use in australia: A review of best practices, Desalination and Water Treatment, 32 (2011) 316-323.

[20] I. Sutzkover-Gutman, D.J.D. Hasson, Feed water pretreatment for desalination plants, 264 (2010) 289-296.

[21] C.A. Rebello, S.J. Couperthwaite, G.J. Millar, L.A. Dawes, Coal seam water quality and the impact upon management strategies, Journal of Petroleum Science and Engineering, 150 (2017) 323-333.

[22] J. Lin, S.J. Couperthwaite, G.J. Millar, Effectiveness of aluminium based coagulants for pre-treatment of coal seam water, Separation and Purification Technology, 177 (2017) 207-222.

[23] J. Lin, S.J. Couperthwaite, G.J. Millar, Applicability of iron based coagulants for pre-treatment of coal seam water, Journal of Environmental Chemical Engineering, 5 (2017) 1119-1132.

[24] L. Lipus, D. Dobersek, Influence of magnetic field on the aragonite precipitation, Chemical Engineering Science, 62 (2007) 2089-2095.

[25] V.S. Jagati, V.C. Srivastava, B.J.S.S. Prasad, Technology, Multi-response optimization of parameters for the electrocoagulation treatment of electroplating wash-water using aluminum electrodes, 50 (2015) 181-190.

[26] N.A. Milne, T. O'Reilly, P. Sanciolo, E. Ostarcevic, M. Beighton, K. Taylor, M. Mullett, A.J. Tarquin, S.R. Gray, Chemistry of silica scale mitigation for RO desalination with particular reference to remote operations, Water Research, 65 (2014) 107-133.

[27] M.H. Isa, E.H. Ezechi, Z. Ahmed, S.F. Magram, S.R.M. Kutty, Boron removal by electrocoagulation and recovery, Water Research, 51 (2014) 113-123.

[28] Y. Xu, J.-Q.J.I. Jiang, E.C. Research, Technologies for boron removal, 47 (2008) 16-24.

[29] A. Davey, R. Howick, R. Armbruster, WATER IN MINING-Treatment of Coal Seam Methane Water in Talinga, Dalby and Moranbah-Relocatable RO plants for the coal seam gas industry, Water-Australian Water and Wastewater Association, 39 (2012) 71.

[30] Y. Chun, S.-J. Kim, G.J. Millar, D. Mulcahy, I.S. Kim, L. Zou, Forward osmosis as a pre-treatment for treating coal seam gas associated water: Flux and fouling behaviour, Desalination, 403 (2017) 144-152.

[31] L.F. Greenlee, D.F. Lawler, B.D. Freeman, B. Marrot, P. Moulin, Reverse osmosis desalination: Water sources, technology, and today's challenges, Water Res., 43 (2009) 2317-2348.

[32] D. Mukhopadhyay, Method and apparatus for high efficiency reverse osmosis operation, in, United States 1999.

[33] Y. Chen, J.C. Baygents, J. Farrell, Evaluating electrocoagulation and chemical coagulation for removing dissolved silica from high efficiency reverse osmosis (HERO) concentrate solutions, Journal of Water Process Engineering, 16 (2017) 50-55.

[34] G.J. Millar, J. Lin, A. Arshad, S.J. Couperthwaite, Evaluation of electrocoagulation for the pre-treatment of coal seam water, Journal of Water Process Engineering, 4 (2014) 166-178.

[35] D.B. Wellner, S.J. Couperthwaite, G.J. Millar, The Influence of Coal Seam Water Composition upon Electrocoagulation Performance Prior to Desalination, Journal of Environmental Chemical Engineering, (2018).

[36] T.A. Moore, Coalbed methane: A review, International Journal of Coal Geology, 101 (2012) 36-81.

[37] I. Hamawand, T. Yusaf, S.G. Hamawand, Coal seam gas and associated water: A review paper, Renewable and Sustainable Energy Reviews, 22 (2013) 550-560.

[38] D. Luo, Y. Dai, Economic evaluation of coalbed methane production in China, Energy Policy, 37 (2009) 3883-3889.

[39] S. Shalhevet, Balancing Socioeconomic and Environmental Risks and Benefits under Multiple Stressor Conditions, in: Real-Time and Deliberative Decision Making, Springer, 2008, pp. 415-425.

[40] J. Veil, C. Clark, Produced water volume estimates and management practices, SPE Production & Operations, 26 (2011) 234-239.

[41] D. Liu, Y. Yao, D. Tang, S. Tang, Y. Che, W. Huang, Coal reservoir characteristics and coalbed methane resource assessment in Huainan and Huaibei coalfields, Southern North China, International Journal of Coal Geology, 79 (2009) 97-112.

[42] Y. Qin, T.A. Moore, J. Shen, Z. Yang, Y. Shen, G. Wang, Resources and geology of coalbed methane in China: a review, International Geology Review, 60 (2018) 777-812.

[43] A. Saghafi, Potential for ECBM and CO2 storage in mixed gas Australian coals, International Journal of Coal Geology, 82 (2010) 240-251.

[44] R. WILKINSON, Eastern Australian coalbed methane supply rivals western offshore conventional resource, Oil & gas journal, 109 (2011).

[45] F. Xu, L.-h. Zhu, Synthesis of methanol from oxygen-containing coalbed methane and environmental benefit analysis, Disaster Advances, 3 (2010) 407-410.

[46] S. Vink, Coal seam gas and water issues, AusIMM Bulletin, 1 (2014) 57-58.

[47] J. Pan, X. Zhang, RETRACTED ARTICLE: Characteristics of produced water from coal mine and coalbed methane well and impact on environment in Liulin mining area, in: 5th International Conference on Bioinformatics and Biomedical Engineering, iCBBE 2011, 2011.

[48] J.M. Bennett, A. Marchuk, S.R. Raine, S.A. Dalzell, D.C. Macfarlane, Managing land application of coal seam water: A field study of land amendment irrigation using saline-sodic and alkaline water on a Red Vertisol, Journal of Environmental Management, 184 (2016) 178-185.

[49] B. Towler, M. Firouzi, J. Underschultz, W. Rifkin, A. Garnett, H. Schultz, J. Esterle, S. Tyson, K. Witt, An overview of the coal seam gas developments in Queensland, Journal of Natural Gas Science and Engineering, 31 (2016) 249-271.

[50] D.A. Post, P.A. Baker, Determining the impacts of coal seam gas extraction on water resources and water-dependent assets, The APPEA Journal, 57 (2017) 519-522.

[51] K.G. Dahm, K.L. Guerra, P. Xu, J.E. Drewes, Composite geochemical database for coalbed methane produced water quality in the Rocky Mountain region, Environmental Science and Technology, 45 (2011) 7655-7663.

[52] K.G. Dahm, K.L. Guerra, P. Xu, J.E. Drewes, Composite Geochemical Database for Coalbed Methane Produced Water Quality in the Rocky Mountain Region, Environ. Sci. Technol., 45 (2011) 7655-7663.

[53] L.D. Nghiem, C. Elters, A. Simon, T. Tatsuya, W. Price, Coal seam gas produced water treatment by ultrafiltration, reverse osmosis and multi-effect distillation: A pilot study, Separation and Purification Technology, 146 (2015) 94-100.

[54] P.J. Davies, D.B. Gore, S.J. Khan, Managing produced water from coal seam gas projects: implications for an emerging industry in Australia, Environmental science and pollution research international, 22 (2015) 10981.

[55] G.J. Millar, S.J. Couperthwaite, C. Moodliar, Strategies for the management and treatment of coal seam gas associated water, Renewable and Sustainable Energy Reviews, 57 (2016) 669-691.

[56] I. Hamawand, T. Yusaf, S.G. Hamawand, Coal seam gas and associated water: A review paper, Renewable and Sustainable Energy Reviews, 22 (2013) 550-560.

[57] M. Taulis, M. Milke, Coal seam gas water from Maramarua, New Zealand: Characterisation and comparison to United States analogues, Journal of Hydrology New Zealand, 46 (2007) 1-17.

[58] E.C.P. Kinnon, S.D. Golding, C.J. Boreham, K.A. Baublys, J.S. Esterle, Stable isotope and water quality analysis of coal bed methane production waters and gases from the Bowen Basin, Australia, International Journal of Coal Geology, 82 (2010) 219-231.

[59] G.H. Li, H.P. Sjursen, Characteristics of produced water during coalbed methane (CBM) development and its feasibility as irrigation water in Jincheng, China, Journal of Coal Science and Engineering, 19 (2013) 369-374.

[60] EPA, 5.5 Turbidity, in, 2012.

[61] M.K. Shuuya, Z. Hoko, Trends and Impacts of Pollution in the Calueque-Oshakati Canal in North-Central Namibia on Water Treatment, in: M. Josephine Phillip (Ed.) Combating Water Scarcity in Southern Africa: Case Studies from Namibia, Springer Netherlands, Dordrecht, 2014, pp. 43-60.

[62] USGS, Turbidity, in, The USGS Water Science School, 2016.

[63] Z. Chen, C. Hu, F. Muller-Karger, Monitoring turbidity in Tampa Bay using MODIS/Aqua 250-m imagery, Remote sensing of Environment, 109 (2007) 207-220.

[64] R.G. Wetzel, Limnology: lake and river ecosystems, Gulf Professional Publishing, 2001.

[65] M.S. Wood, Estimating suspended sediment in rivers using acoustic Doppler meters, US Geological Survey, 2014.

[66] K.L. Benko, J.E. Drewes, Produced water in the Western United States: Geographical distribution, occurrence, and composition, Environmental Engineering Science, 25 (2008) 239-246.

[67] A. Ali, V. Strezov, P. Davies, I. Wright, Environmental impact of coal mining and coal seam gas production on surface water quality in the Sydney basin, Australia, Environmental Monitoring and Assessment, 189 (2017) 408.

[68] Z. Qian, X. Liu, Z. Yu, H. Zhang, Y. JÜ, A Pilot-scale Demonstration of Reverse Osmosis Unit for Treatment of Coal-bed Methane Co-produced Water and Its Modeling, Chinese Journal of Chemical Engineering, 20 (2012) 302-311.

[69] K.L. Hickenbottom, N.T. Hancock, N.R. Hutchings, E.W. Appleton, E.G. Beaudry, P. Xu, T.Y. Cath, Forward osmosis treatment of drilling mud and fracturing wastewater from oil and gas operations, Desalination, 312 (2013) 60-66.

[70] K.R. O'Brien, T.R. Weber, C. Leigh, M.A. Burford, Sediment and nutrient budgets are inherently dynamic: Evidence from a long-term study of two subtropical reservoirs, Hydrology and Earth System Sciences, 20 (2016) 4881-4894.

[71] G.F. Vance, L.A. King, G.K. Ganjegunte, Soil and plant responses from land application of saline-sodic waters: implications of management, J. Environ. Qual., 37 (2008) S/139-S/148.

[72] A. Burkhardt, A. Gawde, C.L. Cantrell, H.L. Baxter, B.L. Joyce, C.N. Stewart, V.D. Zheljazkov, Effects of produced water on soil characteristics, plant biomass, and secondary metabolites, Journal of Environmental Quality, 44 (2015) 1938-1947.

[73] R. Dennis, Ion exchange helps CBM producers handle water, Oil and Gas Journal, 105 (2007) 41-43.

[74] D. Blair, D.T. Alexander, S.J. Couperthwaite, M. Darestani, G.J. Millar, Enhanced water recovery in the coal seam gas industry using a dual reverse osmosis system, Environmental Science: Water Research and Technology, 3 (2017) 278-292.

[75] A. Averina, M.G. Rasul, S. Begum, Management of coal seam gas (CSG) by-product water: a case study on spring gully mine site in Queensland, Australia, in, WSEAS Press, 2008, pp. 169-174.

[76] N. Quevedo, J. Sanz, A. Lobo, J. Temprano, I. Tejero, Filtration demonstration plant as reverse osmosis pretreatment in an industrial water treatment plant, Desalination, 286 (2012) 49-55.

[77] I. Sutzkover-Gutman, D. Hasson, Feed water pretreatment for desalination plants, Desalination, 264 (2010) 289-296.

[78] D. Abdessemed, G. Nezzal, Coupling softening—ultrafiltration like pretreatment of sea water case study of the Corso plant desalination (Algiers), Desalination, 221 (2008) 107-113.

[79] E.C. Dogan, A. Yasar, U. Sen, C. Aydiner, Water recovery from treated urban wastewater by ultrafiltration and reverse osmosis for landscape irrigation, Urban Water Journal, 13 (2016) 553-568.

[80] M.H.D.A. Farahani, S.M. Borghei, V. Vatanpour, Recovery of cooling tower blowdown water for reuse: The investigation of different types of pretreatment prior nanofiltration and reverse osmosis, Journal of Water Process Engineering, 10 (2016) 188-199.

[81] M. Stoller, G. Vilardia, L. Di, A.C. Palmaa, Treatment of olive oil processing wastewater by ultrafiltration, nanofiltration, reverse osmosis and biofiltration, CHEMICAL ENGINEERING, 47 (2016).

[82] H. Le, Innovative commercial and technical solutions for CSG produced water treatment project, Chemical Engineering World, 52 (2017) 32-40.

[83] A. Carter, GE Kenya WTP Queensland Water: Journal of the Australian Water Association, 42 (2015) 28-29.

[84] L. Lunevich, P. Sanciolo, A. Smallridge, S.R. Gray, Silica scale formation and effect of sodium and aluminium ions -29Si NMR study, Environmental Science: Water Research and Technology, 2 (2016) 174-185.

[85] Z. Hu, A. Antony, G. Leslie, P. Le-Clech, Real-time monitoring of scale formation in reverse osmosis using electrical impedance spectroscopy, Journal of Membrane Science, 453 (2014) 320-327.

[86] J. Lipnizki, B. Adams, M. Okazaki, A. Sharpe, Water treatment: Combining reverse osmosis and ion exchange, Filtration and Separation, 49 (2012) 30-33.

[87] C.Y. Teh, P.M. Budiman, K.P.Y. Shak, T.Y. Wu, Recent Advancement of Coagulation-Flocculation and Its Application in Wastewater Treatment, Industrial and Engineering Chemistry Research, 55 (2016) 4363-4389.

[88] P.H. Nelson, Osmosis and thermodynamics explained by solute blocking, European Biophysics Journal, 46 (2017) 59-64.

[89] D.M. Warsinger, E.W. Tow, K.G. Nayar, L.A. Maswadeh, Energy efficiency of batch and semi-batch (CCRO) reverse osmosis desalination, Water Res., 106 (2016) 272-282.

[90] J.C. Crittenden, R.R. Trussell, D.W. Hand, K.J. Howe, G. Tchobanoglous, MWH's water treatment: principles and design, John Wiley & Sons, 2012.

[91] U. Lachish, Optimizing the efficiency of reverse osmosis seawater desalination, in, 2010.

[92] S. Jiang, Y. Li, B.P. Ladewig, A review of reverse osmosis membrane fouling and control strategies, Science of The Total Environment, 595 (2017) 567-583.

[93] Aquatech, High Efficiency Reverse Osmosis (HERO™), in, 2017.

[94] M. Mickley, Survey of high-recovery and zero liquid discharge technologies for water utilities, WateReuse Foundation, 2008.

[95] P.R. Khaled Moftah, HIGH-EFFICIENCY REVERSE OSMOSIS TREATS GRAY WATER FOR POWER GENERATION, in, 2018.

[96] J. Rioyo, V. Aravinthan, J. Bundschuh, M. Lynch, A review of strategies for RO brine minimization in inland desalination plants, Desalination and Water Treatment, 90 (2017) 110-123.

[97] W. Online, HERO™ (High Efficiency Reverse Osmosis) Technology, in.

[98] High efficiency reverse osmosis, Membrane Technology, 1999 (1999) 13.

[99] R.E. Kremesti, HERO ™ - High Efficiency Reverse Osmosis, in, 2017.

[100] J. Morillo, J. Usero, D. Rosado, H. El Bakouri, A. Riaza, F.-J. Bernaola, Comparative study of brine management technologies for desalination plants, Desalination, 336 (2014) 32-49.

[101] W. Stumm, J.J. Morgan, Aquatic chemistry: chemical equilibria and rates in natural waters, John Wiley & Sons, 2012.

[102] S.S. Voi͡utskiĭ, Colloid chemistry, Mir Publishers, Moscow, Russia., 1978.

[103] J.D. Clogston, A.K. Patri, Zeta potential measurement, in: Characterization of nanoparticles intended for drug delivery, Springer, 2011, pp. 63-70.

[104] A. Black, F. Birkner, J. Morgan, The effect of polymer adsorption on the electrokinetic stability of dilute clay suspensions, Journal of Colloid and Interface Science, 21 (1966) 626-648.

[105] A. Rahmani, Removal of water turbidity by the electrocoagulation method, Journal of research in health sciences, 8 (2008) 18-24.

[106] M.Y. Mollah, P. Morkovsky, J.A. Gomes, M. Kesmez, J. Parga, D.L. Cocke, Fundamentals, present and future perspectives of electrocoagulation, Journal of Hazardous Materials, 114 (2004) 199-210.

[107] S. Khoufi, F. Feki, S. Sayadi, Detoxification of olive mill wastewater by electrocoagulation and sedimentation processes, Journal of Hazardous Materials, 142 (2007) 58-67.

[108] M. Vepsäläinen, J. Selin, P. Rantala, M. Pulliainen, H. Särkkä, K. Kuhmonen, A. Bhatnagar, M. Sillanpää, Precipitation of dissolved sulphide in pulp and paper mill wastewater by electrocoagulation, Environmental technology, 32 (2011) 1393-1400.

[109] O. Yahiaoui, H. Lounici, N. Abdi, N. Drouiche, N. Ghaffour, A. Pauss, N. Mameri, Treatment of olive mill wastewater by the combination of ultrafiltration and bipolar electrochemical reactor processes, Chemical Engineering and Processing: Process Intensification, 50 (2011) 37-41.

[110] M. Behloul, H. Grib, N. Drouiche, N. Abdi, H. Lounici, N. Mameri, Removal of malathion pesticide from polluted solutions by electrocoagulation: Modeling of experimental results using response surface methodology, Separation Science and Technology, 48 (2013) 664-672.

[111] N. Drouiche, N. Ghaffour, S. Aoudj, M. Hecini, T. Ouslimane, Fluoride removal from photovoltaic wastewater by aluminium electrocoagulation and characteristics of products, Chem. Eng. Trans, 17 (2009) 1651-1656.

[112] N. Boudjema, N. Drouiche, N. Abdi, H. Grib, H. Lounici, A. Pauss, N. Mameri, Treatment of Oued El Harrach river water by electrocoagulation noting the effect of the electric field on microorganisms, Journal of the Taiwan Institute of Chemical Engineers, 45 (2014) 1564-1570.

[113] G. Chen, Electrochemical technologies in wastewater treatment, Separation and Purification Technology, 38 (2004) 11-41.

[114] N. Drouiche, S. Aoudj, H. Lounici, M. Drouiche, T. Ouslimane, N. Ghaffour, Fluoride removal from pretreated photovoltaic wastewater by electrocoagulation: an investigation of the effect of operational parameters, Procedia Engineering, 33 (2012) 385-391.

[115] N. Drouiche, S. Aoudj, H. Lounici, H. Mahmoudi, N. Ghaffour, M.F. Goosen, Development of an empirical model for fluoride removal from photovoltaic wastewater by electrocoagulation process, Desalination and Water Treatment, 29 (2011) 96-102.

[116] E. Butler, Y.-T. Hung, R.Y.-L. Yeh, M. Suleiman Al Ahmad, Electrocoagulation in wastewater treatment, Water, 3 (2011) 495-525.

[117] M. Changmai, M. Pasawan, M. Purkait, A hybrid method for the removal of fluoride from drinking water: Parametric study and cost estimation, Separation and Purification Technology, (2018).

[118] Y.Ş. Yildiz, A.S. Koparal, Ş. İrdemez, B. Keskinler, Electrocoagulation of synthetically prepared waters containing high concentration of NOM using iron cast electrodes, Journal of Hazardous Materials, 139 (2007) 373-380.

[119] J. Ge, J. Qu, P. Lei, H. Liu, New bipolar electrocoagulation–electroflotation process for the treatment of laundry wastewater, Separation and Purification Technology, 36 (2004) 33-39.

[120] C.G. Rocha, D.A.M. Zaia, R.V. da Silva Alfaya, A.A. da Silva Alfaya, Use of rice straw as biosorbent for removal of Cu (II), Zn (II), Cd (II) and Hg (II) ions in industrial effluents, Journal of Hazardous Materials, 166 (2009) 383-388.

[121] İ.A. Şengil, Treatment of dairy wastewaters by electrocoagulation using mild steel electrodes, Journal of Hazardous Materials, 137 (2006) 1197-1205.

[122] Y. Yavuz, EC and EF processes for the treatment of alcohol distillery wastewater, Separation and Purification Technology, 53 (2007) 135-140.

[123] N. Kannan, G. Karthikeyan, N. Tamilselvan, Comparison of treatment potential of electrocoagulation of distillery effluent with and without activated Areca catechu nut carbon, Journal of Hazardous Materials, 137 (2006) 1803-1809.

[124] M. Kobya, H. Hiz, E. Senturk, C. Aydiner, E. Demirbas, Treatment of potato chips manufacturing wastewater by electrocoagulation, Desalination, 190 (2006) 201-211.

[125] S. Tchamango, C.P. Nanseu-Njiki, E. Ngameni, D. Hadjiev, A. Darchen, Treatment of dairy effluents by electrocoagulation using aluminium electrodes, Science of The Total Environment, 408 (2010) 947-952.

[126] E. Bazrafshan, H. Moein, F. Kord Mostafapour, S. Nakhaie, Application of electrocoagulation process for dairy wastewater treatment, Journal of Chemistry, 2013 (2012).

[127] M. Alimohammadi, M. Askari, M.H. Dehghani, A. Dalvand, R. Saeedi, K. Yetilmezsoy, B. Heibati, G. McKay, Elimination of natural organic matter by electrocoagulation using bipolar and monopolar arrangements of iron and aluminum electrodes, Int. J. Environ. Sci. Technol., 14 (2017) 2125-2134.

[128] S.M. Adapureddy, S. Goel, Optimizing electrocoagulation of drinking water for turbidity removal in a batch reactor, in: Proc., 3rd Int. Conf. on Environment Science and Technology, 2012, pp. 97-102.

[129] S. Pérez-Sicairos, J. Morales-Cuevas, R. Félix-Navarro, O. Hernández-Calderón, Evaluation of the electro-coagulation process for the removal of turbidity of river water, wastewater and pond water, Revista Mexicana de Ingeniería Química, 10 (2011).

[130] C.M. van Genuchten, S.R.S. Bandaru, E. Surorova, S.E. Amrose, A.J. Gadgil, J. Peña, Formation of macroscopic surface layers on Fe(0) electrocoagulation electrodes during an extended field trial of arsenic treatment, Chemosphere, 153 (2016) 270-279.

[131] L.C.A. Gobbi, I.L. Nascimento, E.P. Muniz, S.M.S. Rocha, P.S.S. Porto, Electrocoagulation with polarity switch for fast oil removal from oil in water emulsions, Journal of Environmental Management, 213 (2018) 119-125.

[132] D.B. Wellner, S.J. Couperthwaite, G.J. Millar, Influence of operating parameters during electrocoagulation of sodium chloride and sodium bicarbonate solutions using aluminium electrodes, Journal of Water Process Engineering, 22 (2018) 13-26.

[133] Ã. Fekete, B. Lengyel, T. Cserfalvi, T. Pajkossy, Electrochemical dissolution of aluminium in electrocoagulation experiments, Journal of Solid State Electrochemistry, 20 (2016) 3107-3114.

[134] T.C. Timmes, H.C. Kim, B.A. Dempsey, Electrocoagulation pretreatment of seawater prior to ultrafiltration: Pilot-scale applications for military water purification systems, Desalination, 250 (2010) 6-13.

[135] D.B. Wellner, S.J. Couperthwaite, G.J. Millar, The influence of coal seam water composition upon electrocoagulation performance prior to desalination, Journal of Environmental Chemical Engineering, 6 (2018) 1943-1956.

[136] G.J. Millar, J. Lin, A. Arshad, S.J. Couperthwaite, Evaluation of electrocoagulation for the pre-treatment of coal seam water, Journal of Water Process Engineering, 4 (2014) 166-178.

[137] F. Orssatto, M.H. Ferreira Tavares, F. Manente da Silva, E. Eyng, B. Farias Biassi, L. Fleck, Optimization of the pretreatment of wastewater from a slaughterhouse and packing plant through electrocoagulation in a batch reactor, Environmental Technology (United Kingdom), 38 (2017) 2465-2475.

[138] T. Amani, K. Veysi, W. Dastyar, S. Elyasi, Studying interactive effects of operational parameters on continuous bipolar electrocoagulation–flotation process for treatment of high-load compost leachate, International Journal of Environmental Science and Technology, 12 (2015) 2467-2474.

[139] R. Mores, H. Treichel, C.A. Zakrzevski, A. Kunz, J. Steffens, R.M. Dallago, Remove of phosphorous and turbidity of swine wastewater using electrocoagulation under continuous flow, Separation and Purification Technology, 171 (2016) 112-117.

[140] M. Kobya, E. Gengec, E. Demirbas, Operating parameters and costs assessments of a real dyehouse wastewater effluent treated by a continuous electrocoagulation process, Chemical Engineering and Processing - Process Intensification, 101 (2016) 87-100.

[141] W. Lemlikchi, S. Khaldi, M.O. Mecherri, H. Lounici, N. Drouiche, Degradation of Disperse Red 167 Azo Dye by Bipolar Electrocoagulation, Separation Science and Technology, 47 (2012) 1682-1688.

[142] B. Kimball, High recovery reverse osmosis for treatment of produced water, Off. Proc. - Int. Water Conf., 71st (2010) 643-654.

[143] S. Chalmers, A. Kowse, P. Stark, L. Facer, N. Smith, Treatment of coal seam gas water, Water, 37 (2010) 71-76.

[144] G.J. Millar, S.J. Couperthwaite, S. Papworth, Ion exchange of sodium chloride and sodium bicarbonate solutions using strong acid cation resins in relation to coal seam water treatment, Journal of Water Process Engineering, 11 (2016) 60-67.

[145] R. Vedelago, G.J. Millar, Process evaluation of treatment options for high alkalinity coal seam gas associated water, Journal of Water Process Engineering, 23 (2018) 195-206.

[146] L. Ho, G. Newcombe, Effect of NOM, turbidity and floc size on the PAC adsorption of MIB during alum coagulation, Water Research, 39 (2005) 3668-3674.

[147] T. González, J.R. Domínguez, J. Beltrán-Heredia, H.M. García, F. Sanchez-Lavado, Aluminium sulfate as coagulant for highly polluted cork processing wastewater: Evaluation of settleability parameters and design of a clarifier-thickener unit, Journal of Hazardous Materials, 148 (2007) 6-14.

[148] M. Mahdavi, A.H. Mahvi, H. Pourzamani, A. Fatehizadeh, A. Ebrahimi, High turbid water treatment by kenaf fibers: A practical method for individual water supply and remote areas, Desalination and Water Treatment, 76 (2017) 225-231.

[149] A. Baghvand, A.D. Zand, N. Mehrdadi, A. Karbassi, Optimizing coagulation process for low to high turbidity waters using aluminum and iron salts, American Journal of Environmental Sciences, 6 (2010) 442-448.

[150] S. Du, W. Jin, F. Duan, Research on the Removal of Scale Ions from Circulating Cooling Wastewater by Chemical Coagulation Process, in: E3S Web of Conferences, 2018.

[151] A.J. O'Donnell, D.A. Lytle, S. Harmon, K. Vu, H. Chait, D.D. Dionysiou, Removal of strontium from drinking water by conventional treatment and lime softening in bench-scale studies, Water Research, 103 (2016) 319-333.

[152] H.-H. Cheng, S.-S. Chen, S.-R. Yang, In-line coagulation/ultrafiltration for silica removal from brackish water as RO membrane pretreatment, Separation and Purification Technology, 70 (2009) 112-117.

[153] R. Kleven, J. Alstad, Interaction of alkali, alkaline-earth and sulphate ions with clay minerals and sedimentary rocks, Journal of Petroleum Science and Engineering, 15 (1996) 181-200.

[154] H. Bakraouy, S. Souabi, K. Digua, O. Dkhissi, M. Sabar, M. Fadil, Optimization of the treatment of an anaerobic pretreated landfill leachate by a coagulation–flocculation process using experimental design methodology, Process Safety and Environmental Protection, 109 (2017) 621-630.

[155] A.D. Knowles, C.K. Nguyen, M.A. Edwards, A. Stoddart, B. McIlwain, G.A. Gagnon, Role of iron and aluminum coagulant metal residuals and lead release from drinking water pipe materials, Journal of Environmental Science and Health - Part A Toxic/Hazardous Substances and Environmental Engineering, 50 (2015) 414-423.

[156] D. Hermosilla, R. Ordóñez, L. Blanco, E. de la Fuente, A. Blanco, pH and Particle Structure Effects on Silica Removal by Coagulation, Chemical Engineering and Technology, 35 (2012) 1632-1640.

[157] R.K. Iler, The chemistry of silica: solubility, polimerization, colloid and surface properties, and biochemistry, Wiley Interscience, 1979.

[158] O. Guseva, P. Schmutz, T. Suter, O. von Trzebiatowski, Modelling of anodic dissolution of pure aluminium in sodium chloride, Electrochimica Acta, 54 (2009) 4514-4524.

[159] T. Li, Z. Zhu, D. Wang, C. Yao, H. Tang, The strength and fractal dimension characteristics of alum-kaolin flocs, International Journal of Mineral Processing, 82 (2007) 23-29.

[160] R. Jiao, H. Xu, W. Xu, X. Yang, D. Wang, Influence of coagulation mechanisms on the residual aluminum – The roles of coagulant species and MW of organic matter, Journal of Hazardous Materials, 290 (2015) 16-25.

[161] R.K. Chakraborti, J.F. Atkinson, J.E. Van Benschoten, Characterization of Alum Floc by Image Analysis, Environ. Sci. Technol., 34 (2000) 3969-3976.

[162] F. Pontius, Treatability of a highly-impaired, saline surface water for potential Urban water use, Water (Switzerland), 10 (2018).

[163] M. Umar, F. Roddick, L. Fan, Comparison of coagulation efficiency of aluminium and ferric-based coagulants as pre-treatment for UVC/H$_2$O$_2$ treatment of wastewater RO concentrate, Chemical Engineering Journal, 284 (2016) 841-849.

[164] M. De Julio, T.S. De Julio, L. Di Bernardo, Influence of the apparent molecular size of humic substances on the efficiency of coagulation using Fenton's reagent, Anais da Academia Brasileira de Ciencias, 85 (2013) 833-847.

[165] C. Staaks, R. Fabris, T. Lowe, C.W.K. Chow, J.A. van Leeuwen, M. Drikas, Coagulation assessment and optimisation with a photometric dispersion analyser and organic characterisation for natural organic matter removal performance, Chemical Engineering Journal, 168 (2011) 629-634.

[166] N. Xue, X. Wang, F. Zhang, Y. Wang, Y. Chu, Y. Zheng, Effect of SiO$_2$ nanoparticles on the removal of natural organic matter (NOM) by coagulation, Environmental Science and Pollution Research, 23 (2016) 11835-11844.

[167] M. Kimura, Y. Matsui, K. Kondo, T.B. Ishikawa, T. Matsushita, N. Shirasaki, Minimizing residual aluminum concentration in treated water by tailoring properties of polyaluminum coagulants, Water Research, 47 (2013) 2075-2084.

[168] R. Jiao, R. Fabris, C.W.K. Chow, M. Drikas, J. van Leeuwen, D. Wang, Roles of coagulant species and mechanisms on floc characteristics and filterability, Chemosphere, 150 (2016) 211-218.

[169] C. Ockert, L.M. Wehrmann, S. Kaufhold, T.G. Ferdelman, B.M.A. Teichert, N. Gussone, Calcium-ammonium exchange experiments on clay minerals using a45Ca tracer technique in marine pore water, Isotopes in Environmental and Health Studies, 50 (2014) 1-17.

[170] G. Gascó, A. Méndez, Sorption of Ca2+, Mg2+, Na+and K+by clay minerals, Desalination, 182 (2005) 333-338.

[171] D.T. Moussa, M.H. El-Naas, M. Nasser, M.J. Al-Marri, A comprehensive review of electrocoagulation for water treatment: Potentials and challenges, Journal of Environmental Management, 186 (2017) 24-41.

[172] J. Lin, Millar, G.J., Couperthwaite, S.J. and Mackinnon, I.D.R., Electrocoagulation as a pre-treatment stage to reverse osmosis, in: OzWater 2014, Australian Water Association, Brisbane, 2014.

[173] S. Bellebia, S. Kacha, A.Z. Bouyakoub, Z. Derriche, Experimental investigation of chemical oxygen demand and turbidity removal from cardboard paper mill effluents using combined electrocoagulation and adsorption processes, Environ Prog Sustain, 31 (2012) 361-370.

[174] W.L. Chou, C.T. Wang, S.Y. Chang, Study of COD and turbidity removal from real oxide-CMP wastewater by iron electrocoagulation and the evaluation of specific energy consumption, Journal of Hazardous Materials, 168 (2009) 1200-1207.

[175] T.L. Benazzi, M. Di Luccio, R.M. Dallago, J. Steffens, R. Mores, M.S. Do Nascimento, J. Krebs, G. Ceni, Continuous flow electrocoagulation in the treatment of wastewater from dairy industries, Water Science and Technology, 73 (2016) 1418-1425.

[176] S. Mahesh, K.K. Garg, V.C. Srivastava, I.M. Mishra, B. Prasad, I.D. Mall, Continuous electrocoagulation treatment of pulp and paper mill wastewater: operating cost and sludge study, RSC Advances, 6 (2016) 16223-16233.

[177] S.M. Moosavirad, Treatment and operation cost analysis of greywater by electrocoagulation and comparison with coagulation process in mining areas, Separation Science and Technology (Philadelphia), 52 (2017) 1742-1750.

[178] M.K.N. Mahmad, M.A.Z.M.R. Rozainy, I. Abustan, N. Baharun, Electrocoagulation Process by Using Aluminium and Stainless Steel Electrodes to Treat Total Chromium, Colour and Turbidity, Procedia Chem, 19 (2016) 681-686.

[179] H. Cesar Lopes Geraldino, J. Izabelle Simionato, T. Karoliny Formicoli de Souza Freitas, J. Carla Garcia, N. Evelázio de Souza, Evaluation of the electrode wear and the residual concentration of iron in a system of electrocoagulation, Desalination and Water Treatment, 57 (2016) 13377-13387.

[180] M. Mechelhoff, G.H. Kelsall, N.J.D. Graham, Super-faradaic charge yields for aluminium dissolution in neutral aqueous solutions, Chemical Engineering Science, 95 (2013) 353-359.

[181] M.A. Sari, S. Chellam, Mechanisms of boron removal from hydraulic fracturing wastewater by aluminum electrocoagulation, Journal of Colloid and Interface Science, 458 (2015) 103-111.

[182] K. Brahmi, W. Bouguerra, H. Belhsan, E. Elaloui, M. Loungou, Z. Tlili, B. Hamrouni, Use of Electrocoagulation with Aluminum Electrodes to Reduce Hardness in Tunisian Phosphate Mining Process Water, Mine Water and the Environment, 35 (2016) 310-317.

[183] N. Esmaeilirad, K. Carlson, P. Omur Ozbek, Influence of softening sequencing on electrocoagulation treatment of produced water, Journal of Hazardous Materials, 283 (2015) 721-729.

[184] V.S. Jagati, V.C. Srivastava, B. Prasad, Multi-Response Optimization of Parameters for the Electrocoagulation Treatment of Electroplating Wash-Water using Aluminum Electrodes, Separation Science and Technology (Philadelphia), 50 (2015) 181-190.

[185] P. Somasundaran, J.O. Amankonah, K. Ananthapadmabhan, Mineral—solution equilibria in sparingly soluble mineral systems, Colloids and Surfaces, 15 (1985) 309-333.

[186] J.R. Parga, G. González, H. Moreno, J.L. Valenzuela, Thermodynamic studies of the strontium adsorption on iron species generated by electrocoagulation, Desalination and Water Treatment, 37 (2012) 244-252.

[187] Z. Murthy, S. Parmar, Removal of strontium by electrocoagulation using stainless steel and aluminum electrodes, Desalination, 282 (2011) 63-67.

[188] R. Kamaraj, S. Vasudevan, Evaluation of electrocoagulation process for the removal of strontium and cesium from aqueous solution, chemical engineering research and design, 93 (2015) 522-530.

[189] I. De Oliveira Da Mota, J.A. De Castro, R. De Góes Casqueira, A.G. De Oliveira Junior, Study of electroflotation method for treatment of wastewater from washing soil contaminated by heavy metals, Journal of Materials Research and Technology, 4 (2015) 109-113.

[190] M. Dolati, A.A. Aghapour, H. Khorsandi, S. Karimzade, Boron removal from aqueous solutions by electrocoagulation at low concentrations, Journal of Environmental Chemical Engineering, 5 (2017) 5150-5156.

[191] O.M. Hafez, M.A. Shoeib, M.A. El-Khateeb, H.I. Abdel-Shafy, A.O. Youssef, Removal of scale forming species from cooling tower blowdown water by electrocoagulation using different electrodes, Chemical Engineering Research and Design, 136 (2018) 347-357.

[192] W. Den, C.-J. Wang, Removal of silica from brackish water by electrocoagulation pretreatment to prevent fouling of reverse osmosis membranes, Separation and Purification Technology, 59 (2008) 318-325.

[193] J. Sarapata, Bicarbonate alkalinity in drinking water, Journal of New England Water Works Association, 108 (1994) 277-287.

[194] K. Brahmi, W. Bouguerra, S. Harbi, E. Elaloui, M. Loungou, B. Hamrouni, Treatment of heavy metal polluted industrial wastewater by a new water treatment process: ballasted electroflocculation, Journal of Hazardous Materials, 344 (2018) 968-980.

[195] S.Y. Lee, G.A. Gagnon, Comparing the growth and structure of flocs from electrocoagulation and chemical coagulation, Journal of Water Process Engineering, 10 (2016) 20-29.

[196] J.N. Hakizimana, N. Najid, B. Gourich, C. Vial, Y. Stiriba, J. Naja, Hybrid electrocoagulation/electroflotation/electrodisinfection process as a pretreatment for seawater desalination, Chemical Engineering Science, 170 (2017) 530-541.

[197] S.Q. Yu, D.W. Xiong, X.B. Chen, J.J. You, S. Xiong, H.D. Wang, Treatment of wastewater containing chromium with periodic reversal electrocoagulation, Zhongguo Huanjing Kexue/China Environmental Science, 34 (2014) 118-122.

[198] S. Khan, G. Kordek, Coal seam gas: produced water and solids, Report commissioned for the independent review of coal seam gas activities in NSW by the NSW Chief Scientist & Engineer: School of Civil Environmental Engineering, The University of New South Wales, (2014).

[199] G.J. Millar, S. Papworth, S.J. Couperthwaite, Exploration of the fundamental equilibrium behaviour of calcium exchange with weak acid cation resins, Desalination, 351 (2014) 27-36.

[200] R.S. Dennis, Continuous ion exchange for wyoming CBM produced-water purification: Proven experience, in: SPE E and P Environmental and Safety Conference 2007: Delivering Superior Environmental and Safety Performance, Proceedings, 2007, pp. 321-324.

[201] H.C. Duong, S. Gray, M. Duke, T.Y. Cath, L.D. Nghiem, Scaling control during membrane distillation of coal seam gas reverse osmosis brine, Journal of Membrane Science, 493 (2015) 673-682.

[202] K. Sadeddin, A. Naser, A. Firas, Removal of turbidity and suspended solids by electro-coagulation to improve feed water quality of reverse osmosis plant, Desalination, 268 (2011) 204-207.

[203] R. Jiao, H. Xu, W. Xu, X. Yang, D. Wang, Influence of coagulation mechanisms on the residual aluminum - The roles of coagulant species and MW of organic matter, Journal of Hazardous Materials, 290 (2015) 16-25.

[204] T. Xu, X. Lei, B. Sun, G. Yu, Y. Zeng, Highly efficient and energy-conserved flocculation of copper in wastewater by pulse-alternating current, Environmental Science and Pollution Research, 24 (2017) 20577-20586.

[205] T.C. Timmes, H.C. Kim, B.A. Dempsey, Electrocoagulation pretreatment of seawater prior to ultrafiltration: Bench-scale applications for military water purification systems, Desalination, 249 (2009) 895-901.

[206] X. Mao, S. Hong, H. Zhu, H. Lin, L. Wei, F. Gan, Alternating pulse current in electrocoagulation for wastewater treatment to prevent the passivation of al electrode, Journal Wuhan University of Technology, Materials Science Edition, 23 (2008) 239-241.

[207] P.J. Panikulam, N. Yasri, E.P.L. Roberts, Electrocoagulation using an oscillating anode for kaolin removal, Journal of Environmental Chemical Engineering, 6 (2018) 2785-2793.

[208] L. Zaleschi, M.S. Secula, C. Teodosiu, C.S. Stan, I. Cretescu, Removal of rhodamine 6G from aqueous effluents by electrocoagulation in a batch reactor:

Assessment of operational parameters and process mechanism, Water, Air, and Soil Pollution, 225 (2014).

[209] A. Ciblak, X. Mao, I. Padilla, D. Vesper, I. Alshawabkeh, A.N. Alshawabkeh, Electrode effects on temporal changes in electrolyte pH and redox potential for water treatment, Journal of Environmental Science and Health - Part A Toxic/Hazardous Substances and Environmental Engineering, 47 (2012) 718-726.

[210] H.A. Moreno C, D.L. Cocke, J.A. Gromes, P. Morkovsky, J.R. Parga, E. Peterson, C. Garcia, Electrochemical reactions for electrocoagulation using iron electrodes, Industrial and Engineering Chemistry Research, 48 (2009) 2275-2282.

[211] C.M. Van Genuchten, S.E.A. Addy, J. Peña, A.J. Gadgil, Removing arsenic from synthetic groundwater with iron electrocoagulation: An Fe and As K-edge EXAFS study, Environmental Science and Technology, 46 (2012) 986-994.

[212] J.M. Blengino, M. Keddam, J.P. Labbe, L. Robbiola, Physico-chemical characterization of corrosion layers formed on iron in a sodium carbonate-bicarbonate containing environment, Corrosion Science, 37 (1995) 621-643.

[213] L. Legrand, G. Sagon, S. Lecomte, A. Chausse, R. Messina, A Raman and infrared study of a new carbonate green rust obtained by electrochemical way, Corrosion Science, 43 (2001) 1739-1749.

[214] K.L. Dubrawski, C.M. Van Genuchten, C. Delaire, S.E. Amrose, A.J. Gadgil, M. Mohseni, Production and transformation of mixed-valent nanoparticles generated by Fe(0) electrocoagulation, Environmental Science and Technology, 49 (2015) 2171-2179.

[215] Y. Wei, J. Lu, X. Dong, J. Hao, C. Yao, Coagulation performance of a novel poly-ferric-acetate (PFC) coagulant in phosphate-kaolin synthetic water treatment, Korean Journal of Chemical Engineering, 34 (2017) 2641-2647.

[216] G.J. Millar, A. Schot, S.J. Couperthwaite, A. Shilling, K. Nuttall, M. De Bruyn, Equilibrium and column studies of iron exchange with strong acid cation resin, Journal of Environmental Chemical Engineering, 3 (2015) 373-385.

[217] M. Mechelhoff, G.H. Kelsall, N.J.D. Graham, Electrochemical behaviour of aluminium in electrocoagulation processes, Chemical Engineering Science, 95 (2013) 301-312.

[218] C.M. Van Genuchten, K.N. Dalby, M. Ceccato, S.L.S. Stipp, K. Dideriksen, Factors affecting the Faradaic efficiency of Fe(0) electrocoagulation, Journal of Environmental Chemical Engineering, 5 (2017) 4958-4968.

[219] M. Reffass, R. Sabot, C. Savall, M. Jeannin, J. Creus, P. Refait, Localised corrosion of carbon steel in $NaHCO_3$/NaCl electrolytes: Role of Fe(II)-containing compounds, Corrosion Science, 48 (2006) 709-726.

[220] M. Malakootian, H.J. Mansoorian, M. Moosazadeh, Performance evaluation of electrocoagulation process using iron-rod electrodes for removing hardness from drinking water, Desalination, 255 (2010) 67-71.

[221] F. Widhiastuti, J.Y. Lin, Y.J. Shih, Y.H. Huang, Electrocoagulation of boron by electrochemically co-precipitated spinel ferrites, Chemical Engineering Journal, 350 (2018) 893-901.

[222] G. Sayiner, F. Kandemirli, A. Dimoglo, Evaluation of boron removal by electrocoagulation using iron and aluminum electrodes, Desalination, 230 (2008) 205-212.

[223] W. Den, C. Huang, H.C. Ke, Mechanistic study on the continuous flow electrocoagulation of silica nanoparticles from polishing wastewater, Industrial and Engineering Chemistry Research, 45 (2006) 3644-3651.

[224] E. Mohora, S. Rončević, J. Agbaba, K. Zrnić, A. Tubić, B. Dalmacija, Arsenic removal from groundwater by horizontal-flow continuous electrocoagulation (EC) as a standalone process, Journal of Environmental Chemical Engineering, 6 (2018) 512-519.

[225] T.S. Pertile, E.J. Birriel, Treatment of hydrocyanic galvanic effluent by electrocoagulation: Optimization of operating parameters using statistical techniques and a coupled polarity inverter, Korean Journal of Chemical Engineering, 34 (2017) 2631-2640.

[226] M.M. Emamjomeh, M. Sivakumar, Review of pollutants removed by electrocoagulation and electrocoagulation/flotation processes, Journal of Environmental Management, 90 (2009) 1663-1679.

[227] S. Karpagamoorthy, S. Arunthathp, Review of electrocoagulation efficiency for the pollutants removal from water and wastewater, Pollution Research, 33 (2014) 583-590.

[228] K. Sardari, P. Fyfe, D. Lincicome, S.R. Wickramasinghe, Combined electrocoagulation and membrane distillation for treating high salinity produced waters, Journal of Membrane Science, (2018).

[229] L. Xu, X. Xu, G. Cao, S. Liu, Z. Duan, S. Song, M. Song, M. Zhang, Optimization and assessment of Fe–electrocoagulation for the removal of potentially toxic metals from real smelting wastewater, Journal of Environmental Management, 218 (2018) 129-138.

[230] V.L. Dhadge, C.R. Medhi, M. Changmai, M.K. Purkait, House hold unit for the treatment of fluoride, iron, arsenic and microorganism contaminated drinking water, Chemosphere, 199 (2018) 728-736.

[231] D. Zhao, J. Pan, Numerical simulation on reasonable hole-sealing depth of boreholes for gas extraction, AIP Advances, 8 (2018) 045003.

[232] Z. Wang, X. Tang, New Insights from Supercritical Methane Adsorption in Coal: Gas Resource Estimation, Thermodynamics, and Engineering Application, Energy & Fuels, 32 (2018) 5001-5009.

[233] X. Cheng, G. Zhao, Y. Li, X. Meng, C. Dong, Z. Liu, Researches of fracture evolution induced by soft rock protective seam mining and an omni-directional stereo pressure-relief gas extraction technical system: a case study, Arabian Journal of Geosciences, 11 (2018) 326.

[234] E.V. Mazanik, A.V. Ponizov, S.V. Slastunov, P.N. Paschenkov, MINE STUDIES OF IMPROVED TECHNOLOGY OF UNDERGROUND FRACTURING OF COAL SEAMS FOR THE PURPOSE OF EFFICIENT PRELIMINARY DEGASSING, 2018.

[235] L.O. Villacorte, Y. Ekowati, H.N. Calix-Ponce, V. Kisielius, J.M. Kleijn, J.S. Vrouwenvelder, J.C. Schippers, M.D. Kennedy, Biofouling in capillary and spiral wound membranes facilitated by marine algal bloom, Desalination, 424 (2017) 74-84.

[236] E. Guerra, P. Mahadevan, S. Chefai, Design and commissioning of a laboratory scale electrocoagulation reactor, in: TMS Annual Meeting, 2012, pp. 247-252.

[237] L. Smoczyński, H. Ratnaweera, M. Kosobucka, M. Smoczyński, Image analysis of sludge aggregates, Separation and Purification Technology, 122 (2014) 412-420.

[238] M.A. Sandoval, R. Fuentes, J.L. Nava, O. Coreño, Y. Li, J.H. Hernández, Simultaneous removal of fluoride and arsenic from groundwater by electrocoagulation using a filter-press flow reactor with a three-cell stack, Separation and Purification Technology, (2018).

[239] A. Guzmán, J.L. Nava, O. Coreño, I. Rodríguez, S. Gutiérrez, Arsenic and fluoride removal from groundwater by electrocoagulation using a continuous filter-press reactor, Chemosphere, 144 (2016) 2113-2120.

[240] C. Phalakornkule, S. Polgumhang, W. Tongdaung, B. Karakat, T. Nuyut, Electrocoagulation of blue reactive, red disperse and mixed dyes, and application in treating textile effluent, Journal of Environmental Management, 91 (2010) 918-926.

[241] I. Heidmann, W. Calmano, Removal of Ni, Cu and Cr from a galvanic wastewater in an electrocoagulation system with Fe-and Al-electrodes, Separation and Purification Technology, 71 (2010) 308-314.

[242] P. Canizares, M. Carmona, J. Lobato, F. Martinez, M. Rodrigo, Electrodissolution of aluminum electrodes in electrocoagulation processes, Ind. Eng. Chem. Res., 44 (2005) 4178-4185.

[243] R. Katal, H. Pahlavanzadeh, Influence of different combinations of aluminum and iron electrode on electrocoagulation efficiency: Application to the treatment of paper mill wastewater, Desalination, 265 (2011) 199-205.

[244] Z.-h. Yang, H.-y. Xu, G.-m. Zeng, Y.-l. Luo, X. Yang, J. Huang, L.-k. Wang, P.-p. Song, The behavior of dissolution/passivation and the transformation of passive films during electrocoagulation: Influences of initial pH, Cr(VI) concentration, and alternating pulsed current, Electrochimica Acta, 153 (2015) 149-158.

[245] X. Chen, G. Chen, P.L. Yue, Investigation on the electrolysis voltage of electrocoagulation, Chemical Engineering Science, 57 (2002) 2449-2455.

[246] C.-C. He, C.-Y. Hu, S.-L. Lo, Integrating chloride addition and ultrasonic processing with electrocoagulation to remove passivation layers and enhance phosphate removal, Separation and Purification Technology, 201 (2018) 148-155.

[247] T.H. Nguyen, R. Foley, On the mechanism of pitting of aluminum, Journal of the Electrochemical Society, 126 (1979) 1855-1860.

[248] K.V.K. Ansaf, S. Ambika, I.M. Nambi, Performance enhancement of zero valent iron based systems using depassivators: Optimization and kinetic mechanisms, Water Res., 102 (2016) 436-444.

[249] G. Mouedhen, M. Feki, M.D.P. Wery, H. Ayedi, Behavior of aluminum electrodes in electrocoagulation process, Journal of Hazardous Materials, 150 (2008) 124-135.

[250] C.-C. He, C.-Y. Hu, S.-L. Lo, Evaluation of sono-electrocoagulation for the removal of Reactive Blue 19 passive film removed by ultrasound, Separation and Purification Technology, 165 (2016) 107-113.

[251] P. Maha Lakshmi, P. Sivashanmugam, Treatment of oil tanning effluent by electrocoagulation: Influence of ultrasound and hybrid electrode on COD removal, Separation and Purification Technology, 116 (2013) 378-384.

[252] A. Ciblak, X. Mao, I. Padilla, D. Vesper, I. Alshawabkeh, A.N. Alshawabkeh, Electrode effects on temporal changes in electrolyte pH and redox potential for water treatment, Journal of Environmental Science and Health, Part A, 47 (2012) 718-726.

[253] T.C. Timmes, H.-C. Kim, B.A. Dempsey, Electrocoagulation pretreatment of seawater prior to ultrafiltration: pilot-scale applications for military water purification systems, Desalination, 250 (2010) 6-13.

[254] É. Fekete, B. Lengyel, T. Cserfalvi, T. Pajkossy, Electrochemical dissolution of aluminium in electrocoagulation experiments, Journal of Solid State Electrochemistry, 20 (2016) 3107-3114.

[255] C.-T. Wang, W.-L. Chou, L.-S. Chen, S.-Y. Chang, Silica particles settling characteristics and removal performances of oxide chemical mechanical polishing

wastewater treated by electrocoagulation technology, Journal of Hazardous Materials, 161 (2009) 344-350.

[256] P. Cañizares, C. Jiménez, F. Martínez, M.A. Rodrigo, C. Sáez, The pH as a key parameter in the choice between coagulation and electrocoagulation for the treatment of wastewaters, Journal of Hazardous Materials, 163 (2009) 158-164.

[257] İ.A. Şengil, M. Özacar, The decolorization of CI Reactive Black 5 in aqueous solution by electrocoagulation using sacrificial iron electrodes, Journal of Hazardous Materials, 161 (2009) 1369-1376.

[258] S. Zhi, S. Zhang, Effect of co-existing ions on electrode behavior in electrocoagulation process for silica removal, Desalination and Water Treatment, 56 (2015) 3054-3066.

[259] N. Esmaeilirad, K. Carlson, P.O. Ozbek, Influence of softening sequencing on electrocoagulation treatment of produced water, Journal of Hazardous Materials, 283 (2015) 721-729.

[260] A. Ozkan, A.G. Sener, H. Ucbeyiay, Investigation of coagulation and electrokinetic behaviors of clinoptilolite suspension with multivalent cations, Separation Science and Technology (Philadelphia), 53 (2018) 823-832.

[261] J.A.G. Gomes, P. Daida, M. Kesmez, M. Weir, H. Moreno, J.R. Parga, G. Irwin, H. McWhinney, T. Grady, E. Peterson, D.L. Cocke, Arsenic removal by electrocoagulation using combined Al-Fe electrode system and characterization of products, J. Hazard. Mater., 139 (2007) 220-231.

[262] E.D. Güven, E. Güler, G. Akıncı, A. Bölükbaş, Influencing Factors in the Removal of High Concentrations of Boron by Electrocoagulation, Journal of Hazardous, Toxic, and Radioactive Waste, 22 (2017) 04017031.

[263] B. Zeboudji, N. Drouiche, H. Lounici, N. Mameri, N. Ghaffour, The influence of parameters affecting boron removal by electrocoagulation process, Separation Science and Technology, 48 (2013) 1280-1288.

[264] Z. Zaroual, M. Azzi, N. Saib, E. Chainet, Contribution to the study of electrocoagulation mechanism in basic textile effluent, Journal of Hazardous Materials, 131 (2006) 73-78.

[265] C. Jiménez, C. Sáez, F. Martínez, P. Cañizares, M.A. Rodrigo, Electrochemical dosing of iron and aluminum in continuous processes: a key step to explain electro-coagulation processes, Separation and Purification Technology, 98 (2012) 102-108.

[266] M. Mechelhoff, G.H. Kelsall, N.J. Graham, Electrochemical behaviour of aluminium in electrocoagulation processes, Chemical Engineering Science, 95 (2013) 301-312.

[267] T. Milligan, An examination of the settling behaviour of a flocculated suspension, Netherlands Journal of Sea Research, 33 (1995) 163-171.

[268] C. Ricordel, A. Darchen, D. Hadjiev, Electrocoagulation-electroflotation as a surface water treatment for industrial uses, Sep. Purif. Technol., 74 (2010) 342-347.

[269] J.C. Pashin, M.R. McIntyre-Redden, S.D. Mann, D.C. Kopaska-Merkel, M. Varonka, W. Orem, Relationships between water and gas chemistry in mature coalbed methane reservoirs of the Black Warrior Basin, International Journal of Coal Geology, 126 (2014) 92-105.

[270] H. Le, S. Chalmers, Australia's first build own operate CSG produced water treatment and beneficial reuse project, in: Proceedings - SPE Annual Technical Conference and Exhibition, 2015, pp. 3661-3670.

[271] L. De Buren, A. Sharbat, Inland desalination and brine management: Salt recovery and beneficial uses of brine, in: World Environmental and Water Resources

Congress 2015: Floods, Droughts, and Ecosystems - Proceedings of the 2015 World Environmental and Water Resources Congress, 2015, pp. 1219-1230.

[272] P. Chelme-Ayala, D.W. Smith, M.G. El-Din, Membrane concentrate management options: A comprehensive critical review, Canadian Journal of Civil Engineering, 36 (2009) 1107-1119.

[273] S.J. Khan, D. Murchland, M. Rhodes, T.D. Waite, Management of concentrated waste streams from high-pressure membrane water treatment systems, Critical Reviews in Environmental Science and Technology, 39 (2009) 367-415.

[274] P. Xu, T.Y. Cath, A.P. Robertson, M. Reinhard, J.O. Leckie, J.E. Drewes, Critical review of desalination concentrate management, treatment and beneficial use, Environmental Engineering Science, 30 (2013) 502-514.

[275] A. Pérez-González, A.M. Urtiaga, R. Ibáñez, I. Ortiz, State of the art and review on the treatment technologies of water reverse osmosis concentrates, Water Research, 46 (2012) 267-283.

[276] Y. Kim, Y.C. Woo, S. Phuntsho, L.D. Nghiem, H.K. Shon, S. Hong, Evaluation of fertilizer-drawn forward osmosis for coal seam gas reverse osmosis brine treatment and sustainable agricultural reuse, Journal of Membrane Science, 537 (2017) 22-31.

[277] H.C. Duong, M. Duke, S. Gray, B. Nelemans, L.D. Nghiem, Membrane distillation and membrane electrolysis of coal seam gas reverse osmosis brine for clean water extraction and NaOH production, Desalination, 397 (2016) 108-115.

[278] D. Mukhopadhyay Method and apparatus for high efficiency reverse osmosis operation, US6537456B2, (2003).

[279] K. Moftah, High pH RO for wastewater treatment, Pollution Engineering, 34 (2002) 30-35.

[280] X. Long, Q. Zhu, X.Y. Wang, J.H. Shi, Application of high-efficiency reverse osmosis technology in reclaimed water treatment in power plants, in: Advanced Materials Research, 2014, pp. 108-114.

[281] Y. Oren, E. Korngold, N. Daltrophe, R. Messalem, Y. Volkman, L. Aronov, M. Weismann, N. Bouriakov, P. Glueckstern, J. Gilron, Pilot studies on high recovery BWRO-EDR for near zero liquid discharge approach, Desalination, 261 (2010) 321-330.

[282] P. Cañizares, M. Carmona, J. Lobato, F. Martínez, M.A. Rodrigo, Electrodissolution of aluminum electrodes in electrocoagulation processes, Industrial and Engineering Chemistry Research, 44 (2005) 4178-4185.

[283] D.Y. Sorokin, J.G. Kuenen, Haloalkaliphilic sulfur-oxidizing bacteria in soda lakes, FEMS microbiology reviews, 29 (2005) 685-702.

[284] L. Lunevich, P. Sanciolo, N. Milne, S.R. Gray, Silica fouling in coal seam gas water reverse osmosis desalination, Environmental Science: Water Research and Technology, 3 (2017) 911-921.

[285] C.J. Gabelich, K.P. Ishida, F.W. Gerringer, R. Evangelista, M. Kalyan, I.H. Suffet, Control of residual aluminum from conventional treatment to improve reverse osmosis performance, Desalination, 190 (2006) 147-160.

[286] W.Y. Shih, J. Gao, A. Rahardianto, J. Glater, Y. Cohen, C.J. Gabelich, Ranking of antiscalant performance for gypsum scale suppression in the presence of residual aluminum, Desalination, 196 (2006) 280-292.

[287] W. Wang, H. Yang, X. Wang, J. Jiang, W. Zhu, Factors effecting aluminum speciation in drinking water by laboratory research, Journal of Environmental Sciences, 22 (2010) 47-55.

[288] S.Y. Lee, G.A. Gagnon, Growth and structure of flocs following electrocoagulation, Separation and Purification Technology, 163 (2016) 162-168.

[289] D.G. Kim, R.J.S. Palacios, S.O. Ko, Characterization of sludge generated by electrocoagulation for the removal of heavy metals, Desalination and Water Treatment, 52 (2014) 909-919.

[290] C. Jimenez, B. Talavera, C. Saez, P. Canizares, M.A. Rodrigo, Study of the production of hydrogen bubbles at low current densities for electroflotation processes, J. Chem. Technol. Biotechnol., 85 (2010) 1368-1373.